Waseda University

Doctoral Dissertation

Studies on Spectrum Sensing and MAC layer Protocol for Wireless Mesh Networks

メッシュ型無線ネットワークにおけるスペクトラム検知と MAC 層プロトコルに関する研究

November 2011

Graduate School of Global Information and Telecommunication Studies

Bingxuan ZHAO

Contents

List of Figures

List of Tables

Acknowledgement

This dissertation summarizes the achievements of my research in Graduate School of Global Information and Telecommunication Studies, Waseda University, Japan, under the supervision of Prof. Shigeru Shimamoto. Firstly, I would like to express my grate acknowledgement to my supervisor, Prof. Shimamoto, for his valuable guidance, insightful suggestions, kind and constant help and encouragement during the past three years.

I also would like to give my thanks to all the members in Shimamoto Laboratory, especially, Ms. Jiang Liu, Mr. Dec Tu Ho, Mr. Jun Wu, Ms. Rabarijaona Verotiana Hanitriniala, Ms. Wasinee Noonpakdee, Ms. Chunxiao Li, Mr. Jin Qi, Ms. Zhenni Pan, Mr. Thomas Bourjeois, TungWu Chiu, Mr. and Ms. Shiho Saruta for their continuous encouragement, support, and technical discussions. Also, I would like to thank all my friends in GITS, Waseda Univeristy.

In addition, I really appreciate Dr. Chunyi Song in the National Institute of Information and Communications Technology, Japan, Prof. Jianjun Wu in Peiking University, China, and my supervisor in the master course, Prof. Gang Wu, in University of Science and Technology of China for their kind help and meaningful discussions.

I am very proud of being awarded the Monbukagakusho scholarship from Ministry of Education, Culture, Sports, Science and Technology, Japan. I would like to thanks their financial support.

Last but not least, I would like to show my respect and deep gratitude to my parents, and my wife. Their understanding, encouragement and support, have helped me to complete this work.

Bingxuan ZHAO
November 2011

Summary

The current spectrum regulatory rule, which exclusively allocates wireless spectrum to different specific applications and forbids violation from unlicensed users, has resulted in the unbalanced spectrum utilization. On one hand, some spectrum bands such as the ISM band are very crowded; on the other hand, most of the allocated spectrum bands are significantly underutilized in different locations and times. Such an unbalanced spectrum utilization problem can be alleviated by the emerging dynamic spectrum access techniques such as cognitive radio. As the fundamental component of dynamic spectrum access, implementing spectrum sensing is one of the most important goals in cognitive radio networks due to its key functions of protecting licensed primary users from harmful interference and identifying spectrum holes for the improvement of spectrum utilization. However, the performance of the local spectrum sensing, performed by a single cognitive radio, cannot work well when it is suffering from multi-path fading, shadowing, and receiver uncertainty. To overcome such challenges, cooperative spectrum sensing is usually employed. Since the typical architecture of cooperative spectrum sensing is similar to the wireless mesh networks, the cognitive wireless mesh networks have attracted more and more attentions in the recent years. Therefore, this dissertation focuses on the study of the cooperative spectrum sensing for cognitive wireless mesh networks, specially, two aspects of which are involved in this dissertation: the spectrum sensing to effectively find the white spaces in the primary spectrum bands, and the MAC protocol for data transmission in the cognitive secondary networks. Although various local spectrum sensing techniques can be utilized, energy detection is the most widely used technique in the cooperative spectrum sensing because of its simplicity and no requirement on the prior knowledge of the primary signals. Thus, it is utilized in the cooperative spectrum sensing investigated by this dissertation. In spectrum sensing, there exist several challenges that compromise its performance, i.e., the inter-channel interference, the threshold setting, and the reporting channel allocation. This dissertation tries to address such challenges.

In chapter 1, the wireless mesh network and the spectrum sensing for cognitive

radio are briefly introduced. At first, the architecture, characteristics, and the application scenarios of wireless mesh networks are described. Then, two main characteristics, cognitive ability and reconfigurability, are presented. Cognitive ability enables the radio technology to capture or collect the information from its operating environment. It consists of four steps: the spectrum sensing, management, sharing, and mobility. The reconfigurability is the capability of adjusting the transmission parameters of the radio to adapt to the working environment without any modification of the hardware.

In chapter 2, the well known spectrum sensing techniques and MAC protocols of wireless mesh network are briefly overviewed. In the local sensing, the pros and cons of various sensing techniques are analyzed and compared. Such techniques include energy detection, covariance detection, eigenvalue detection, cyclostationary detection, and wavelet detection. In cooperative spectrum sensing, the implementation model and evaluation metrics are firstly introduced. Then, the implementation steps, pros, and cons of hard combining and soft combining are presented, respectively. In the review of MAC protocols of wireless mesh network, the typical single radio single channel MAC, single radio multi-channel MAC, and the multi-radio multi-channel MAC are briefly introduced. The advantages and disadvantages of such MAC protocols are analyzed and compared.

In chapter 3, the performance improvement through interference cancellation is firstly analyzed. The analysis indicates that the performance of cooperative spectrum sensing can be improved by interference cancellation in terms of probability of detection and probability of false alarms. Then, the non-coherent power decomposition-based energy detection method for cooperative spectrum sensing is proposed to alleviate the impact of the inter-channel interference and improve the detection performance. Due to its use of power decomposition, the interference power, background noise power, and the target signal power can be individually separated from the superposed received power, and thus, interference cancellation can be applied in energy detection by subtracting it from the total received power. The proposed power decomposition does not require any prior knowledge of the primary signals. The power decomposition with its interference cancellation can be implemented indirectly by solving a non-homogeneous linear equation set with a coefficient matrix that involves only the distances between primary transmitters and cognitive secondary users (SUs).

The optimal number of SUs for sensing a single channel and the number of channels that can be sensed simultaneously are also derived. The simulation results show that the proposed method is able to cope with the expected interference variation and achieve higher probability of detection and lower probability of false alarm than the conventional method in both hard combining and soft combining scenarios. Since the proposed power decomposition scheme depends on the distances between primary transmitters and cognitive SUs, the position accuracy of both primary transmitters and cognitive SUs has an impact on the performance of cooperative spectrum sensing. However, the analysis of position accuracy indicates that the impact is so weak that it can be ignored when the inaccuracy of both primary transmitters and cognitive SUs is very small compared to the distances between these two kinds of nodes.

In chapter 4, both the threshold setting problem and the reporting channel problem are addressed. In order to address the threshold setting problem, different from the conventional method, which cannot optimize both the probability of false alarm and the probability of detection since it sets the determination threshold to a target probability of false alarm, an optimal threshold setting method is proposed in this chapter. The optimal threshold is able to minimize the sum of the probabilities of false alarms and missed detection. It depends only on the means and variances of the power samples when the primary signals are absent and when they are present. The derivation process of optimal threshold setting indicates that it is more accurate when the number of samples of test statistic is large due to the application of central limit theorem, which corresponds to the cases that the SINR is low. Then, it is successfully applied in the power decomposition method described in chapter 3. In addition, the reporting channel will become the bottleneck when the number of cognitive radios need to be coordinated becomes large in the soft combing scenario. In order to address the bottleneck problem, multiple in-band orthogonal channels are designated as reporting channels. In this scheme, a multi-radio conflict graph is utilized to model the co-channel interference, and the vertex coloring algorithm is applied to the multi-radio conflict graph to figure out the reporting channel allocation results. By considering the traffic pattern of sensed data transmission, a Breadth First Search (BFS) in a bottom-up order is applied in the vertex coloring algorithm to decrease the complexity. Simulations verify the feasibility of the optimal threshold setting and show that it can work well in the low SINR range

and can achieve low sensing delay.

In chapter 5, the MAC protocol of secondary wireless mesh network is investigated. In this chapter, a two-stage coordination multi-radio multi-channel MAC (TSC-M2MAC) is proposed. It can be utilized to solve the bottleneck problem, resulted from the increasing number of concurrent traffic flows in the single common control channel. It designates all the available in-band orthogonal channels as both control channels and data channels in a time division manner through a two-stage coordination. On the first stage, similar to the reporting channel allocation in chapter 4, the multiple control channels allocation is performed. However, the vertex coloring algorithm is performed in a top-down order since the links with less hop counts should be given higher priority of allocating channels with less interference according to the traffic pattern of wireless mesh networks. On the second stage, a REQ/ACK/RES mechanism is proposed to dynamically channel allocation for data transmission. The control messages, i.e., REQ, ACK, RES, and periodically transmitted beacons and pilots, are exchanged in the pre-allocated control channels on the first stage. In this stage both the primary channel and the secondary channels can be allocated. The proposed TSC-M2MAC is able to alleviate the multi-channel hidden terminal problem when using multiple control channels and cope with the variation of the number of concurrent traffic flows. In addition, a power saving mechanism is designed for TSC-M2MAC to decrease its power consumption. Simulation results show that the TSC-M2MAC protocol is able to achieve higher throughput and lower end-to-end packet delay than conventional schemes. They also show that the TSC-M2MAC can achieve load balancing, save energy, and remain stable when the network becomes saturated.

In chapter 6, I conclude the dissertation and state the future works.

Chapter 1
Introduction

As an emerging and promising technology, a wireless mesh network (WMN) can provide high QoS to end users as the last mile technique for data delivery over the Internet. Its capabilities of self-organizing, self-healing, and self-configuring significantly reduce the complexity of deployment and enhance the robustness of the network. Its infrastructure consists of wireless routers and gateways, through which mesh clients connect to the Internet. Obviously, the gateway has much stronger computing capability than other nodes in WMNs.

Since most of the consumer devices in WMNs work in the unlicensed frequency band for industrial, scientific, and medical (ISM) applications, similar to other networks such as ad hoc networks, WMNs also suffer from the crowded spectrum in the ISM band. Meanwhile, many licensed frequency bands are shown to be greatly under-utilized even in the most crowded urban areas [1, 2]. Such unbalanced spectrum utilization can be alleviated using dynamical spectrum access (DSA) techniques such as cognitive radio [3-7]. Obviously, applying cognitive technique to WMNs is able to more effectively utilize the spectrum and significantly decrease the complexity of deployment and enhance the robustness of the network. Therefore, our work focuses on the cognitive Wireless Mesh network. In this chapter, I will first introduce the WMN and cognitive radio especially the spectrum sensing; then, I will list the contributions of our work; finally, I will show the organizational structure of this dissertation.

1.1 Wireless Mesh Networks

In WMN, there are two main kinds of nodes: mesh routers and mesh clients. Compared to mesh clients, the mesh routers are usually with low mobility. So, they generally have lower power constraints and more powerful computing capabilities. A WMN is dynamically self-organized, self-configured with other nodes in the network.

The nodes are able to establish or cancel the connections automatically when they join in or depart from the network. These features incur many advantages to WMNs such as robustness, low up-front investment, easy network maintenance, and reliable service coverage [8-10]. Therefore, WMN is a very attractive technique and can be used in many application scenarios. In this section, I will introduce the WMN from three aspects: the architecture, the characteristics, and the application scenarios.

1.1.1 Architecture of WMNs

As it is mentioned before, WMN consists of mesh routers and mesh clients. Compared to conventional wireless routers in other networks such as ad hoc network, Wireless Local Area Network (WLAN), and Worldwide Interoperability Microwave Access (WiMAX), mesh routers have additional functions apart from the routing function. For example, a mesh router can be quipped with multiple interfaces to improve the network capacity since a router can transmit, receive, and forward packets using different interfaces working on different frequency bands. In addition, a wireless mesh router is able to achieve the same coverage with much lower transmission power through multi-hop communication [8, 9, 11].

Similar with the conventional wireless routers, wireless mesh routers can work as gateways. They can also be built on both dedicated computer system like the embedded systems and general purpose computer systems like laptop.

Mesh clients can also provide the routing function when it is necessary although they are less powerful than the routers. However, they cannot work as a gateway of bridge. Obviously, they are much simpler and easier to be implemented than the mesh routers. So, mesh clients are more diversifying and can be laptops, PDAs, IP phones, RFID readers, and many other devices [8].

Although the architectures of WMNs can be divided into three groups: Backbone WMNs, clients WMNs, and hybrid WMNs according to the functionality of the mesh nodes, the hybrid one is believed the most applicable architecture. Here, we only introduce the architecture of hybrid WMNs.

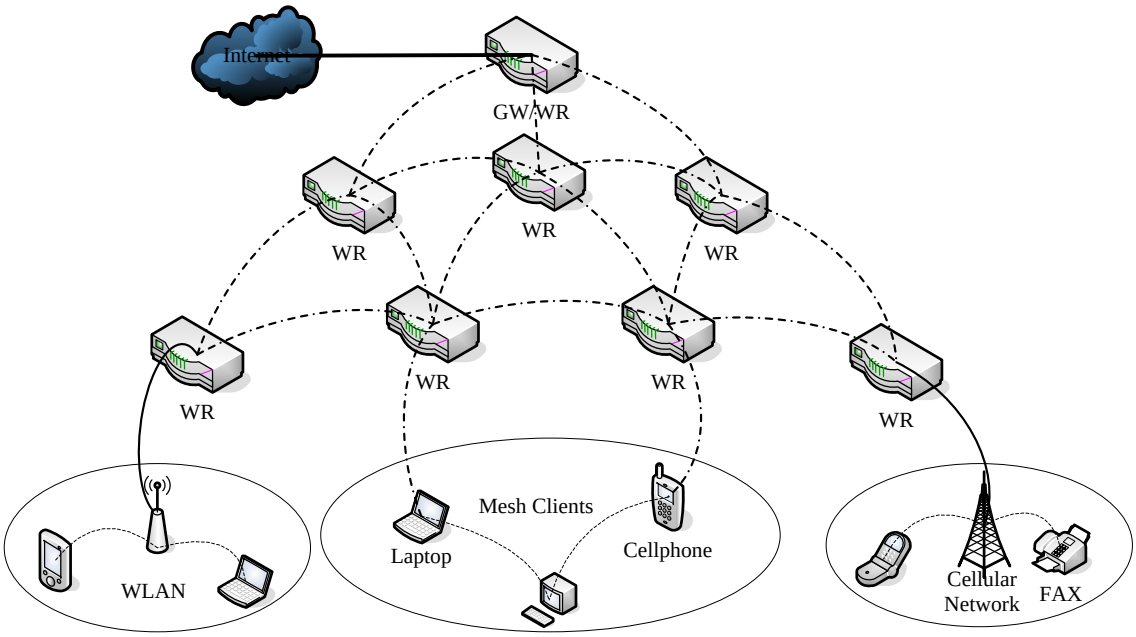

Figure 1-1 A typical architecture of a hybrid WMN

A typical architecture of a hybrid WMN is shown in Figure 1-1. In this figure, the solid and dashed lines indicate the wired and wireless links, respectively. The mesh routers including the gateways form an infrastructure/backbone for mesh clients and other networks such as WLAN, cellular network, and so on. The backbone can be built using different kinds of radio techniques, in addition to IEEE 802.11 technique, which becomes very crowd since Wi-Fi becomes very popular and widely used nowadays. Through the gateway, all the users, including the mesh clients and Wi-Fi users, are able to access the Internet. In addition to accessing the Internet, the mesh nodes can exchange data among themselves. In general, there are two types of radio equipped on the mesh routers: long range communication radio for backbone data exchanging, e.g., the radio with directional antenna; and the short range communication radio for data exchanging between the mesh routers on the edge and the mesh clients, e.g., the radio with omni-directional antenna in order to achieve large coverage.

1.1.2 Characteristics of WMNs

As an emerging and promising technique, WMNs have a lot of attractive characteristics. They will be introduced as follows.

- Multi-hop wireless network. There are two main motivations to develop WMNs. The first one is to extend the coverage of the currently existing wireless networks like the Wi-Fi without sacrificing the channel capacity. The second motivation is to provide nonline-of-sight (NLOS) connectivity since no line-of-sight (LOS) links exist in some cases between the sources and destinations. To achieve these objectives, mesh-style multi-hopping is unavoidable [8, 12]. They point out that mesh-style multi-hopping is able to achieve higher throughput without sacrificing coverage range through coordination between nodes by selecting shorter distance and less interference links. In this case, the frequency band can be effectively reused [8].

- Self-organizing, self-healing, and self-configuring. Generally, WMNs have flexible architecture. They are easy to deploy and configure. In addition, WMNs can achieve fault tolerance and multipoint-to-multi-point communications. Therefore, WMNs have low upfront investment requirement and the network can grow gradually as needed [8, 9].

- Mobility. In WMNs, mesh routers and clients have different mobility styles. In general, mesh routers have lower mobility, but the mesh clients can be stationary or mobile. Obviously, mesh nodes is different from the nodes in ad hoc networks.

- Compatibility and interoperability with existing wireless networks. As it is mentioned in section 1.1.1, WMNs is an integration of multiple types of wireless networks. Therefore, in order to provide connectivity for such existing networks to the internet and the data exchanging among them, WMNs built on IEEE 802.11 technology must be compatible with IEEE 802.11 standards to support both mesh-capable and conventional Wi-Fi applications [8, 9]. They also need to be interoperable with other wireless networks such as WiMAX, ZigBee, Cellular networks, and so on [8, 9].

- Power consumption constraints. Since the mesh routers are always with low mobility, they are usually power sufficient. However, power saving is needed for mesh clients. Therefore, MAC and routing protocols optimized for the mesh routers may not work well for the mesh clients, since power efficiency is

the primary concern for mesh clients like the wireless sensors [8, 13].

1.1.3 Application Scenarios of WMNs

Since the research and development of WMNs is driven by applications, they can be used in various scenarios. In such scenarios, the current existing wireless networks such as WLAN, ad hoc networks, etc, cannot be directly applied. WMNs can be applied in, but no limited to, the following scenarios.

- Broadband home networking. Currently, home networking is usually implemented by the IEEE 802.11 WLAN. However, WLAN has the several disadvantages. The first one is the coverage. There are generally several dead zones that cannot be covered by the Wi-Fi service. The second disadvantage is that all data exchanging should be forwarded by the affiliated access point. This is really inefficient for broadband communications. WMNs can solve such problems. At first, the dead zones can be eliminated by deploying more wireless mesh routers. Second, in WMNs, end users are able to directly exchange data among themselves rather than requiring the access points to forward. This is important for some protocols like peer-to-peer (P2P).
- Community and neighborhood networking. The common used architecture for network access in a community is based on the infrastructure connected to the internet by fiber or digital subscriber line (DSL) with a wireless router for the last hop access. However, such a scheme has the following shortcomings. First, the data shared in the community still has to flow through the internet, which will occupy more bandwidth of the internet and degrade the network performance. Second, a part of areas between houses will not be covered by the wireless services [8]. Third, only a single path is available for one home to access the internet or communicate with other neighbors [8]. However, WMNs can be used to solve the above problems through flexible connectivities. In addition, WMNs can enable many other applications such as distributed file storage, P2P file exchanging, etc.

In addition to the applications introduced above, WMNs can also be used to enterprise networking, metropolitan area networks, transportation system, and etc.

interested people can refer to [8, 9].

Since the there are differences between WMN and the existing networks, the design of the protocol should take into account its unique features to achieve better performance.

1.2 Cognitive Radio and Spectrum Sensing

It has been shown by the Federal Communications Commission (FCC) that the current fixed spectrum allocation has resulted in low spectrum utilization in almost all the allocated spectrum band [14]. The utilization of the assigned spectrum ranges from 15% to 85% at different positions and times [1, 2, 15, 16]. On the other hand, the open spectrum access has made great success in the industrial, scientific, and medical (ISM) radio band. In ISM band, the spectrum band is not allocated to any specific applications. Instead, all the devices can operate in this band as long as they can tolerate the interference from other equipment operating in this band. Examples of applications in this band include WLAN devices, Bluetooth, microwave ovens, and diathermy machines. Because of its open spectrum policy, ISM band has caused an impressive variety of important technologies and innovative applications. As the increasing of applications in this band, it becomes crowd. Such unbalanced spectrum utilization can be alleviated by using the dynamic spectrum access (DSA) technique, i.e., cognitive radio (CR), which can be defined as follows:

A “Cognitive Radio” is a radio than can change its transmitter parameters based on the interaction with the environment in which it operates [15, 16].

In cognitive radio, the primary users (PUs) are referred to the licensed users that have higher priority or legacy rights on the usage of the part of the licensed spectrum band [17]. The secondary users (SUs) are referred to the unlicensed users that want to utilize the spectrum opportunities in the licensed band for communications [18]. The cognitive radio has two main characteristics: cognitive ability and reconfigurability.

1.2.1 Cognitive ability

Cognitive ability refers to the ability of the radio technology to capture or collect the information from its operating environment. It enables real time interaction with the environment to find the spectrum hole or white space shown in Figure 1-2, i.e., a band of frequencies assigned to a licensed user (primary user), but, at a particular time and a specific geographic location, the band is not being utilized by that user [19]. If so, the cognitive radio should adapt its transmission parameters to explore the white space. These tasks are implemented by five steps [15, 20]:

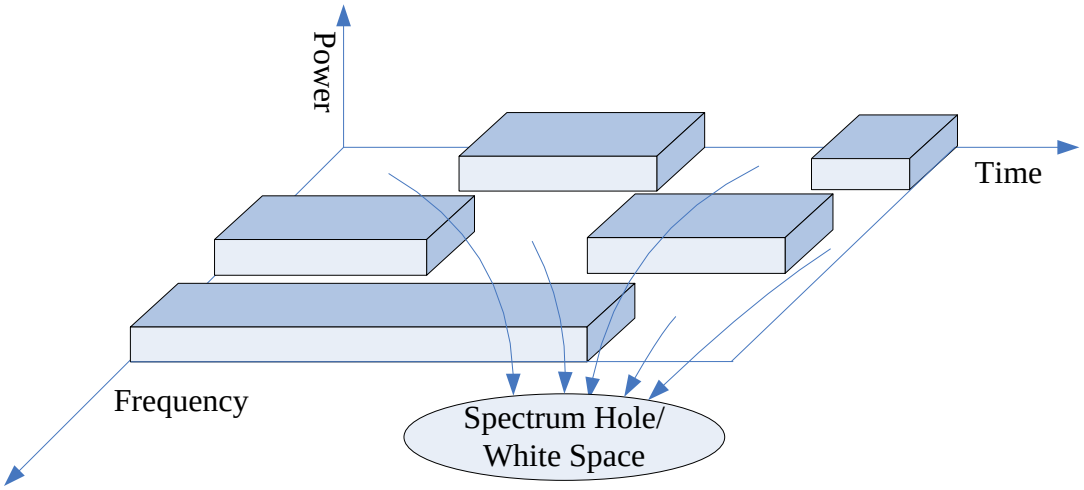

Figure 1-2 Spectrum Holes/White Space

- Spectrum sensing. It is used to detect whether the primary signals are present or absent. Nowadays, there are various types of such detections. They can be mainly categorized into two groups: primary transmitter detection and primary receiver detection. Since the emitted power by the primary receiver is usually too weak to be measured, most of the existing detection schemes are of primary transmitter detection. It is an issue of physical layer.

- Spectrum analysis. Since the characteristics of detected spectrum holes vary over time and geographic locations, analysis is necessary for the cognitive radio in the physical layer to understand them. Hence, it is essential to define parameters such as interference level, channel error rate, path-loss, link layer delay, etc [15].

- Spectrum decision. The transmission parameters, modulation and coding schemes,

data rate, and the spectrum bandwidth should be determined by the cognitive radio in order that the appropriate spectrum band can be selected according to the quality of service (QoS) requirements. Both spectrum analysis and decision can be considered as spectrum management.

- Spectrum sharing. After the white spaces being detected, the secondary users should be coordinated to decide which one can access them. Then, the secondary users can switch to the target primary channel to share it.
- Spectrum mobility. When the primary signals are detected, the secondary users should vacate its operating primary channel to avoid interference with the licensed primary user.

1.2.2 Reconfigurability

Reconfigurability is the capability of adjusting the parameters of the transmission without any modification on the hardware component. That is why the cognitive radio was initially considered as an extension of software-defined radio. This capacity enables the cognitive radio to adapt its parameters easily to its operating environment. The parameters that can be incorporated into the cognitive radio are listed as follows [15, 16, 20]:

- Operating frequency. The capacity of switching the operating frequency is the most basic requirement for the cognitive radio. Based on the spectrum sensing result, the most appropriate center frequency and bandwidth are able to be determined. After changing the frequency, the communication can be dynamically performed.
- Modulation and coding scheme (MCS). A cognitive radio should adapt its modulation and coding scheme to satisfy the QoS requirements and the channel conditions. For example, in the case of delay sensitive applications such as the voice over IP (VoIP), the packet transmission rate is more important than the packet error rate. Consequently, the MCS that can provide higher spectral efficiency should be selected. On the contrary, in the case of pack loss sensitive applications such as file transfer system, the MCS that can decrease the packet error rate are preferred.

- Transmission power. In cognitive radio system, a spectrum band can be shared by multiple users. Therefore, such users will interfere with each other when they operate simultaneously in the same frequency band. If a higher power operation is not necessary, the transmitter should limit its transmission power on a lower level in order to reduce the interference with other users and improve the capacity of the spectrum band.
- Communication technology. As it is stated in section 1.1.1, the cognitive radio should be able to interoperate among different communications systems. This requires the cognitive radio to operate on different standards.

The transmission parameters of a cognitive should be able to be reconfigured not only at the beginning of a session but also during the ongoing session. According to the sensing result, a cognitive radio should be able to switch to the white space or vacate the current operating channel. Then, both the transmitters and receivers should reconfigure their parameters to satisfy the QoS requirement and the channel conditions.

1.3 Organization of the Dissertation

Since cognitive wireless mesh network is an emerging technique, there are various research challenges to be addressed. The open research issues include, but are not limited to, spectrum sensing in physical layer, spectrum sharing and allocation in the MAC layer, and upper layer issues such as routing, flow control and congestion control. However, this dissertation only involves in the spectrum sensing in the physical layer and the design of MAC layer protocol. As we know, there are different kinds of schemes for spectrum sensing and various types of MAC protocol, the spectrum sensing investigated in this dissertation is based on the energy detection, and the MAC protocol is designed for the multi-radio multi-channel application. However, an overview of both spectrum sensing and MAC protocol for cognitive wireless mesh networks will be given in this dissertation.

The remainder of this dissertation is organized as follows:

In chapter 2, the overview of spectrum sensing and MAC protocol is given. In the review of spectrum sensing schemes, the pros and cons of both primary transmitter

detection and primary receiver detection will be listed. I will compare them from both the theoretical and implemental aspects and point out the reason why the primary transmitter detection is widely used in the previous literature. In the primary transmitter detection, the advantages and disadvantages of coherent and non-coherent spectrum sensing will be listed. Moreover, some of the typical schemes proposed in the previous literature will be introduced. In the review of MAC layer protocol, the MAC protocols designed for the single radio single channel (SRSC), the single radio multiple channel (SRMC), and multiple radio multiple channel (MRMC) will be introduced. The pros and cons of such MAC protocols will be analyzed. In addition, the typical MAC protocols in these three categories will be introduced. In this chapter, the motivation of my work will also be presented.

In chapter 3, I will present a non-coherent power decomposition based energy detection for cooperative spectrum sensing scheme. This scheme is proposed for general cognitive networks, so, it can certainly be used for cognitive wireless mesh networks. As the fundamental component of dynamic spectrum access, implementing spectrum sensing is one of the most important goals in cognitive radio networks due to its key functions of protecting licensed primary users from harmful interference and identifying spectrum holes for the improvement of spectrum utilization. However, its performance is generally compromised by the interference from adjacent primary channels. To cope with such interference and improve detection performance, this chapter proposes a non-coherent power decomposition-based energy detection method for cooperative spectrum sensing. Due to its use of power decomposition, interference cancellation can be applied in energy detection. The proposed power decomposition does not require any prior knowledge of the primary signals. The power detection with its interference cancellation can be implemented indirectly by solving a non-homogeneous linear equation set with a coefficient matrix that involves only the distances between primary transmitters and cognitive secondary users (SUs). The optimal number of SUs for sensing a single channel and the number of channels that can be sensed simultaneously are also derived. The simulation results show that the proposed method is able to cope with the expected interference variation and achieve higher probability of detection and lower probability of false alarm than the conventional method in both hard combining and soft combining scenarios. The content of this chapter corresponds to [21].

In chapter 4, we propose an optimal spectrum sensing with inter-channel interference cancellation for cognitive wireless mesh network. The traffic pattern of wireless mesh network is considered when the control channel is allocated. Different from the conventional threshold setting that determine the threshold with a target probability of false alarm, the optimal threshold setting determine it to minimize the sum of probability of false alarm and probability of missed detection. We apply the optimal threshold setting in the power decomposition method, which is called inter-channel interference cancellation because it is emphasized in this chapter. Moreover, in order to decrease the sensing delay, especially the reporting delay, a scheme utilizing multiple control channels is proposed. In control channel allocation, the multi-radio conflict graph is used to model the co-channel interference, then, a vertex coloring algorithm in a bottom-up order is applied to the multi-radio conflict graph to allocate the control channel. Simulations validate the proposed scheme and show that the proposed scheme is able to minimize the sum of probability of false alarm and probability of missed detection. Meanwhile, the control channel allocation utilizing multiple control channels is able to decrease the reporting delay. The content of this chapter corresponds to [22, 23]

In chapter 5, we proposed a two-stage coordination multi-radio multi-channel MAC protocol for the secondary wireless mesh network. The first stage is the control channel allocation, which is similar to the method used in the chapter 4. Then, a dynamic data channel allocation scheme is proposed. The coordination for data channel allocation is implemented by a REQ/ACK/RES mechanism, which is similar to RTS/CTS mechanism. The data channel allocation and data transmission are performed in a time division manner in which the time line is divided into beacon intervals by the periodical beacons. Each beacon interval is further divided into two sub-intervals. One is for data channel negotiation and allocation (CNA sub-interval), another is for data transmission (DT sub-interval). The control messages such as periodical beacons, data pilots, REQ, ACK, RES, are exchanged through the multiple control channels allocated at the first stage. In order to cope with the variation of the number of traffic flows at different times, an adaptive adjusting algorithm for CNA sub-interval is proposed. In addition, a power saving mechanism unique to the proposed MAC protocol is presented to improve the efficiency of its energy consumption. The content of this chapter

corresponds to [24, 25]

In chapter 6, we conclude this dissertation and outline the future works.

The main work of this dissertation consists of three chapters, i.e., chapter 3, chapter 4, and chapter 5. The relations among the three chapters can be described as follows: chapter 3 and chapter 4 focus on the cooperative spectrum sensing. The schemes in chapter 4 can further improve the performance of the power decomposition method proposed in chapter 3. To efficiently utilize the spectrum holes from spectrum sensing, chapter 5 focuses on the dynamic spectrum access scheme. In this chapter, I proposed a two-stage coordination multi-radio multi-channel MAC protocol.

It would be the honor of the author if this work could contribute towards the accuracy improvement of the spectrum sensing and the efficiency increase at the multi-radio multi-channel MAC protocol for cognitive wireless mesh networks.

Chapter 2

Overview of Spectrum Sensing and MAC Protocol of Cognitive WMNs

Due to the remarkable growth of wireless applications and the rapid development of wireless devices over the past decades, the spectrum becomes very scarce. There are two ways to meet the increasing demand for the spectrum: to look for white spaces in various primary channels and to improve the utilization of the spectrum that can be used for the secondary cognitive networks. The first way is generally implemented by spectrum sensing, i.e., detecting the presence or absence of the primary signals to find the white spaces. Since there are many challenges in spectrum sensing to be faced, it becomes a very active research topic in recent years [26]. The second way is able to be implemented by many techniques such as power control, interference cancellation, and exploring multiple orthogonal channels allocated by many standards such as IEEE 802.11 a/b/g. However, this chapter focuses only on the spectrum sensing and utilizing multiple orthogonal channels.

In the following, the overview of spectrum sensing will be first given. Then, the MAC layer protocols utilizing multiple orthogonal channels for WMN will be reviewed.

2.1 Overview of Spectrum Sensing

There are two main objectives of spectrum sensing. The first one is to prevent the primary users from harmful interference from the secondary users. So, the interference caused by secondary users should be limited at an acceptable level. The second objective is to efficiently identify the white spaces which can be exploited by the secondary networks to improve the network throughput and meet the requirement of the QoS.

The performance of the spectrum sensing is generally evaluated by probability of false alarm (p_{FA}) and probability of detection (p_D) or probability of missed detection (p_{MD}), which equals 1- p_D. A false alarm indicates that the cognitive radio declares the presence of primary signals when they are actually absent. A missed detection indicates that the cognitive radio declares the absence of primary signals when they are indeed present. In case of false alarms, some of the white spaces in the target primary channel will be wasted, and so, the performance of the secondary network will be degraded. On the other hand, in case of missed detections, the secondary users will communicate on the target primary channel, which will cause serious interference to the primary users and adversely impact the performance of primary networks. Therefore, a good spectrum sensing should try to minimize the probability of false alarm and maximize the probability of detection.

However, the spectrum sensing method cannot improve the probability of detection arbitrarily high and decrease the probability of false alarm arbitrarily low at the same time. In general, if the probability of detection is too high, to some extent, the probability of false alarm will become higher, and vise versa. Therefore, the probability of detection is tried to be improved as high as possible while to keep the probability of false alarm to a target value.

2.1.1 Spectrum Sensing Techniques

As it is mentioned before, one of the most important components of cognitive radio is the ability to measure, sense, learn, and be aware of parameters related to characteristics of primary channels, the availability of primary spectrum band, the radio's operating environment, and the QoS of the secondary users [17, 27]. Thus, the spectrum sensing is the fundamental components of cognitive radio since it can enable the cognitive radio to adapt its operating environment.

There are two categories of primary signal detection: primary transmitter detection and primary receiver detection. Obviously, the most effective way to detect the primary signals in the primary band is to detect the emitted signal by the primary receivers that are receiving data within the sensing range of the cognitive radios [28]. However, the emitted signal power from the primary receiver is usually too weak to be measured.

Currently, the primary receiver detection is only feasible in the detection of TV receivers [29]. Therefore, most of the existing spectrum sensing schemes focus on the primary transmitter detection, i.e., the detection of primary signals emitted from the primary transmitters.

The primary transmitter detection can mainly be divided into two categories: non-coherent techniques and coherent techniques. The well-known non-coherent spectrum sensing techniques include energy detection, covariance-based detection, eigenvalue-based detection, etc. The typical coherent spectrum sensing techniques contain matched filter detection, cyclostationary detection, wavelet detection, and so on. The classification of spectrum sensing techniques is shown in Figure 2-1. In the following, such typical and well known spectrum sensing techniques will be briefly introduced.

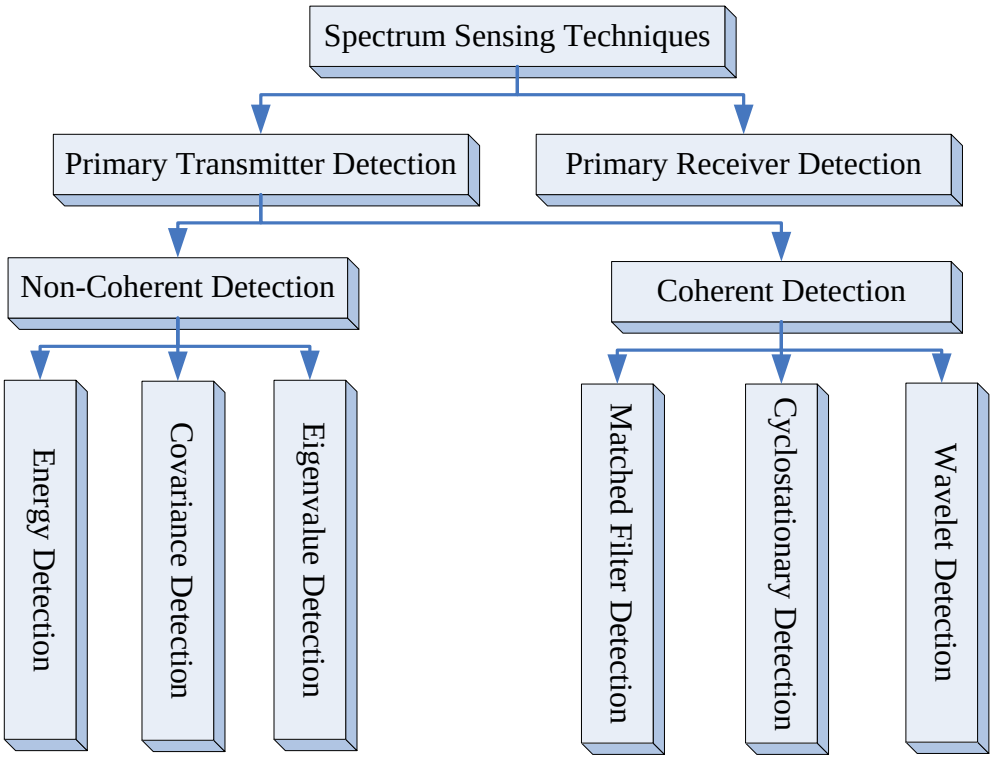

Figure 2-1 Categories of spectrum sensing techniques

2.1.1.1 Energy Detection

Energy detection is a non-coherent detection method. If the knowledge of primary

signals is unknown, the energy detection method is optimal for detecting any zero-mean constellation signals [30]. In energy detection, the signal energy emitted from the radio-frequency front-end of the primary transmitters or the received signal strength indicator is measured by the cognitive secondary users to determine whether the primary signals are present or not. This process can be summarized by the following steps. First, the input signal is filtered by a band-pass filter to select the frequency range of interest. Second, the output signal from the band-pass filter is squared and integrated over the observation interval, which can be either in time domain or in frequency domain. Third, the output of the integrator is compared to a predefined threshold to infer the presence or absence of the primary signals. When the spectral is analyzed in the digital domain, fast Fourier transform (FFT) based method should be utilized. For example, if the received signal $X(t)$, sampled in a time window, is first passed through an FFT device to get the spectral $|X(f)|^2$. The peak of the power spectral is then located. After windowing the peak of the spectrum, we can get $|Y(f)|^2$. The signal energy can be collected in the frequency domain [17].

Due to its simplicity and on requirement on a prior knowledge of primary signals, energy detection is the most popular technique [1]. However, energy detection has several shortcomings. First, it has poor performance under low signal to interference-plus-noise radio (SINR) condition. Second, it cannot differentiate primary signals from secondary signals. As a result, cognitive radio users need to be tightly synchronized and refrain from transmission during an interval called quiet period in cooperative spectrum sensing, which will be introduced in the following context. Third, the detection performance is subject to the uncertainty of the interference and background noise power. In spite of such problems, energy detection still be the most common used mechanism in cooperative sensing because some of the issues such as the performance degradation due to the uncertainty of interference and noise can be mitigated by the diversity gain resulting from cooperation [1]. Furthermore, the proposed power decomposition method is believed to be able to differentiate the target primary signals from the inter-channel interference and to decrease the uncertainty of interference and noise.

2.1.1.2 Covariance Detection

In general, the statistical covariance matrices or autocorrelations of the signal and noise are different. Considering this fact, a covariance detection method was proposed in [31, 32]. In covariance detection, the off-diagonal elements of the covariance matrix of the received signals are observed. If the off-diagonal elements are zero, it declares that the primary signals are absent; otherwise, they are inferred to be present. Specially, the statistical covariance of the noise is determined by the receiving filter. Therefore, its structure is known to the receiving. By using the same structure of the receiving filter, the covariance of the primary signal can be turned into another matrix. When there is no primary signal, the off-diagonal elements are zeros. However, when the primary signals are present, some of the off-diagonal elements in the resulting matrix are non-zeros. Based on this property, the off-diagonal elements in the covariance matrix resulted from the structure of receiving filter can be used to compare with that of the transformed matrix to determine the presence or absence of the primary signals.

2.1.1.3 Eigenvalue Detection

Eigenvalue detection is based on the covariance detection and was proposed or used in [33-39]. By applying eigen-decomposition of the covariance matrix, the eigenvalues can be achieved. Many detection schemes are proposed based on the eigenvalue detection. For example, the maximum-minimum eigenvalue detection [34] and the maximum eigenvalue detection [39]. The essence of the eigenvalue detection lies in the significant difference of the eigenvalue of the variance of the received signal when the primary signal is present or absent [17].

2.1.1.4 Matched Filter Detection

Matched filter detection is a type of coherent detection methods and was used in [40-43]. When the prior knowledge of the primary signal is known to the cognitive secondary users, the optimal detector in the stationary Gaussian noise is the matched filter detection because it is able to maximize the received SNR [30]. A matched filter is obtained by correlating a known signal or its template with an known signal to detect

the presence of the template in the unknown signal. In essential, it is equivalent to convolving the unknown signal with a time-reversed version of the template [17]. While the main advantage of the matched filter detection is that it needs less time to achieve higher process gain due to the coherency, its significant shortcoming is that it requires a dedicated sensing receiver for all primary signal types, which should have the prior knowledge of the primary signal such as the modulation type and order, the pulse shape, and the packet format [1, 17, 30]. Therefore, if such information of the primary signal is unknown or inaccurate, the matched filter detection cannot be used or its performance becomes very poor. The use of this method is still possible if partial information of the primary signal is known for cognitive secondary users for coherent detection. Such information includes pilot, preambles, synchronization word or spreading codes [1, 17, 44].

2.1.1.5 Cyclostationary Detection

Cyclostationary detection [45-52] is also a coherent detection. If the primary signals exhibit strong cyclostationary properties, it can be detected at very low SINR values by exploiting the cyclostationary featured information embedded in the received signal by the cognitive secondary user. If the autocorrelation of a signal is a periodic function of time *t* with some period, the signal is said to be cyclostationary. In general, the modulated signals are coupled with sine wave carriers, pulse trains, repeating spreading, hopping sequences, or cyclic prefixes, which usually lead to built-in periodicity and are generally cyclostationary signals. The cyclostationary detection can be performed as follows [17]. First, the cyclic autocorrelation function of the observed signal $x(t)$ is calculated as $E\left\{x(t+\tau)\cdot x^{*}(t-\tau)e^{-i2\pi\alpha t}\right\}$, where $E\{\cdot\}$ denotes the operation of the statistical expectation and α is the cyclic frequency. Second, the spectral correlation function $S(f,\alpha)$ can be obtained from discrete Fourier transformation of the cyclic autocorrelation function. Obviously, the spectrum correlation function is a two-dimension function in terms of frequency f and the cyclic frequency α. Third, the detection is completed by searching for the unique cyclic frequency corresponding to the peak in the spectral correlation function.

The significant advantage of spectral correlation function is that it is able to differentiate the noise energy from the modulated signal energy since the noise can be treated as a wide-sense stationary signal with no correlation while the modulated signal is cyclostationary with spectral correlation due to the embedded redundancy of signal periodicity [15]. Therefore, the cyclostationary detection is robust to random noise and interference from other modulated signals since the noise has only a peak of spectral correlation function when the cyclic frequency equals zero and other different modulated signals have different cyclic frequencies from that of target signal.

In [47], the cyclostationary detection is employed to detection primary signals in 802.22 applications, i.e., the advanced television systems committee (ATSC) DTV signals in wireless regional area networks (WRAN). The experimental results show that it can achieve superior detection performance even in very low SINR region.

Besides, the cyclostationary detection is able to detect the primary signals from other secondary signals over the same frequency band provided that the cyclic features of primary signals and secondary signals are different from each other. In general, the precondition is true since different wireless systems usually utilize different signal structures and parameters. For example, when the primary users work in a GSM network while the secondary users work in an OFDM-based WLAN, the information of channel allocation can be extracted, which has been implemented in spectrum pooling systems based on the difference between the cyclostationary characteristics of primary signals and secondary signals [52].

However, the disadvantage of cyclostationary detection lies in the fact that it requires high computational complexity and significantly long observation time.

2.1.1.6 Wavelet Detection

Wavelet detection [53-58] is also a non-coherent detection method. In wavelet detection, the wavelet transform of the power spectral of the received signals is explored. Wavelet transform is a multi-resolution analysis mechanism where an input signal is decomposed into different frequency components. Then, each component is investigated with resolutions matched to its scales. Different from Fourier transform which uses regularly shaped waves such as sine and cosines as basic functions, the wavelet

transform employs irregularly shaped wavelets as basic functions and thus can offer better tools to represent shape change and local features [17, 54]. For signal detection over wide band channels, the wavelet approach is able to provide lower implementation cost and higher flexibility in adapting to dynamic spectrum access, compared to the conventional use of multiple narrow band bandpass filters [17, 53]. To identify the locations of vacant frequency bands, the entire wide-band is modeled as a chain of consecutive frequency sub-bands. In this case, the power spectral characteristic is smooth within each sub-band but changes abruptly on the border of two neighboring sub-bands. By taking the wavelet transformation of the power spectral density (PSD) of the received signal $x(t)$, the singularities of the power spectral density $S(f)$ can be located and thus the vacant frequency band can be identified. However, there is a crucial challenge when the wavelet detection is performed, i.e., the high sampling rates for characterizing the wide bandwidth. To address this problem, a dual-stage spectrum sensing algorithm is proposed in [58]. In their scheme, the wavelet transformation-based detection is employed as a coarse sensing stage and a temporal signature detection is explored as a fine sensing stage.

2.1.2 Cooperative Spectrum Sensing

Generally, the performance of the spectrum sensing is compromised by many practical factors such as multi-path fading, shadowing, and the receiver uncertainty problem. Such factors can be illustrated in Figure 2-2. CR1, CR2, and CR3 are in the transmission range of the primary transmitter, while CR4 is outside of it. As it is shown in this figure, CR1 suffers from multi-path fading; CR2 suffers from shadowing; and CR4 suffers from receiver uncertainty. Therefore, the sensing results from CR1, CR2, and CR4 are not reliable and will easily incur false alarm and missed detection. However, it is unlikely for all spatially distributed CR users to concurrently experience multi-path fading, shadowing, or receiver uncertainty. If CR users, most of which can observe strong primary signals like the CR3 in Figure 2-2, can cooperate and share their sensing results with other users, the combined cooperative sensing result derived from spatially distributed CR users can overcome the deficiency of individual CR users. And thus, the sensing performance can be significantly improved. The cooperative spectrum

sensing has become very attractive to cope with multi-path fading, shadowing, and receiver uncertainty. Also, this dissertation focuses on cooperative spectrum sensing. In addition, only energy detection is considered in the cooperative spectrum sensing in this dissertation.

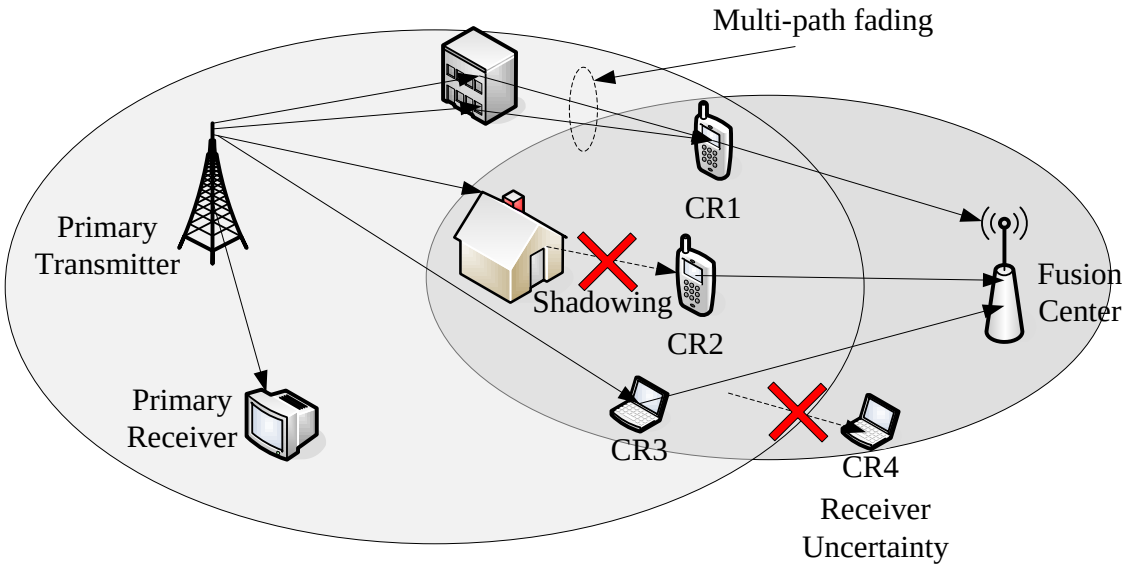

Figure 2-2 Cooperative SS with Fading, Shadowing, and Receiver Uncertainty

2.1.2.1 Model of Cooperative Spectrum Sensing

In spectrum sensing, multi-path fading, shadowing, and receiver uncertainty, corresponding to CR1, CR2, and CR4, respectively in Figure 2-2, are the most crucial challenges. The cognitive users suffering such three factors are referred to hidden terminal problem [17]. As it is mentioned before, cooperative spectrum sensing can be used to address this problem [59-69]. It has been shown in [64] that the cooperative spectrum sensing can significantly improve the probability of detection in fading channels. In general, cooperative spectrum sensing contains three steps:

1) Each cognitive radio performs its own local spectrum sensing individually.

2) The cognitive radio transmits the sensing result to its affiliated fusion center (FC).

3) The fusion makes final decision whether the primary signal is present or not.

Depending on the transmitted data on step 2, the cooperative spectrum sensing can

be divided into two groups: hard combing and soft combining. If the transmitted data on step 2 is the binary decision made by each cognitive radio on step 1, the combining method in the cooperative spectrum sensing is referred to hard combing. Instead, if the cognitive radio does not make any decision, but, transmits the raw measured data to the fusion center, and the fusion center makes the final decision according the raw data collected by cognitive radios, the combing method for cooperative spectrum sensing is called soft combing. Obviously, the soft combing can be treated as an amplify-and-forward protocol in cooperative networks. The hard combing requires less bandwidth of the reporting channel, which is defined as the channel used to transmit raw data (or locale decision results) to the fusion center. On the contrary, the soft combing will need much more bandwidth of the reporting channel.

It can be seen that cooperative spectrum sensing involves two successive channels: sensing channel, i.e., the target primary channel from the primary transmitter to the cognitive radio, and the reporting channel. As it is stated before, the cooperative spectrum sensing is able to achieve spatial diversity gain due to the multiple spatially distributed cognitive radios. Moreover, the cooperative spectrum sensing can achieve mutual benefit brought forward by communicating with each other to improve the performance of spectrum sensing [17, 59]. For example, when a cognitive radio is far from the primary transmitter, the received signal may be too weak to make a reliable detection. In this case, if there is a cognitive radio near to the primary radio and in the communication range of the far cognitive radio, the near one can work as a relay to forward its sensed data to the far cognitive radio, which can make reliable detection.

2.1.2.2 Performance Analysis

The analysis of local spectrum sensing and cooperative spectrum sensing will be presented in this subsection, respectively.

1) *Local spectrum sensing*. The essence of the local spectrum sensing can be modeled by a binary hypothesis-testing problem:

H_0 : Primary signal is **absent** in the target sensing channel
H_0 : Primary signal is **present** in the target sensing channel

Then, the above mentioned evaluation metrics can be defined as follows. The probability of false alarm and the probability of false alarm are $prob\{Decision = H_1 | H_0\}$ and $prob\{Decision = H_0 | H_1\}$, respectively. As a result, the probability of correct detection is $1 - prob\{Decision = H_0 | H_1\}$.

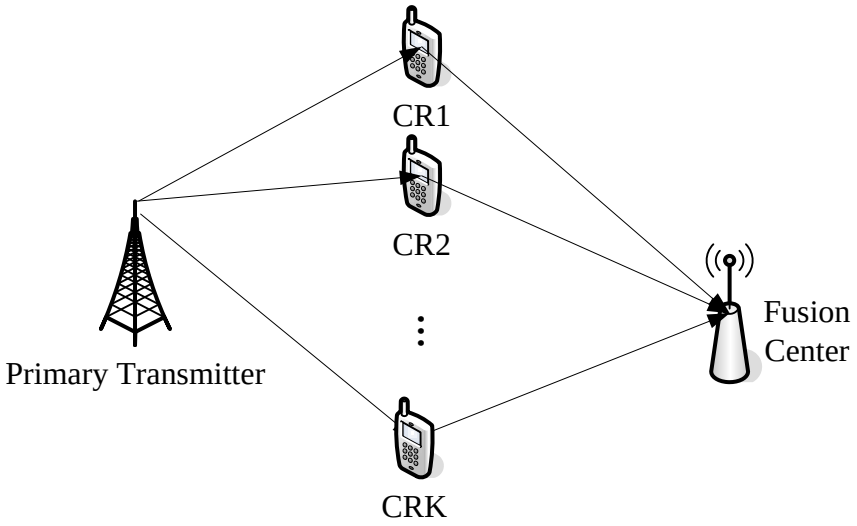

Figure 2-3 A Typical Structure of Cooperative Spectrum Sensing

A typical structure of cooperative spectrum sensing is shown in Figure 2-3. In this structure, only K cognitive radios and a fusion center are considered. The cognitive secondary network is managed by the fusion center. The fusion center sends instructions to the cognitive radios to tell them to sense which primary channel. In order to clearly show how the energy detector works, only the ith cognitive radio is focused on in the following. The local spectrum sensing for the ith cognitive radio to determine whether the primary signal is present or not is to select between the two hypothesizes:

$$r_i(t) = \begin{cases} n_i(t), & for\ H_0 \\ h_i s(t) + n_i(t), & for\ H_1 \end{cases} \tag{2.1}$$

Where $r_i(t)$ is the received signal at the ith cognitive radio, $s(t)$ is the primary transmitted signal, $n_i(t)$ is the additive white Gaussian noise (AWGN), and h_i is the complex channel gain of the target sensing channel between the primary transmitter and the ith cognitive radio. Here, the co-channel and inter-channel interference is not

considered, and the sensing channel is assumed to be time-invariant during the sensing process.

The energy detection can be performed in either time domain or frequency domain. If it is performed in time domain, the power should be measured in the frequency range of the target sensing channel. The collection of samples of the output of the bandpass filter applied to the target signal is measured as the sensing metric. If it is performed in frequency domain, the time-domain signal should be transformed to frequency domain using FFT. The collection of the samples in the range of target sensing channel is measured as the sensing metric. Here, we only take the frequency-domain detection as an example.

In frequency-domain energy detection, the energy of the received signal $r_i(t)$ is measured in a fixed bandwidth W over an observation time window T. If the energy collected in the frequency domain is denoted by E_i, which serves as the decision statistic, E_i can be modeled by the following distribution [17, 69-72]:

$$E_i \sim \begin{cases} \chi^2_{2u}, & for\ H_0 \\ \chi^2_{2u}(2\gamma_i), & for\ H_1 \end{cases} \tag{2.2}$$

Where χ^2_{2u} stands for a central chi-square distribution with $2u$ degrees of freedom and $\chi^2_{2u}(2\gamma_i)$ stands for a non-central chi-square distribution with $2u$ degrees of freedom and a non-centrality parameter $2\gamma_i$, respectively. The instantaneous SNR of the received signal at the ith cognitive radio is γ_i, and the time-bandwidth product is $u = TW$. The decision of energy detection is made by comparing E_i with a predefined threshold λ_i. Then, the probability of false alarm, the probability of detection, and probability of missed detection can be represented respectively as:

$$p_f^i = prob\{E_i > \lambda_i | H_0\} \tag{2.3}$$

$$p_d^i = prob\left\{E_i > \lambda_i \middle| H_1\right\} \tag{2.4}$$

$$p_{md}^i = prob\left\{E_i < \lambda_i \middle| H_1\right\} = 1 - p_d^i \tag{2.5}$$

Over the Rayleigh fading channels, the three above evaluation metrics have been derived in a closed-form in [72] and can be given respectively by:

$$p_f^i = \frac{\Gamma\left(u, \frac{\lambda_i}{2}\right)}{\Gamma(u)} \tag{2.6}$$

$$p_d^i = e^{-\frac{\lambda_i}{2}} \sum_{p=0}^{u-2} \frac{1}{p!}\left(\frac{\lambda_i}{2}\right)^p + \left(\frac{1+\overline{\gamma_i}}{\overline{\gamma_i}}\right)^{u-1}\left[e^{-\frac{\lambda_i}{2\left(1+\overline{\gamma_i}\right)}} - e^{-\frac{\lambda_i}{2}} \sum_{p=0}^{u-2} \frac{1}{p!}\left(\frac{\lambda_i \overline{\gamma_i}}{2\left(1+\overline{\gamma_i}\right)}\right)^p\right] \tag{2.7}$$

$$p_{md}^i = 1 - p_d^i \tag{2.8}$$

Where $\overline{\gamma_i}$ denotes the average SNR at the *ith* cognitive radio, $\Gamma(a,x)$ is the incomplete gamma function given by:

$$\Gamma(a,x) = \int_x^{+\infty} t^{a-1} e^{-t} dt \tag{2.9}$$

And $\Gamma(a)$ is the gamma function.

The energy detection performance of one cognitive radio usually gets worse, i.e., the probability of false alarm significantly increase and the probability of detection becomes decrease when the SNR is low. Such case usually occurs when heaving fading or shadowing is encountered. In such a scenario, the cooperative spectrum sensing can be used to improve the sensing performance with the help of multiple cognitive users [17, 61, 64].

2) *Cooperative spectrum sensing*.

As it is shown before, compared to local spectrum sensing, cooperative spectrum sensing involves two addition operations: cooperative user selection and data fusion. Both of them play important roles in determining the performance of cooperative

spectrum sensing.

User selection. It can be utilized to improve the cooperative gain and address the hidden terminal problem in cooperative spectrum sensing. For example, when some of the cognitive user experience multi-path fading, shadowing, or receiver uncertainty, as it is shown in Figure 2-2, it is shown in [60] that selecting independent cognitive users is able to improve the robustness of the sensing. Moreover, removing malicious users from cooperation ensures the security and the reliability of the network [1]. In the previous literature, there are two kinds of user selection method to address overhead issues such as correlated shadowing, cooperation efficiency, security, energy, and mobility: centralized user selection and cluster based user selection

In centralized scheme, cooperative users are selected by the fusion center. In this case, the fusion center is able to collect the information about the sensing channel from the cognitive radio users among their coordination. For example, fusion center can select independent users for cooperation to cope with the effect of correlated shadowing based on the location estimation of the cognitive users. In [73], three user selection algorithms with different degrees of knowledge of cognitive radio user positions are proposed for cooperative sensing to cope with the correlated shadowing in cellular systems. The first algorithm is taken to be briefly introduced here. It is to find a set of cooperation users with the minimum correlation measure through a greedy approach. In this algorithm, users with the largest summed correlation are removed one at a time until the desired number of cognitive users for cooperation is reached. Based on the knowledge of user locations, the correlation can be estimated from the distances between two cognitive users. In all the three algorithms proposed in [73], the cognitive users should be partitioned into two categories: uncorrelated users and correlated users. The complexity is evaluated by two bounds: sphere packing upper bound and random selection lower bound. The upper bound indicates the maximum number of users that experience uncorrelated shadowing in a cellular area. The lower bound is the expected number of randomly placed cognitive radio users in a cellular area.

Compared to centralized selection, which may incur higher overhead such as control channel bandwidth, energy efficiency, and reporting delay when the number of cognitive radio users needed to cooperate is large, the cluster-based selection is more

effective and is able to reduce the cooperation range and the incurred overhead by grouping the cooperating users into clusters [74-77] or coalitions [78]. For example, in [76], clustering is utilized to employ user selection diversity to improve the detection performance through reporting channels under Rayleigh fading. In each cluster, the cognitive radio user with the largest reporting channel gain is selected as the cluster head to decrease the reporting errors. The cluster head collects the local sensed data from the members of the cluster and forward the data to the fusion center [1]. The results show that this method outperforms the conventional cooperating sensing schemes.

When the user selection scheme is designed, cooperation footprint and the coordination overhead should be taken into account. The cooperation footprint refers to the area where the cognitive users cooperate with each other. As it is pointed out in [1], since cooperative gain is obtained from spatial diversity, cooperation footprint is an important parameter to evaluate the performance and the overhead in cooperative sensing. Thus, user selection schemes should consider the distribution of CR users and the area covered by their cooperation, not just the distance between the CR users. Obviously, the user selection is strongly related to every type of cooperative sensing overhead, among others, from control channel bandwidth, energy efficiency, to security issues. Therefore, there exists a tradeoff between the detection performance and the abovementioned overhead [1].

Data fusion. In cooperative spectrum sensing, data fusion refers to the process of local sensed data combination for finial decision. According to the bandwidth requirement of the reporting channel, the reported sensed data may have different forms, types, and sizes. As a result, as it is mentioned before, the data fusion can be performed in two ways: soft combing and hard combining.

Soft combining. There exist several diversity techniques that can be utilized for soft combination of local sensed data, for example, the equal gain combination and the maximal ratio combination. In [79], an optimal soft combination scheme based on NP criterion is proposed to combine the weighted local sensed data. The proposed scheme reduces to equal gain combination at high SNR and reduces to maximal ratio combination at low SNR. Since such a soft combining scheme results in large overhead,

a softened two-bit hard combining scheme is also proposed in [79] for energy detection. In this method, there are three decision thresholds dividing the whole range of test statistics into four regions. Each CR user reports the quantized two-bit information of its local test statistics. This method shows the comparable performance with the EGC scheme with less complexity and overhead.

Hard combing. In cooperative spectrum sensing, each cognitive radio makes local decision independently on whether the primary signal is present or not. Such a local decision is only based on its local sensed data without neither exchanging data nor cooperating with other cognitive radios. Then, such binary local decision results are forwarded to the fusion center, which makes final decision to infer the presence or absence of the primary signal according to different combination rules. If $D_i \in \{0,1\}$ is utilized to denote the local sensing result of the *ith* cognitive radio, where $\{0\}$ denotes the cognitive radio infers the absence of the primary signal in the target sensing band while $\{1\}$ indicate that the cognitive radio infers the presence of the primary signal in the sensed band, the collected local sensed data from each cognitive radio by the fusion center can be fused together by the following fusion rule:

$$decision = \begin{cases} \mathcal{H}_1, & \sum_{i=1}^{K} D_i \geq n \\ \mathcal{H}_0, & \sum_{i=1}^{K} D_i < n \end{cases} \tag{2.10}$$

Where $\mathcal{H}_1$ and $\mathcal{H}_0$ denote the final decision made by the fusion center that the primary signal is present and absent, respectively. (2.10) clearly shows that the fusion center determine the primary signal being transmitted, i.e., $\mathcal{H}_1$, when there exists at least n out of K cognitive radio users determining H_1. Otherwise, the fusion center makes a decision that the primary signal is not being transmitted, i.e., $\mathcal{H}_0$. The mentioned "AND" rule and "OR" rule in the many literature corresponds to the $n = K$ and $n = 1$, respectively. For the "OR" rule, the fusion center determines the primary

signal being transmitted as long as at least one cognitive radio user making the decision H_1. Therefore, it is conservative for the cognitive users to utilize the target primary spectrum band. As a result, the chances of interfering with the primary users can be minimized. It has been found in [62] that for many practical cases, "OR" rule is the best among the fusion rules.

The probability of false alarm in cooperative spectrum sensing based on the "OR" rule can be derived by:

$$Q_f = 1 - \prod_{i=1}^{K} \left(1 - p_f^i\right) \tag{2.11}$$

Where p_f^i is the probability of false alarm of the ith cognitive radio user in its local spectrum sensing, and can be obtained from (2.6) under Rayleigh fading channel.

Similarly, the probability of missed detection can also be easily derived:

$$Q_{md} = \prod_{i=1}^{K} p_{md}^i \tag{2.12}$$

Where p_{md}^i denotes the probability of missed detection of the ith cognitive radio user in its local spectrum sensing, and can be obtained from (2.8) under Rayleigh fading channel.

When the data fusion is conducted, some practical issues should be carefully considered. For example, there exist tradeoffs between sensing duration and performance, and between cooperation and sensing, respectively. A longer sensing duration is able to achieve a better sensing performance but lead to longer waiting time for cognitive radio to access the target primary channel for data transmission, which undoubtedly decrease the throughput and increase the delay of the cognitive secondary network. Such a phenomenon cannot be tolerated in some applications such as real time phones. Therefore, such practical issues should be considered when devise the cooperative spectrum sensing schemes.

2.2 Overview of MAC Protocols for Cognitive WMNs

As we know, the medium access control (MAC) has three main functions. First, it provides an interface between physical layer and higher layer protocols to interpret bit stream and convert them into packets and vice versa. Second, MAC has to coordinate the transmission and reception of packets among multiple nodes in order to improve the network performance. Third, MAC has to provide error control function to decrease the packet errors.

Different from the MAC for wired networks, the key task of wireless networks such as WMN is to coordinate the process of sharing the same medium among multiple users to improve the network throughput and satisfy the QoS requirements such as end-to-end delay, delay jitter, and packet loss rate. As it is mentioned in Chapter 1 the unique feature of WMNs such as the network topology should be taken into account when designing the MAC protocols. It is more challenging than the designing the MAC protocol in single hop wireless networks such as cellular networks and WLAN.

When designing the MAC protocol for WMNs, the following component should be carefully considered.

1. *Packet processing and queuing for both transmission and reception*. It is the interface between MAC layer and the upper layer protocols.

2. *Coordination of medium access*. It is the most important component of a MAC protocol, which involves many different tasks depending on the type of MAC protocols to be designed. Specially, for WMNs, most of the designs of MAC protocols are based on the widely used random access MAC protocol such as carrier sense multiple access with collision avoidance (CSMA/CA). Therefore, it is taken for an example. The key issue of CSMA/CA is to find out the best solution for minimizing collision and fast recovery when it is still happens. Since there is no available reservation, collision becomes serious when the number of users need to be coordinated becomes large. Moreover, because of the use of exponentially backoff mechanism, the contention time will become increasingly high when collision occurs frequently. As a result, it is difficult to ensure a required QoS for such a MAC protocol. However, random access

protocol has two main advantages. The first advantage is its simplicity i.e., it does not require separate signaling and reservation in the protocol. The second advantage is its compatibility with the connectionless networks such as the Internet. However, the reservation based MAC protocols such as time division multiple access (TDMA), code division multiple access (CDMA), always has the problem of integration with a connectionless network.

3. *Adaptive rate control*. To better utilize the capability of adaptive coding and modulation in the physical layer in many current wireless networks, the MAC protocol should consider the adaptive rate control for packet transmissions.

4. *Network formation and association*. This component is actually the network management part for a MAC protocol and is particularly important for WMNs. Without this information, the nodes in WMNs cannot recognize each other and accordingly start the MAC protocol.

According to the number of radios equipped on the nodes in the WMNs and the number of operating channels, the MAC protocols for WMNs can be categorized into three groups: single radio single channel (SRSC) MAC, single radio multiple channel (SRMC) MAC, and multiple radio multiple channel MAC (M2MAC). All of these three groups will be briefly overviewed in the following context.

2.2.1 SRSC MAC Protocols

Single radio single channel MAC protocol is the most common MAC protocol in WMNs. Various SRSC MAC protocols have been proposed. According to their characteristics, SRSC MAC protocols can be divided into the following types: modification of CSMA/CA [80-83], TDMA over CSMA/CA [84], IEEE 802.16 MAC in mesh mode [85], MAC for ultra-wideband (UWB) WMNs [86], and CDMA MAC [87, 88]. In this subsection, only the first two types of MAC protocols will be introduced.

2.2.1.1 Modification of CSMA/CA

The most well-known SRSC MAC protocol is the CSMA/CA. It can be used in the ad hoc mode of IEEE 802.11 to form a meshed WLAN. There exist various schemes

based on the modified CSMA/CA in order to improve the performance of WMNs. The following are the typical modified schemes.

Adjust physical carrier sense. Two well known issues in CSMA/CA MAC are the hidden terminal problem and exposed terminal problem. When the sensing range of each node is too large, many mesh nodes become exposed nodes. On the contrary, when it is two small, some of them become hidden nodes. Some proposals for using dynamic carrier sensing range have been proposed in [83] in order to address the hidden and exposed problems. However, as it is pointed out in [8], how to develop a scheduling scheme for all node in WMNs to dynamically fine-tune the sensing range is still not resolved. For example, the widely accepted method to dynamically fine-tune the sensing range is to use directional antenna [82]. However, it usually leads to the partition of the network, the hidden and exposed terminal problems.

Improve virtual carrier sense. Virtual carrier sensing is able to effectively address the hidden terminal problem, but can lead to more exposed nodes. In order to deal with this problem, a directional virtual carrier sensing is proposed in [81]. It can ensure that the operation of virtual carrier sensing based on the request to send (RTS)/clear to send (CTS) matches the scenario when both directional and omni-antennas exist in the same work. Obviously, this scheme requires the topology information of the network.

Dynamic tuning of backoff procedure. The backoff procedure can be modified in different ways. First, instead of using the binary exponential backoff, other backoff can be utilized, although it is not recommended when the compatibility is considered [8]. The second way is to adjust the minimum and maximum size of the contention window for different nodes in WMNs. A similar scheme has been proposed in [80], the simulation results of which show that it can significantly improve the throughput of the networks.

2.2.1.2 TDMA over CSMA/CA

Instead of fine-tuning the parameters of CSMA/CA, a new system architecture is proposed in [84] to integrate TDMA with CSMA/CA. In this scheme, the software retransmission is proposed to disable the hardware level retransmission in an 802.11 MAC. Based on it, packet transmission and reception can be limited to a particular time

slot, and thus crossing slot-boundary can be avoided [8, 84]. In addition, a distributed scheme is developed to coordinate packet transmissions in different nodes in WMNs and the QoS is also considered in time slot allocation.

2.2.2 SRMC MAC Protocol

As we know, the interference range is much larger than the transmission range of a node. As a result, to avoid interference with each other, some of the nodes in the inference range but outside of the transmission range have to stop communicating. Thus, the time-spatial-reuse efficiency of a channel becomes low, which unavoidablely degrades the network performance. To address this problem, multiple orthogonal channels can be utilized in the same network. Actually, several of the existing standards can provide multiple orthogonal channels. For example, IEEE 802.11b/g can provide 3 orthogonal channels and the IEEE 802.11a can provide as many as 11 orthogonal channels. Obviously, employing multiple channels simultaneously for data transmission can significantly improve the network performance.

There are two ways of utilizing multiple orthogonal channels: equipping a mesh node with single radio (interface/transceiver) and multiple radios, respectively. For the first case, the radio should be switchable among multiple frequency bands. This subsection only involves the single radio case, and the multiple radios case will be left for the next subsection.

When multiple orthogonal channels are utilized in a network, the communication pairs (transmitter-receiver pairs) should be carefully designated to different channels to maximize the throughput and satisfy the QoS requirements since only the transmitter and the receiver in a communication pair operates in a same channel, can they exchange data. It is the task of the SRMC MAC. Many SRMC MAC protocols have been proposed in the previous literature, e.g., the multi-channel MAC [89] and the slotted seeded channel hopping MAC [90].

2.2.2.1 Multi-channel MAC

In fact, multi-channel MAC is proposed for ad hoc networks. However, since the

mobility is not taken into account, it is more suitable for WMNs [8]. Its objective is to solve the multi-channel hidden node problem when the IEEE 802.11 MAC is applied for multi-channel operation. The multi-channel MAC has an assumption, i.e., the underlying techniques of a wireless node are based on the IEEE 802.11 CSMA/CA protocol with the RTS/CTS mechanism.

In multi-channel MAC, the channel is selected according to the proposed preferable channel list. The channels are divided into three different preferable levels: high preference, medium preference, and low preference. The preference is determined by the traffic load in each channel. The higher the traffic load, the lower the preference. The traffic load of each channel is represented by the count of source-destination pairs that have been operating on each channel.

2.2.2.2 Slotted Seeded Channel Hopping (SSCH) MAC

Similar to the multi-channel MAC, SSCH also works on the top of IEEE 802.11 protocol, i.e., the CSMA/CA with RTS/CTS mechanism. SSCH has the following ideas. First, different channel hopping schedules are employed on different nodes in order to reduce the interference between these nodes as low as possible and to avoid the logical topology partition. Second, in order to coordinate different channel hopping schedules on different nodes, channel hopping is performed slot by slot. Same as the requirements in most time division schemes, the nodes in the WMN have to be strictly synchronized to perform this MAC scheme.

In SSCH, each node is assumed to be capable of hopping from one channel to another slot by slot. In order to avoid interference among communication pairs in a interference range, SSCH develops a random process with a unique seed to generate independent channel hopping schedules. It can be described as follows. Each node maintains four time slots with different channel hopping sequences. The channel hopping schedule is represented by the (channel, seed) pairs, denoted by (x_i, a_i), where the channel x_i is an integer in the range $[0,12]$ (13 possibilities), and the seed a_i is an integer in the range $[1,12]$. Each node iterates through all of the channels in the

current schedule, switching to the channel designated in the schedule in the next slot. The node then increments each of the channels in its schedule using the seed,

$$x_i \leftarrow (x_i + a_i) \bmod 13 \tag{2.13}$$

and repeats the process. In this case, the co-channel interference can be reduced as low as possible in the interference range. Simulation results in [90] show that SSCH is able to achieve better performance than the IEEE 802.11 MAC.

2.2.3 Multi-radio Multi-channel MAC (M2MAC)

Compared to the SRMC, M2MAC hare more freedom in resource allocation, which leads to at least two additional advantages. First, it does not need to switch the only single radio among multiple radios, which will simplify the design of the protocol and reduce the switching overhead (no switching delay). Second, compared with SRMC MAC, M2MAC can further improve the network capacity since the same node can transmit and receive data using different radios operating on different orthogonal channels.

The design of a M2MAC usually involves two aspects: how the channels are allocated on different radio and how the MAC protocol is designed. Although several previous literature focus on the latter case, e.g., the multi-channel unification protocol [91] and multi-radio two-phase protocol [92, 93], most of them including the proposed method in this dissertation focus on the first case. Therefore, such a case is briefly introduced in this sub-section.

The superimposed code is proposed in [94] for channel allocation by using a particular coding scheme. In this scheme, each node maintains a channel codeword indicating a set of primary and secondary channels of this node. Based on the information of the local node and its neighboring nodes, the channel allocated to this node is determined.

An interference-aware multi-radio MAC protocol is proposed in [95] to minimize the co-channel interference in the network. A multi-radio conflict graph is proposed to model the co-channel interference, then, a vertex coloring algorithm is applied to the

multi-radio conflict graph to figure out the channel allocation. However, this scheme designates one of the orthogonal channels as the common control channel, which also serves as the data channel. As a result, the designated channel will become the bottleneck and significantly degrade the performance of the network when the number of concurrent flows becomes large. Aiming to address this problem, a two-stage coordination M2MAC is proposed in this dissertation. The proposed M2MAC designates all in-band orthogonal channels as control channels, which is different from the conventional M2MAC protocols utilizing a single common control channel. The proposed two-stage M2MAC is able to improve the network performance especially when the number of concurrent flows becomes large. It will be presented in detail in Chapter 5

2.3 Conclusion

In this chapter, the well known spectrum sensing techniques and MAC protocols for cognitive wireless mesh networks are briefly overviewed. In the local spectrum sensing, the pros and cons of many techniques are analyzed and compared. Such techniques include energy detection, covariance detection, eigenvalue detection, cyclostationary detection, and wavelet detection. The implementation methods of such detections are introduced. In cooperative spectrum sensing, its implementation model and evaluation metrics are firstly introduced. Then, the implementation steps, pros, and cons of hard combing and soft combing are presented, respectively. Based on the hard combing, by using the "OR" rule, the performance is analyzed. In the review of MAC protocols of cognitive WMN, the typical single radio single channel MAC, single radio multiple channels MAC, and the multiple radios multiple channels MAC are briefly introduced. In addition, the advantages and disadvantages of such MAC protocols are analyzed and compared.

Chapter 3
Non-Coherent Power Decomposition-based Energy Detection for Cooperative Spectrum Sensing

As the fundamental component of dynamic spectrum access, implementing spectrum sensing is one of the most important goals in cognitive radio networks due to its key functions of protecting licensed primary users from harmful interference and identifying spectrum holes for the improvement of spectrum utilization. However, its performance is generally compromised by the interference from adjacent primary channels. To cope with such interference and improve detection performance, this chapter proposes a non-coherent power decomposition-based energy detection method for cooperative spectrum sensing. Due to its use of power decomposition, interference cancellation can be applied in energy detection. The proposed power decomposition does not require any prior knowledge of the primary signals. The power detection with its interference cancellation can be implemented indirectly by solving a non-homogeneous linear equation set with a coefficient matrix that involves only the distances between primary transmitters and cognitive secondary users (SUs). The optimal number of SUs for sensing a single channel and the number of channels that can be sensed simultaneously are also derived. The simulation results show that the proposed method is able to cope with the expected interference variation and achieve higher probability of detection and lower probability of false alarm than the conventional method in both hard combining and soft combining scenarios.

3.1 Introduction

Over the past few decades, the remarkable growth of wireless applications and the rapid development of wireless devices have been significantly aggravated the spectrum

scarcity. Meanwhile, the licensed spectrum bands for some systems have been shown to remain heavily underutilized. According to the Federal Communications Commission (FCC), utilization of the licensed spectrum ranges from 15% to 85% at different positions and times [1, 2, 15, 16]. Since it uses Dynamic Spectrum Access (DSA), cognitive radio (CR) has emerged to improve spectrum utilization by allowing cognitive Secondary Users (SUs) to share the unused or underutilized spectrum licensed for primary users (PUs) without causing harmful interference for the PUs [69, 96].

In cognitive radio technology, Spectrum Sensing (SS) is one of the essential components as it should be performed before DSA [69, 96-98]. The objective of SS is to efficiently detect the presence or absence of primary signals. The detection results are used by the SUs to determine whether they can access the primary spectrum and how long they can occupy this spectrum while limiting PU interference to an acceptable level [1]. Therefore, as the fundamental component of DSA, the performance of spectrum sensing is crucial to both primary and secondary networks.

Generally, the most effective way to detect the availability of the spectrum band is to detect signals emitted by the primary receivers that are receiving data within the sensing range of the SU. However, the signal power emitted by the receivers is typically too weak to be measured when noise uncertainty is considered. Therefore, most existing methods of SS, including the method proposed in this chapter, focus on the detection of primary transmitted signals [17, 99]—i.e., primary transmitter detection. In terms of signal detection, SS techniques for primary transmitter detection can be categorized into two groups: coherent and non-coherent detection. Coherent detection—e.g., cyclo-stationary feature-based detection [45, 100]—requires a prior knowledge of the characteristics of the primary signal [1]. In addition, its high computational complexity and long sensing time compromise the gain of its robustness for noise variation. In contrast, non-coherent detection—e.g., energy detection—does not require any prior knowledge and provides lower computational complexity and shorter sensing time. Due to its simplicity and the advantages listed above, energy detection is the most popular technique of SS [1, 29, 70, 72, 101]. However, in order to get better detection accuracy, two challenging issues must be addressed: the difficulty in differentiating the varying interference from background noise and the poor performance under a low Signal to Interference-plus-Noise Ratio (SINR) [1, 2, 101]. In an effort to address such challenges,

this chapter proposes a non-coherent power decomposition method for cooperative SS.

From the perspective of energy detection rather than signal demodulation, co-channel interference can be considered part of the signal, while inter-channel interference should be cancelled as much as possible, since it is harmful for the energy detection on the target primary channel. Generally, the received power at the cognitive SU can be regarded as a superposition of three parts: the signal power, the interference power from adjacent channels (inter-channel interference), and the background noise power. Obviously, if the superposition can be decomposed into the summation of individual parts—termed as power decomposition in this chapter—then the interference and background noise can be differentiated. Consequently, the SINR can be improved by subtracting the inter-channel interference from the superposition, also called interference cancellation in this chapter. It is different from the conventional coherent interference cancellation techniques which emphasize signal demodulation with lower BER. Compared to these techniques, the proposed power decomposition and the resulting interference cancellation method are non-coherent and simple to implement. The aim of the proposed method is to detect the presence or absence of the primary signals with higher accuracy. It can be implemented indirectly by solving a non-homogeneous linear equation set with a coefficient matrix that involves only the distances between primary transmitters and cognitive SUs. The specific features of the proposed method for spectrum sensing are as follows:

- A non-coherent power decomposition method is proposed for energy detection to individually decompose the power superposition consisting of signals, interference, and background noise. It does not require the prior knowledge of the primary signals.

- The resulting interference cancellation from the power decomposition is used to cope with the interference from adjacent primary channels.

- The optimal number of SUs for sensing a single channel and the number of channels that can be sensed simultaneously are derived in the power decomposition method.

- The collected energy multiplied by the corresponding SINR of the SU is

defined as the test statistic in order to further improve detection performance.

The rest of the chapter is organized as follows. In section 3.2, we describe the system model and performance analysis. Power decomposition and the resulting interference cancellation are presented in section 3.3. A simulation-based performance evaluation for the proposed method is illustrated in section 3.4. We discuss the impact of location inaccuracy on the power decomposition scheme in section 3.5 and present our conclusions in section 3.6.

3.2 System Model and Performance Analysis

3.2.1 System Model

A typical cognitive radio network is shown in Figure 3-1. We only consider primary transmitter detection; primary receiver detection is beyond the scope of this chapter. Without loss of generality, the main assumptions are as follows. The primary spectrum band is divided into M primary Additive White Gaussian Noise (AWGN) channels. There are Cj primary transmitters, denoted as $\{Tx(j,1), Tx(j,2),\cdots,Tx(j,Cj)\}$, operating on channel j, $j=(1,2,\cdots,M)$. The secondary network consists of K clusters of secondary users. In cluster i, $i=(1,2,\cdots,K)$, there are Ni secondary cognitive nodes denoted as $\{S(1,i), S(2,i),\cdots,S(Ni,i)\}$ including an Access Point (AP) which also functions as the combination and decision making node. We assume that each cluster as a whole conducts SS in one primary channel under instructions from the gateway. In addition, we assume that the gateway is able to obtain the number and locations of all primary transmitters operating on all primary channels by querying a remote database, as in [1, 102-105]. The essence of SS for a primary signal can be modeled as a binary hypothesis testing problem:

- H0: absence of target primary signals operating on the target-sensing channel
- H1: presence of target primary signals operating on the target-sensing channel

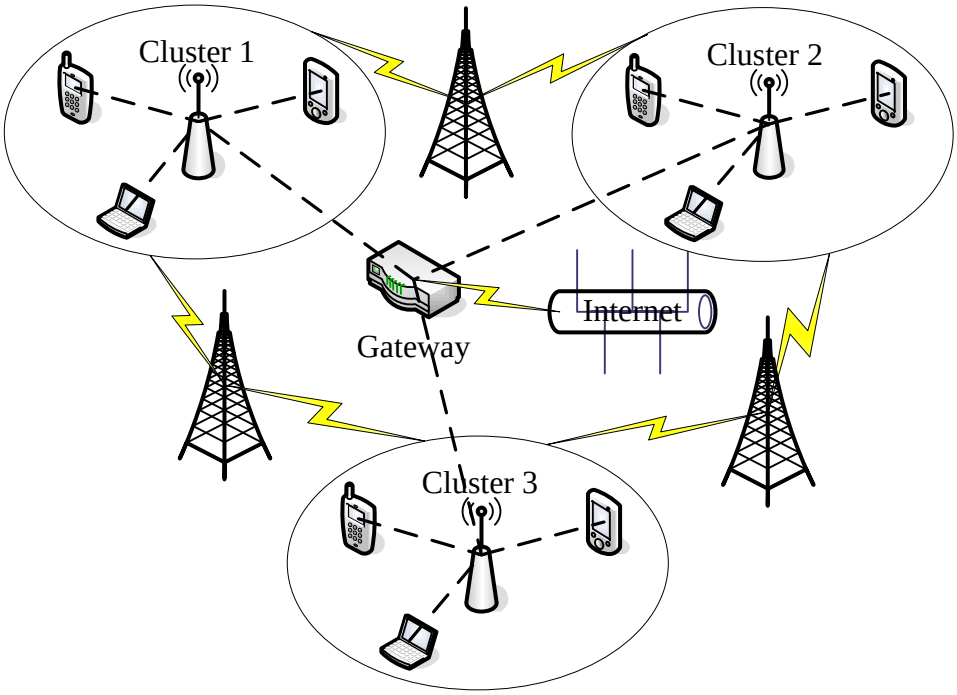

Figure 3-1 Architecture of a typical cognitive radio network

The general process of energy detection-based cooperative SS can be divided into three steps:

a) CRs in the network perform local energy measurement for SS;

b) CRs report their sensing results to their affiliated APs through the reporting channels, which are assumed in this chapter to be perfect;

c) APs combine the sensing results and reach the final decisions.

There are two types of combination in step c: hard combining (HC) and soft combining (SC) [1, 101]. In HC, each CR makes a local binary decision according to its measured data and reports it to its AP, which makes a cooperative decision regarding the presence or absence of primary signals; in SC, each CR reports the measured data, instead of the binary decision, to its AP. The AP combines such data in different ways, such as maximum ratio combination (MRC), and reaches a final decision indicating the absence or presence of the primary signals operating on the target sensing channels. Obviously, SC could achieve better detection performance, but it must occupy more bandwidth of the reporting channel, which will lead to higher overhead than that required by the HC [1]. In this chapter, we will demonstrate the performance

improvement in both HC and SC contributed by power decomposition and its concomitant interference cancellation.

3.2.2 Performance Improvement through Power Decomposition and Interference Cancellation

Motivated by the MRC, in order to more explicitly demonstrate the impact of the SINR on detection performance, the energy multiplied by the SINR of the SU is defined as a test statistic in energy detection. The energy detection performance is evaluated mainly using two metrics: probability of false alarm, $prob_f$, and probability of detection, $prob_d$. Assuming the decision threshold is λ, then $prob_f$ and $prob_d$ can be expressed as:

$$\begin{aligned} prob_f &= prob\left\{E \times SINR > \lambda \middle| H_0\right\} \\ prob_d &= prob\left\{E \times SINR > \lambda \middle| H_1\right\} \end{aligned} \tag{3.1}$$

A good detection method should try to: 1) decrease $prob_f$, since a false alarm will reduce utilization of the primary spectrum; and 2) increase $prob_d$, since a missed detection will cause interference with PUs.

If we use power to measure energy, then the total detected energy $E[S_j(c,i)]$ and the $SINR[S_j(c,i)]$ on channel j at the secondary node $S_j(c,i)$, $c=(1,2,\cdots,Ni)$ can be expressed by (3.2) and (3.3):

$$E\left[S_j(c,i)\right] = \alpha P_r\left[S_j(c,i)\right] + N + I\left[S_j(c,i)\right] \tag{3.2}$$

$$SNIR\left[S_j(c,i)\right] = \frac{\alpha P_r\left[S_j(c,i)\right]}{\left(N + I\left[S_j(c,i)\right]\right)} \tag{3.3}$$

Where $\alpha = 1$ when primary signals are present on the target-sensing channel and $\alpha = 0$ otherwise, $P_r[S_j(c,i)]$ and $I[S_j(c,i)]$ are, respectively, the signal power and the interference power received at $S_j(c,i)$; N is the background noise power, which is the same for all primary channels with same bandwidth at the same instant. We assume that N is given or can be estimated by noise sampling based on the environment of the network deployment, as in [96]. The SINR approaches zero when the primary signals

are absent. Thus, we demonstrate how power decomposition can simultaneously increase the probability of detection and decrease the probability of false alarm in both HC and SC.

In HC, each CR will make the local binary decision according to its measurement of the power. Such binary decisions are then reported to the affiliated AP for the final decision regarding the presence or absence of primary signals, using different combination rules such as AND, OR, or majority rules [1, 69]. Consequently, $prob_f$ and $prob_d$ for local binary decisions can be expressed by (3.4) and (3.5), respectively.

$$\begin{aligned} prob_f[HC] &= prob\left\{E\left[S_j(c,i)\right]\times SINR\left[S_j(c,i)\right] > \lambda \middle| H_0\right\} \\ &= prob\left\{\left(N + I\left[S_j(c,i)\right]\right)\times SINR\left[S_j(c,i)\right] > \lambda \middle| H_0\right\} \\ &\xrightarrow{SINR\to 0} 0 \end{aligned} \tag{3.4}$$

$$\begin{aligned} prob_d[HC] &= prob\left\{E\left[S_j(c,i)\right]\times SINR\left[S_j(c,i)\right] > \lambda \middle| H_1\right\} \\ &= prob\left\{\frac{P_r^2\left[S_j(c,i)\right]}{N + I\left[S_j(c,i)\right]} + P_r\left[S_j(c,i)\right] > \lambda\right\} \\ &< prob\left\{\frac{P_r^2\left[S_j(c,i)\right]}{N} + P_r\left[S_j(c,i)\right] > \lambda\right\} \end{aligned} \tag{3.5}$$

By using power decomposition, the signal power and interference power can be decomposed from the superposition of the receiving power at a cognitive SU $S_j(c,i)$. The absence of primary signals leads to the SINR's approach toward zero; thus, the probability of false alarm shown in (3.4) approaches zero. At the same time, formula (3.5) clearly indicates that removing the interference item $I[S_j(c,i)]$, also called interference cancellation, can increase the probability of detection. As a result, after HC, the final probabilities of false alarm and detection could be decreased and increased, respectively, regardless of the combination rule used.

In SC, CRs do not make any decision; instead, they report the measured data to the affiliated AP. The AP combines the data and reaches a final decision regarding the presence or absence of primary signals. If we assume that the decision threshold in SC is λ^*, then the probabilities of false alarm and detection can be described by (3.6) and

(3.7).

$$
\begin{aligned}
prob_f\left[SC\right] &= prob\left\{\frac{1}{N_c}\sum_{c=1}^{N_c}\left(E\left[S_j(c,i)\right]\times SINR\left[S_j(c,i)\right]\right) > \lambda^* \middle| H_0\right\} \\
&= prob\left\{\frac{1}{N_c}\sum_{c=1}^{N_c}\left(\left(N + I\left[S_j(c,i)\right]\right)\times SINR\left[S_j(c,i)\right]\right) > \lambda^* \middle| H_0\right\} \\
&\xrightarrow{SINR\to 0} 0
\end{aligned}
\tag{3.6}
$$

$$
\begin{aligned}
prob_d\left[SC\right] &= prob\left\{\frac{1}{N_c}\sum_{c=1}^{N_c}E\left[S_j(c,i)\right]\times SINR\left[S_j(c,i)\right] > \lambda^* \middle| H_1\right\} \\
&= prob\left\{\frac{1}{N_c}\sum_{c=1}^{N_c}\left(\frac{P_r^2\left[S_j(c,i)\right]}{N + I\left[S_j(c,i)\right]} + P_r\left[S_j(c,i)\right]\right) > \lambda^*\right\} \\
&< prob\left\{\frac{1}{N_c}\sum_{c=1}^{N_c}\left(\frac{P_r^2\left[S_j(c,i)\right]}{N} + P_r\left[S_j(c,i)\right]\right) > \lambda^*\right\}
\end{aligned}
\tag{3.7}
$$

Similar to HC, when SC is used, we can come to the same conclusion: that the probability of false alarm will approach zero after power decomposition due to the absence of primary signals, and the probability of detection will be increased by subtracting or removing the items $I[S_j(c,i)]$, $c=(1,2,\cdots,N_c)$.

Therefore, the above analysis shows that the power decomposition and the resulting interference cancellation are able to improve the detection performance of cooperative SS. In next section, we will discuss the implementation of the power decomposition and the concomitant interference cancellation.

3.3 Power Decomposition and Interference Cancellation

In this section, we will first introduce the model of interference from adjacent channels and the interference factor proposed in [106], after which we will present the proposed power composition and the resulting interference cancellation method. Finally, we will discuss problem solving and derive the optimal number of SUs for sensing a single channel, as well as the number of channels that can be sensed simultaneously for

a given cognitive radio network.

3.3.1 Model of Interference from Adjacent Channels

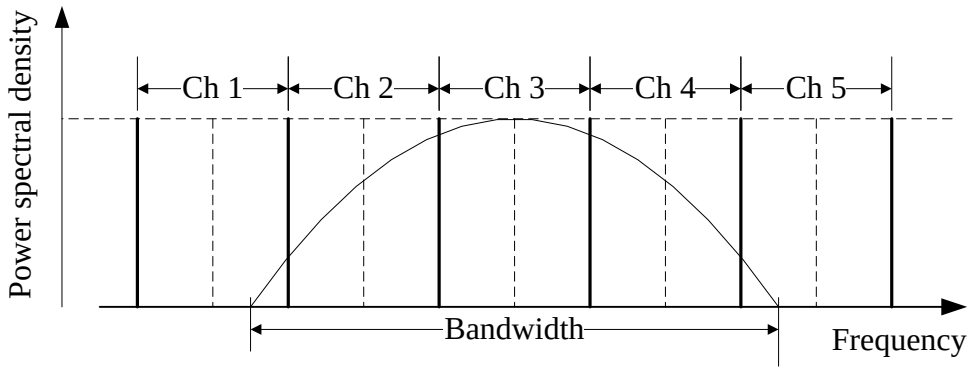

Figure 3-2 Interference from adjacent channels

Although a time-limited signal has a theoretically infinite power spectral in the frequency domain, most of its energy concentrates in a finite frequency range—i.e., the bandwidth. Generally, the licensed primary spectrum is always split into multiple channels in order to reduce the contention problem. If the bandwidth of the transmitted signals is wider than that of the channel, as it is shown in Figure 3-2, interference will be inevitable when transmissions over adjacent channels overlap in the time domain. For example, the incurred interference power on channel 2 (Ch. 2 in Figure 3-2) from the transmission on channel 3 (Ch. 3 in Figure 3-2) can be obtained by:

$$IF(3,2) = \int_{f_2-\frac{B}{2}}^{f_2+\frac{B}{2}} Tx(f)\,Fl(f-B)\,df \tag{3.8}$$

where *Tx(f)* is the Fourier transform of the transmitted signal, and *Fl(f)* is the impulse response of the band-pass filter with the same center frequency f_2 and bandwidth *B* as channel 2. A more general closed-form expression of obtaining the receiving power—i.e., the interference power on channel *v* produced by the transmitter on channel *u*—is derived in [19] by applying the two-ray ground model [107] as follows:

$$P_r = d^{-\beta}[r,tx]P^t I(u,v)\phi_c \tag{3.9}$$

$$\phi_c = G_t G_r h_t^2 h_r^2 \tag{3.10}$$

Where *d[r,tx]* is the distance between the transmitter and the receiver. G_t and G_r are the antenna gains of the transmitter and the receiver, respectively; h_t and h_r are the antenna heights of the transmitter and the receiver, respectively. Thus, ϕ_c is constant. β is typically between 2 and 4. *I(u,v)* is the interference factor, which can be obtained through power mask requirement [106], and *I(u,v)=1* when *u=v*. Although the interference factor is used in the derivation process of power decomposition, it is not necessary when power decomposition is performed.

3.3.2 Problem Formulation of Power Decomposition

The receiving power of a cognitive SU is a superposition of three parts: the signal power produced by the primary transmitters on the target-sensing channel, the interference power (leakage power) produced by primary transmitters operating in other primary channels, and the background noise power. As a result, to sense primary signals on channel *c*, the receiving power $p_{s(i,j)}$ at the j^{th} cognitive SU, and *s(i,j)* in cluster *i* can be expressed by (3.11):

$$p_{s(i,j)} = \sum_{m=1}^{M} pl_{s(i,j)}^{m} + N \tag{3.11}$$

where $pl_{s(i,j)}^{m}$ is the power leaked from channel *m* as expressed by (3.12)

$$pl_{s(i,j)}^{m} = \phi_c I(m,c) \sum_{\zeta=1}^{Cm} \left(d^{-\beta}\left[s(i,j), Tx(m,\zeta) \right] \times p^{t}\left[Tx(m,\zeta) \right] \right) \tag{3.12}$$

Each item of the summation in (3.12) is the leaked power from the transmitter $Tx(m,\zeta)$. If we let:

$$\vec{\mathbf{D}}\left[s(i,j), Tx(m) \right] = \left\{ d^{-\beta}\left[s(i,j), Tx(m,1) \right], \ldots, d^{-\beta}\left[s(i,j), Tx(m,Cm) \right] \right\} \tag{3.13}$$

And

$$\vec{\mathbf{p}}^{t}(m)=\phi_c I(m,c)\left\{p^{t}\left[Tx(m,1)\right],\ldots,p^{t}\left[Tx(m,Cm)\right]\right\} \tag{3.14}$$

Then $pl^{m}_{s(i,j)}$ can be rewritten in vector form as:

$$pl^{m}_{s(i,j)}=\vec{\mathbf{D}}\left[s(i,j),Tx(m)\right]\bullet\vec{\mathbf{p}}^{t}(m)^{\#} \tag{3.15}$$

where "#" is the transpose operator.

Moreover, let

$$\vec{\mathbf{D}}\left[s(i,j)\right]=\left\{\vec{\mathbf{D}}\left[s(i,j),Tx(1)\right],\ldots,\vec{\mathbf{D}}\left[s(i,j),Tx(M)\right]\right\} \tag{3.16}$$

And

$$\vec{\mathbf{p}}=\left\{\vec{\mathbf{p}}^{t}(1),\ldots,\vec{\mathbf{p}}^{t}(M)\right\} \tag{3.17}$$

Since the dimensions of the vector $\vec{\mathbf{D}}\left[s(i,j)\right]$ and the vector $\vec{\mathbf{p}}$ are equal to $n_d=\sum_{m=1}^{M}Cm$, $p_{s(i,j)}$ can be rewritten as:

$$p_{s(i,j)}=\vec{\mathbf{D}}\left[s(i,j)\right]\bullet\vec{\mathbf{p}}^{\#}+N \tag{3.18}$$

Note that $\vec{\mathbf{p}}$ has no relation to any cognitive SU. Therefore, the receiving power of other nodes can also be obtained from (3.18) with the same $\vec{\mathbf{p}}$ and different distance vectors. The receiving power of all cognitive SUs in the cluster *i* can be written in a matrix form:

$$\begin{bmatrix}\vec{\mathbf{D}}\left[s(i,1)\right]\\ \vec{\mathbf{D}}\left[s(i,2)\right]\\ \vdots\\ \vec{\mathbf{D}}\left[s(i,N_i)\right]\end{bmatrix}_{N_i\times n_d}\bullet\vec{\mathbf{p}}^{\#}=\begin{bmatrix}p_{s(i,1)}-N\\ p_{s(i,2)}-N\\ \vdots\\ p_{s(i,N_i)}-N\end{bmatrix} \tag{3.19}$$

(3.19) is a non-homogeneous linear equation set. The items of the coefficient matrix are the distances between the cognitive SUs in cluster *i* and the primary

transmitters on all primary channels. The items of the vector on the right side of the matrix equation are the differences between the total receiving power of cognitive SUs and the background noise power (recall that it is assumed or can be obtained as in [96]). $\vec{\mathbf{p}}$ can be solved from (3.19) when the coefficient matrix is given and adheres to some constraints, which will be discussed later.

Let

$$\vec{\mathbf{T}} = \{Tx(1,1),\ldots,Tx(1,C1),\ldots,Tx(M,1),\ldots,Tx(M,CM)\} \tag{3.20}$$

$$\alpha = \sum_{j=1}^{m-1} Cj \tag{3.21}$$

and use *p[l]* and *Tx[l]* to index the l^{th} factor of vectors $\vec{\mathbf{p}}$ and $\vec{\mathbf{T}}$, respectively; then, the part of the received power at *s(i,j)* produced by the transmitter *l* operating on the primary channel *m* can be extracted from the superposition of receiving power and can be expressed as:

$$p[Tx(m,l)] = p[l]d^{-\beta}[s(i,j),Tx(l)] \tag{3.22}$$

And the part of the received power at *s(i,j)* produced by all of the primary transmitters on channel *m* can be expressed as:

$$p_m = \sum_{l=\alpha+1}^{\alpha+Cm} p[l]d^{-\beta}[s(i,j),Tx(l)] \tag{3.23}$$

(3.22) and (3.23) clearly show that the part of power produced by each transmitter on any primary channel can be decomposed from the superposition of the receiving power. The received power produced by all of the transmitters operating on each primary channel can thereby be decomposed. If the target channel is *j*, and the signal power is p_j, the corresponding interference power can be expressed by:

$$I_p(j) = \sum_{m=1,m\neq j}^{M} p_m \tag{3.24}$$

Now, the task of power decomposition has been transformed into the need to solve the non-homogeneous linear equation set in (3.19), which will be analyzed in the next section.

3.3.3 Problem Solving

Since the positions of all primary transmitters on all channels are assumed to be known, the distance between each transmitter to all SUs can be easily calculated. Therefore, the coefficient matrix in (3.19) is known. According to the property of the non-homogeneous linear equation set, solving for $\vec{\mathbf{p}}$ is only related to the coefficient matrix. We can rewrite (3.19) in a simple form as:

$$\vec{\mathbf{D}}\left[s(i)\right] \bullet \vec{\mathbf{p}}^{\#} = \vec{\mathbf{p}}^{*}\left[s(i)\right] \tag{3.25}$$

Where $\vec{\mathbf{D}}\left[s(i)\right]$ and $\vec{\mathbf{p}}^{*}\left[s(i)\right]$ correspond to the coefficient matrix and the vector on the right side of (3.19), respectively. By fine-tuning the position of the SUs, the rank of the coefficient matrix can always satisfy:

$$rank\left\{\vec{\mathbf{D}}\left[s(i)\right]\right\} = \min\left(N_i, n_d\right) \tag{3.26}$$

As a result, the solution for the non-homogeneous linear equation set has the following three possible cases:

1) If $N_i < n_d$—i.e., the number of cognitive SUs is smaller than the number of primary transmitters—then the equation set only has a general solution rather than a unique solution vector. The general solution is a linear combination of a particular solution vector and $(n_d - Ni)$ basis vectors. This means that the powers produced by the primary transmitters cannot be decomposed from the superposition.

2) If $N_i = n_d$—i.e., the number of cognitive SUs is equal to the number of primary transmitters—then the equation set has a unique solution. In this case, the coefficient matrix in (3.25) is invertible, and the unique solution set can be solved as:

$$\vec{\mathbf{p}}^{\#} = \vec{\mathbf{D}}^{-1}\left[s(i)\right] \bullet \vec{\mathbf{p}}^{*}\left[s(i)\right] \tag{3.27}$$

The part of the power produced by each primary transmitter and that produced by the primary transmitters operating on each primary channel can be calculated by (3.22) and (3.23), respectively. Then the signal power and interference power on any primary channel can be obtained by (3.23) and (3.24), respectively.

3) If $N_i > n_d$—i.e., the number of cognitive SUs is larger than the number of primary transmitters—then the equation set becomes over-determined. In general, an over-determined equation set has no solution vector unless the equations are non-contradictive. However, we can select any *k*-order complementary minor $\vec{\mathbf{D}}^{*}$ with a rank equal to *k* from $\vec{\mathbf{D}}[s(i)]$ to replace $\vec{\mathbf{D}}[s(i)]$ in order to get the unique solution vector by (3.27). Similar to case 2) above, the signal and interference power on each primary channel can also be obtained.

From the three cases discussed above, we can conclude that the optimal number of required cognitive SUs for sensing a primary channel equals the total number of primary transmitters operating in all primary channels. Note that the gateway is assumed to be able to obtain the total number of primary transmitters, saying N_{tx}, by querying the remote database as in [1, 102-105]. Therefore, the number of primary channels that can be detected simultaneously, denoted by N_{cap}, is the integer part of the quotient of the number of cognitive SUs in the network divided by N_{tx}. If N_{cap} is equal to or larger than *m*, it means that all primary channels can be detected simultaneously. Otherwise, only N_{cap} channels among the *m* primary channels can be detected. If the cognitive SUs in a certain cluster are not sufficient, the redundant cognitive SUs in other clusters can be borrowed through coordination in order to sense the target primary channel. In the coordinated scenario, the sensed data are forwarded by the gateway. The coordination method and the selection algorithm of collaborative SUs can be described as follows:

a) The gateway collects the information of all the free SUs, including their cluster number and the number of hop counts from the gateway.

b) The cluster that does not have enough SUs to sense a target primary channel sends a

request to the gateway for the number of required SUs.

c) The gateway schedules the claimed number of SUs by the requesting cluster with the least number of hop counts from the gateway to minimize the sensing delay as much as possible.

The derivations above show that the solving of the non-homogeneous linear equation set for $\bar{\mathbf{p}}$ and the calculation of individual power produced by each primary transmitter or transmitters on a specific primary channel do not require any information about the primary signals or the interference factor. Therefore, the power decomposition and the resulting interference cancellation are non-coherent.

3.4 Simulation-based Performance Evaluation

In this section, we will validate the proposed power decomposition-based cooperation SS and evaluate its performance based on the two metrics discussed in section 2.2: probability of false alarm and probability of detection in soft combining and hard combining, respectively. We will show the effectiveness of the proposed power decomposition method by comparing it with the conventional method. Here, we define the conventional method as hard combining and soft combining without canceling the interference. The conventional method does not differentiate interference from background noise, treating both as noise. On the other hand, the power decomposition method individually decomposes the signal, the interference, and the background noise from the received power. The combining methods used in the conventional method and the power decomposition method are the same in HC and SC, respectively, as described in section 2.1.

The analysis in section 2 indicates that the method of SS for multiple primary channels is similar to that of SS for a single primary channel in that both exploit the proposed power decomposition method. For the sake of simplicity, we only simulate the SS for a single primary channel. In addition, section 3.3 shows that the number of cognitive SUs required to sense a single primary channel should be larger than or equal to that of the primary transmitters operating in all primary channels. Although more SUs can be expected to achieve more cooperative gain, in order to illustrate the validity and

efficiency of the power decomposition scheme, this simulation only focuses on the lower bound of its performance—i.e., only the equal number of primary transmitters and cognitive SUs are used. The main parameters of our simulation are as follows. We randomly distribute 6 primary transmitters and 6 cognitive SUs, including an AP, in two circular regions with the same central point and radiuses equal to 10km and 200m, respectively. The primary transmitters operate in 6 primary channels and the SUs, as a whole, are used to sense one of them. All cognitive SUs are within the transmission ranges of the AP and all primary transmitters. The two-ray ground propagation model is used and the path loss exponent β is set at 3. We model the transmission power of primary transmitters as uniform random variables and model the background noise as a Gaussian random variable with a uniformly varying means and a very small constant standard deviation for different runs. We observe the variation tendency of the probability of false alarm and the probability of detection with the decrease in the SINR. This decrease in the SINR is implemented by increasing the means of transmission power of primary transmitters operating in adjacent primary channels, while the parameters for the transmission power of primary transmitters operating in the target channel and the background noise remain unchanged. When calculating the SINR labeled in Figure 3-3 and Figure 3-4, the means of the receiving power produced by the transmitters operating in the target primary channel and in other channels are treated as the signal power and interference power, respectively. Also, the mean of the background noise is treated as noise power.

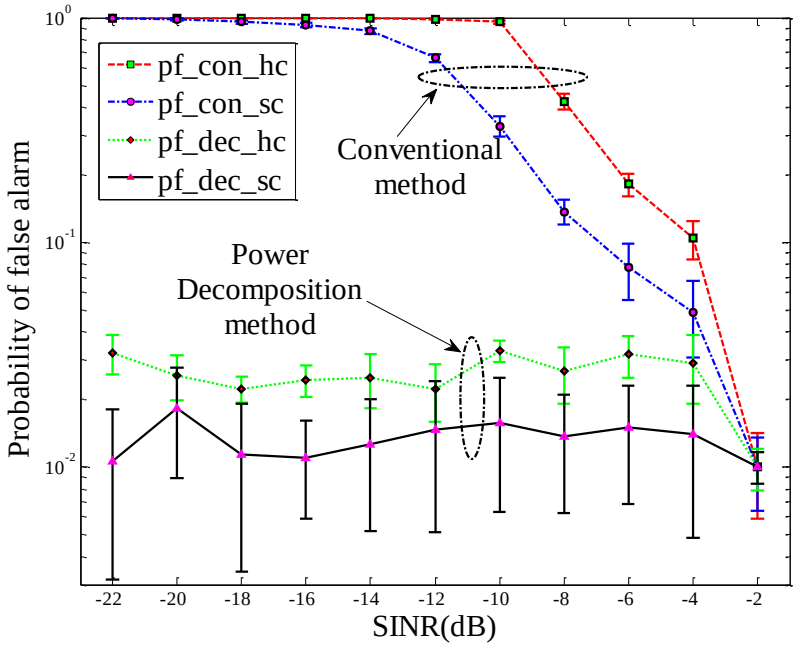

Figure 3-3 Probability of False Alarm (fixed threshold).

The threshold is set based on the scenario that the interference level is equal to 0 with an aimed $prob_f$ equal to 0.01. It is then fixed when the SINR decreases due to improvement of the interference.

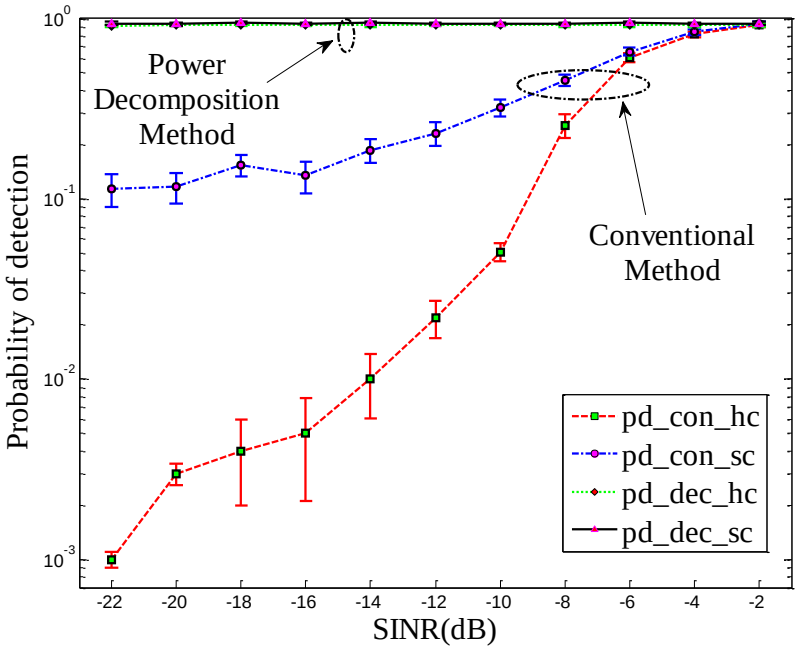

Figure 3-4 Probability of Detection

According to the analysis in section 2.2, the decision threshold should be

determined before calculating the $prob_f$ and $prob_d$. Obviously, we cannot set the threshold arbitrarily high for $prob_d$ and low for $prob_f$ at the same time, since a higher threshold resulting in a lower $prob_f$ will lead to a lower $prob_d$, and vice versa. Also, it is difficult to set the threshold based on $prob_d$ since we have little prior knowledge of the signal. Therefore, the threshold is determined based on $prob_f$ under hypothesis H_0 [26, 69, 97, 108]. However, the closed-form formula exploited in previous literature [26, 69, 70, 97, 98, 108] to determine the threshold for a given target $prob_f$ is based on an assumption—i.e., that the noise is white and Gaussian—and no interference is considered. It is difficult to determine the threshold when the real-time interference is considered in a practical system. Therefore, we do not use an adaptive threshold for different SINRs caused by variation of the interference power. Instead, we set the threshold according to the method introduced in [26, 97, 108] based on the case that the interference is zero—i.e., only the background noise exists—with a target $prob_f$ equal to 0.01. Then, we fix the threshold in the simulation when the SINR decreases due to improvement of the interference.

We perform the simulations in both hard combining and soft combining. In hard combining, we use the "OR" rule for combination when calculating the probability of false alarm and use the "AND" rule for combination when calculating the probability of detection. For each combining method, we compare the probabilities of false alarm and detection achieved by power decomposition and the resulting interference cancellation method with those achieved by the conventional method (without using power decomposition). The curves of the probability of false alarm and the probability of detection are shown in Figure 3-3 and Figure 3-4, respectively. Each point in the plots is an average of 30 runs, and the error bars show the 95% confidence intervals for the difference of each run.

Figure 3-3 shows that the probabilities of false alarm in soft combining and hard combining using the conventional method—denoted as *pf_con_hc* and *pf_con_sc*, respectively—increase rapidly with the decrease in the SINR caused by improvement of the interference. This indicates that the system will create more and more false alarms when the SINR becomes lower. The false alarm shows that the SS will report the spectrum to be occupied by the licensed primary users when it is actually vacant. In this case, some opportunities to exploit the primary spectrum will be wasted and spectrum

utilization will become low. Thus, the performance of the secondary network will be degraded. On the other hand, when the power decomposition method is used and the interference is cancelled, the probabilities of false alarm in hard combining and soft combining—denoted as *pf_dec_hc* and *pf_dec_sc*, respectively—remain flat with the decrease in the SINR. Compared with the conventional method, the power decomposition method is able to achieve a lower probability of false alarm, especially when the SINR becomes low in both hard and soft combining. Therefore, the power decomposition method is more effective and can achieve higher spectrum utilization and higher performance than the conventional method. In addition, Figure 3-3 indicates that *pf_con_hc* and *pf_con_sc* become increasingly higher than *pf_dec_hc* and *pf_dec_sc* as the SINR decreases. This shows that the power decomposition method is able to cope with the inter-channel interference in both hard combining and soft combining. We can also see that soft combining always offers a lower probability of false alarm than hard combining, as is shown in some of the previous literature [1, 97]. However, the improvement shown by the power decomposition method compared with the conventional method in soft combining is not as high as that in hard combining.

Similarly, Figure 3-4 shows that the probabilities of detection in hard combining and soft combining using the conventional method—denoted as *pd_con_hc* and *pd_con_sc*, respectively—decrease rapidly with the decrease in the SINR. However, the probabilities of detection under power decomposition and interference cancellation—denoted as *pd_dec_hc* and *pd_dec_sc*, respectively—remain stationary with the decrease in the SINR. In addition, *pd_con_hc* and *pd_con_sc* become increasingly lower than *pd_dec_hc* and *pd_dec_sc*, respectively, as the SINR decreases. As we know, the lower the probability of detection, the higher the probability of missed detection. Thus, Figure 3-4 indicates that the conventional method has a higher probability of missing the presence of primary signals when the SINR is low. Missed detection means that the SS system reports the absence of primary signals when they are actually present. In this case, the cogitative SUs will access the spectrum specified by the SS system, which will interfere with the licensed primary users. Therefore, the power decomposition method has a higher probability of avoiding interference with the primary users than the conventional method. It is also able to cope with the interference. In addition, Figure 3-4 shows that soft combining has a better probability of detection

than hard combining, as is validated in other studies [1, 97], but the improvement of *pd_dec_sc* compared with *pd_dec_hc* is not as great as that of *pd_con_sc* compared with *pd_con_hc*.

Although Figure 3-3 and Figure 3-4 also show that soft combining can offer a lower $prob_f$ and higher $prob_d$ than hard combining in the proposed power decomposition scheme, the improvement is relatively small in terms of these two metrics, and this strays from common sense. This phenomenon can be interpreted in two ways. First of all, most of the previous literature evaluates these two schemes in terms of $prob_d$ with the same target $prob_f$ rather than using both as they are used in this chapter. According to Figure 3-3, in order to achieve the same target $prob_f$ with the same collected energy, one has to either increase the threshold in hard combining or decrease the threshold in soft combining, which will result in either a decrease in $prob_d[HC]$ in hard combining or an increase in $prob_d[SC]$ in soft combining. Consequently, the difference will become larger. This is in accordance with common sense. Second, the difference between hard combining and soft combining in terms of $prob_d$ depends on the SNR where the interference equals zero. If the SNR becomes higher when the threshold is set at a target $prob_f$, the difference between these two combining schemes in terms of $prob_d$ will become larger.

Both Figure 3-3 and Figure 3-4 show that the proposed power decomposition method and its resulting interference cancellation can cope with high inter-channel interference and achieve better SS performance than the conventional method in terms of the probability of false alarm and the probability of detection.

3.5 Discussion of Location Inaccuracy and a Case Study

From (3.19), we can see that the accuracy of the power decomposition depends on the coefficient matrix involving only the distances between the primary transmitters and the cognitive SUs. The distances are determined by the locations of the primary transmitters and cognitive SUs. Obviously, the location inaccuracy of both leads to a similar impact on the performance of the power decomposition. Therefore, in order to

simplify the analysis and not lose generality, we only use analysis of the location inaccuracy of a primary transmitter as an example.

If the location of the l^{th} primary transmitter in (3.20) is inaccurate, the factors in the l^{th} column, determined by the distances between the l^{th} primary transmitter and all SUs, are inaccurate. If we take the k^{th} row in the coefficient matrix as an example and use $d_{k,l}^{-\beta}$ to denote the factor in the k^{th} row and l^{th} column, we can obtain the $p[l]$ from (3.19) as follows:

$$p[l] = d_{k,l}^{\beta}\left(p_{s(i,k)} - N - \sum_{\xi=1,\xi\neq l}^{n_d} d_{k,\xi}^{-\beta} p[\xi] \right) \tag{3.28}$$

(3.28) clearly shows that the inaccuracy of the location of primary transmitters will degrade the performance of the power decomposition scheme. If we assume that the maximum variance of $d_{k,l}$ caused by the inaccuracy of the l^{th} primary transmitter is $\Delta_{k,l}$, and use $p^*[l]$ to denote the $p[l]$ resulting from the inaccuracy, we can express the ratio between $p^*[l]$ and $p[l]$ as:

$$\frac{p^*[l]}{p[l]} = \left(1 + \frac{\Delta_{k,l}}{d_{k,l}}\right)^{\beta} \tag{3.29}$$

(3.29) shows that if the $\Delta_{k,l}$ is far less than $d_{k,l}$, the impact caused by the location inaccuracy of the primary transmitter on the power decomposition is not large. Otherwise, the impact will significantly degrade the accuracy of the power decomposition.

Let's examine a case study of the location inaccuracy of the primary transmitter in IEEE 802.22. According to [109], the DTV protection contour, also referred to as the noise-limited contour, occurs at 134.2 km from the DTV transmitter. In this case, the actual field strength exceeds 41 dBu, the value defined by the FCC for noise-limited service, at 50% of locations for 90% of the time. Thus, [109] recommends that the distances between the DTV transmitter and the SUs be further than 134.2 km. On the other hand, it is easy to make the location error less than 100 m by using the GPS [110].

In this case, if we substitute the location error and the protection contour in (3.29) and let β be 3, we can obtain:

$$\frac{p^*[l]}{p[l]} = \left(1+\frac{100}{1.34\times10^5}\right)^3 < \left(1+\frac{100}{1\times10^5}\right)^3 \approx 1.003 \qquad (3.30)$$

(3.30) shows that the impact caused by the location inaccuracy of the primary transmitters is almost negligible in the applications for IEEE 802.22.

However, for some conditions, if the distances between the primary transmitters and the cognitive SUs are not far compared to the distance variance, the impact caused by the location inaccuracy cannot be negligible. Thus, it will degrade the performance of the power decomposition scheme.

3.6 Conclusions

This chapter proposed a non-coherent power decomposition method used for energy detection in cooperative spectrum sensing. The power decomposition is implemented indirectly by solving a non-homogeneous linear equation set with a coefficient matrix that involves only the distances between primary transmitters and cognitive SUs. It does not require any prior knowledge of the primary signals. The optimal number of SUs for sensing a single channel is derived in the proposed method, as is the number of channels that can be sensed simultaneously by a cognitive radio network. We use the energy multiplied by the SINR of each SU as the test statistic to perform energy detection. The two widely used metrics, the probability of false alarm and the probability of detection, are exploited to evaluate the performance of power decomposition method and its resulting interference cancellation. Simulations validate the proposed method and show that it can efficiently cope with the interference leaked from adjacent primary channels. The simulations also show that, when the SINR decreases, the power decomposition method and its resulting interference cancellation are able to both greatly increase the probability of detection and significantly decrease the probability of false alarm in hard combining and soft combining compared with the conventional method.

Chapter 4
Optimal Cooperative Spectrum Sensing with Non-coherent Inter-Channel Interference Cancellation for Cognitive Wireless Mesh Networks

In the proposed power decomposition method in last chapter, the determination threshold is set for a given probability of false alarm when the in-channel interference is zero, and then the threshold is fixed. However, as it is analyzed in this chapter, this threshold setting method is not optimal. Therefore, an optimal threshold set method is proposed in this chapter. It is able to minimize the sum of the probability of false alarm and probability of missed detection. In addition, as it is stated in the chapter 2, in the cooperative spectrum sensing, the local sensed data should be transmitted to the fusion center through the reporting channel, which will become the bottleneck when the number of the affiliated cognitive radio users with the fusion center is large or when the single reporting channel suffers from fading. Aiming at addressing this problem, a multiple reporting channels method is proposed in this chapter. It designated multiple in-band channels as reporting channels through which the local sensed data is transmitted. These two measures are applied into the proposed power decomposition method to improve its performance. Simulations show that the modified cooperative spectrum sensing method can efficiently cope with the inter-channel interference and achieve much better performance than the conventional methods in the low signal to interference-plus-noise ratio range.

4.1 Introduction

A wireless mesh network (WMN) is considered a promising technique to provide high-quality service and ubiquitous connectivity to end-consumers in the last mile. Its capabilities of self-organizing, self-healing, and self-configuring significantly reduce the complexity of deployment and enhance the robustness of the network. Its infrastructure consists of wireless routers and gateways, through which mesh clients connect to the Internet. Obviously, the gateway has much stronger computing capability than other nodes in WMNs.

Since most of the consumer devices in WMNs work in the unlicensed frequency band for industrial, scientific, and medical (ISM) applications, similar to other networks such as ad hoc networks, WMNs also suffer from the crowded spectrum in the ISM band. Meanwhile, many licensed frequency bands are shown to be greatly under-utilized even in the most crowded urban areas [1, 2]. Such unbalanced spectrum utilization can be alleviated using dynamical spectrum access (DSA) techniques such as cognitive radio [3-5, 111]. As the first step of the cognitive technique, spectrum sensing (SS) plays an important role in two respects: first, SS should efficiently identify the spectrum holes in the primary (licensed) bands for the secondary (unlicensed) users (SUs); second, SS should limit the interference with the primary users (PUs) caused by the SUs at an acceptable level [1].

SS techniques can mainly be divided into two categories: non-coherent detection, such as energy detection [69, 101], and coherent detection, such as cyclostationary feature-based detection [45, 46]. Although coherent detection can achieve higher detection accuracy in lower signal to interference-plus-noise ratio (SINR) area, it cannot be performed without prior knowledge of the primary signal. On the contrary, non-coherent detection does not require prior knowledge of the primary signal and has lower complexity for implementation. As a result, non-coherent detection, especially energy detection, is the most widely used technique for SS. However, the accuracy of energy detection becomes poor as the SINR decreases and is affected by the uncertainty of interference. Unlike signal demodulation, in energy detection, co-channel interference is helpful, whereas the inter-channel interference (ICI) should be cancelled

as much as possible because it is harmful for signal detection on the target primary channel.

Aiming to cancel ICI and improve the SINR, this chapter proposed a non-coherent cooperative SS method with ICI cancellation for WMNs. In particular, the proposed method has the following features:

1) An optimal threshold for SS is derived to minimize the sum of probabilities of false alarms and missed detection.

2) ICI is cancelled indirectly by solving a non-homogeneous linear equation set with a coefficient matrix depending only on the distances between the primary transmitters and SUs.

3) In contrast to a single common control channel (CCC), to decrease the sensing delay, an intelligent algorithm for utilizing multiple in-band control channels is proposed for the transmission of sensed data, which is treated as control messages.

The rest of the chapter is organized as follows. The system model is shown in section 4.2. The determination of optimal threshold for SS and the ICI cancellation are given in sections 4.3 and 4.4, respectively. The algorithm of control channel allocation is described in section 4.5. Section 4.6 illustrates the simulation-based performance evaluation. We conclude this chapter in section 4.7.

4.2 System Model

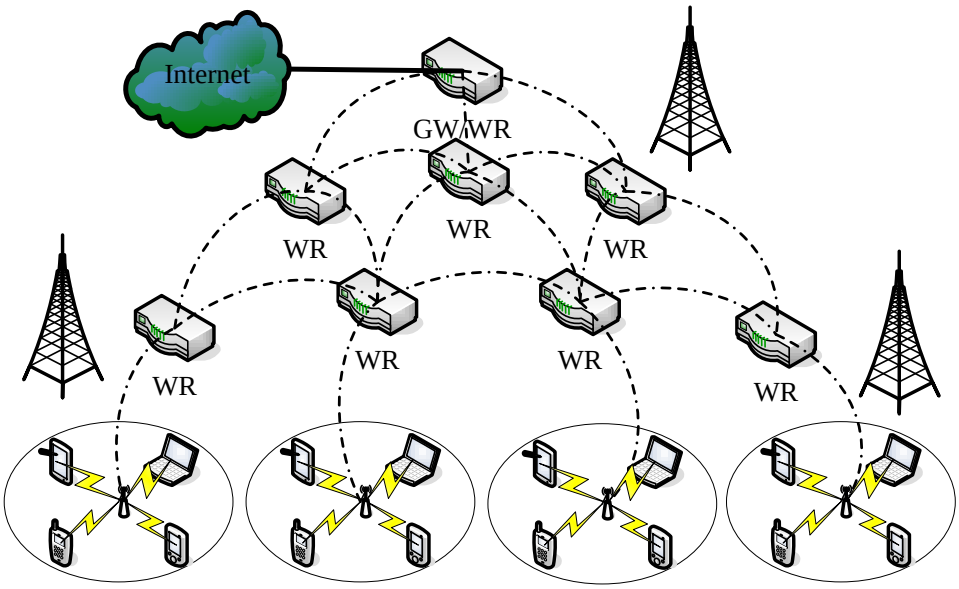

Figure 4-1 A typical architecture of a cognitive WMN

A typical cognitive WMN is shown in Figure 4-1. It consists of a gateway, wireless (mesh) routers, and sensing clusters. The process of the proposed SS consists of three steps: 1) sensing nodes in different clusters conduct local measurement. 2) Sensing nodes report their sensed data (or sensing results) to the corresponding fusion centers (FCs), i.e., the access points in Figure 4-1. The sensed data (or sensing results) are transmitted through multiple control channels rather than a single CCC in our system. The allocation algorithm for control channels is conducted by the gateway in a centralized way. 3) FCs make decisions regarding whether primary transmitters on the sensing channels are present or not and report these decisions to the gateway. The gateway then allocates channels for data (not control messages) transmission according to the sensing results. By applying different clusters to sense different primary channels, the proposed architecture of cognitive WMNs is able to sense multiple primary channels simultaneously.

The main assumptions are as follows: the position of primary transmitters and cognitive SUs are known; the primary spectrum band is divided into M channels; there are C_j primary transmitters, denoted as $\{Tx(j,1),Tx(j,2),\ldots,Tx(j,C_j)\}$, operating on

channel *j, j=(1,2,…,M)*. The secondary network consists of *K* clusters of secondary users. In cluster *i*, *i=(1,2,⋯,K)*, there are *Ni* secondary cognitive nodes denoted as *{S(1,i), S(2,i),⋯, S(N_i,i)}* and the corresponding FC. In general, SS can be modeled as a binary hypothesis testing problem:

- H_0: the absence of primary signals on the target channel
- H_1: the presence of primary signals on the target channel

The accuracy of the SS can be evaluated by the probabilities of false alarms P_{FA} and missed detection P_{MD}:

$$P_{FA} = prob\{T > S_T | H_0\} \tag{4.1}$$

$$P_{MD} = prob\{T < S_T | H_1\} \tag{4.2}$$

where T is the sensing metric and S_T is the threshold to determine whether the primary signals are present or absent. Obviously, a good sensing method should try to minimize P_{FA} and P_{MD} at the same time.

4.3 Determination of Optimal Threshold for SS

In energy detection-based SS, the total received power is utilized as the sensing metric. The sensing metric can be obtained in either the time domain or the frequency domain. In the case of the time domain, the power should be measured in the frequency range of the target channel. The samples of the output of the bandpass filter applied to the target signal are collected as the sensing metric. Otherwise, the time-domain signal should be transformed to the frequency domain using FFT. The samples on all frequency bins in the range of the target channel are collected as the sensing metric. Without loss of generality, the received signal can be expressed as follows:

$$R(n) = S(n) + I(n) + N(n) \tag{4.3}$$

where *S(n)*, *I(n)*, and *N(n)* are the superposition of the target signals, the superposition of the ICI, and the Gaussian background noise, respectively; *n* is the sample index. We assume that the samples of *S(n)*, *I(n)*, and *N(n)* are independent, respectively. We also

assume that the signal, ICI, and background noise are independent of each other. In this case, $|R(n)|^2$ is a sequence of independent and identically distributed, i.e., IID, variables. The sensing metric for energy-aware detection can be given by:

$$T=\sum_{n=0}^{N_S-1}\left|R(n)\right|^2=\begin{cases}\sum_{n=0}^{N_S-1}\left|I(n)+N(n)\right|^2 \ \ for\ H_0\\ \sum_{n=0}^{N_S-1}\left|S(n)+I(n)+N(n)\right|^2 \ \ for\ H_1\end{cases} \tag{4.4}$$

where N_s is the number of collected samples for measurement. The mean and variance of $\left|I(n)+N(n)\right|^2$ (μ_0 and σ_0^2) and $\left|S(n)+I(n)+N(n)\right|^2$ (μ_1 and σ_1^2) can be obtained from the samples when the primary signals are absent and present, respectively. According to the central limit theorem in Lindberg-Levy form, when the number of samples N_s becomes large enough, T_0 and T_1 can be approximated by normal distributions with means and variances as follows:

$$\begin{cases}\mu_{T_0}=N_S\mu_0,\sigma_{T_0}^2=N_S\sigma_0^2\\ \mu_{T_1}=N_S\mu_1,\sigma_{T_1}^2=N_S\sigma_1^2\end{cases} \tag{4.5}$$

The probability density functions of T_0 and T_1 can be express as:

$$f_{T_0}(x)=\frac{1}{\sqrt{2\pi}\sigma_{T_0}}\exp\left(-\frac{\left(x-\mu_{T_0}\right)}{2\sigma_{T_0}^2}\right) \tag{4.6}$$

$$f_{T_1}(x)=\frac{1}{\sqrt{2\pi}\sigma_{T_1}}\exp\left(-\frac{\left(x-\mu_{T_1}\right)}{2\sigma_{T_1}^2}\right) \tag{4.7}$$

Then, the probabilities of false alarms P_{FA} and missed detection P_{MD} can be calculated by (4.8) and (4.9), respectively:

$$P_{FA}=\int_{S_T}^{+\infty}f_{T_0}(x)dx=\int_{\frac{S_T-\mu_{T_0}}{\sigma_{T_0}}}^{+\infty}\frac{1}{\sqrt{2\pi}}\exp\left(-\frac{u^2}{2}\right)du=Q\left(\frac{S_T-\mu_{T_0}}{\sigma_{T_0}}\right) \tag{4.8}$$

$$P_{MD}=\int_{-\infty}^{S_T}f_{T_1}(x)dx=1-\int_{\frac{S_T-\mu_{T_1}}{\sigma_{T_1}}}^{+\infty}\frac{1}{\sqrt{2\pi}}\exp\left(-\frac{u^2}{2}\right)du=Q\left(\frac{S_T-\mu_{T_1}}{\sigma_{T_1}}\right) \tag{4.9}$$

Where, $Q(\bullet)$ denotes the Q function.

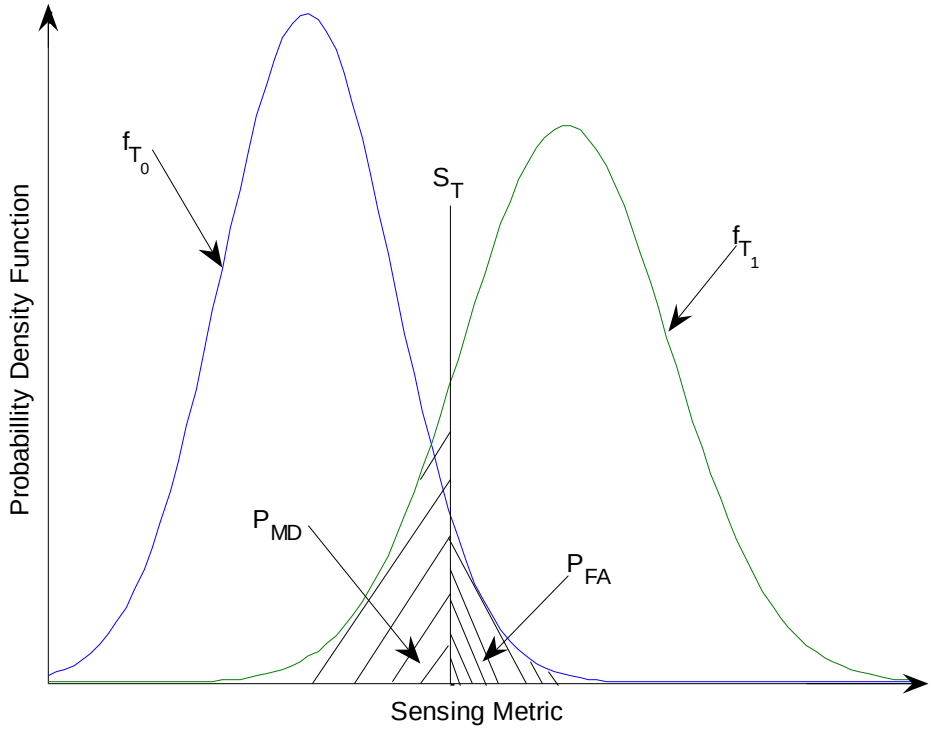

Figure 4-2 Impact caused by the variation of the threshold on the P_{FA} and P_{MD}

An illustration of P_{FA} and P_{MD} is shown in Figure 4-2. In general, the threshold is determined by minimizing P_{MD} (or P_{FA}) for a target P_{FA} (or P_{MD}). However, Figure 4-2 indicates that the decreasing P_{FA} implemented by improving the threshold S_T will result in the increase in P_{MD} and vice versa. In addition, it shows that the sum of P_{FA} and P_{MD} has a minimum value corresponding to a specific threshold. In other words, a trade-off exists between P_{FA} and P_{MD} with a minimum sum. The corresponding threshold is termed as the optimal threshold here. To obtain the optimal threshold, we let

$$P = P_{FA} + P_{MD} = \int_{S_T}^{+\infty} f_{T_0}(x)dx + \int_{S_T}^{+\infty} f_{T_1}(x)dx \tag{4.10}$$

And let

$$\frac{\partial P}{\partial S_T} = 0 \tag{4.11}$$

Then, the optimal threshold minimizing the sum of P_{FA} and P_{MD} can be obtained by

solving (4.11) as:

$$S_{T_{opt}} = \frac{1}{\sigma_{T_1}^2 - \sigma_{T_0}^2}\left[\mu_{T_0}\sigma_{T_1}^2 - \mu_{T_1}\sigma_{T_0}^2 + \sigma_{T_0}\sigma_{T_1}\sqrt{\left(\mu_{T_0} - \mu_{T_1}\right) + 2\left(\sigma_{T_0}^2 - \sigma_{T_1}^2\right)\log\frac{\sigma_{T_0}}{\sigma_{T_1}}}\right] \quad (4.12)$$

(4.12) shows that the optimal threshold depends only on the means and variances of the power samples when the primary signals are absent and when they are present. Consequently, P_{FA} and P_{MD} can be obtained by submitting (4.12) into (4.8) and (4.9), respectively.

The derivation process for the optimal threshold indicates that its accuracy depends on the number of power samples considering the condition for applying the central limit theorem. In general, the number of power samples is small in the case of high SINR. In contrast, this sample number is large in the case of low SINR. Therefore, the proposed method for determining the optimal threshold can get better performance when the SINR is low.

4.4 Inter-channel Interference Cancellation

In this section, we will first introduce the model of ICI proposed in [106]. Then, we will present how the ICI cancellation can be achieved by solving a non-homogeneous linear equation set and, finally, discuss the condition to cancel the ICI.

4.4.1 Model of ICI

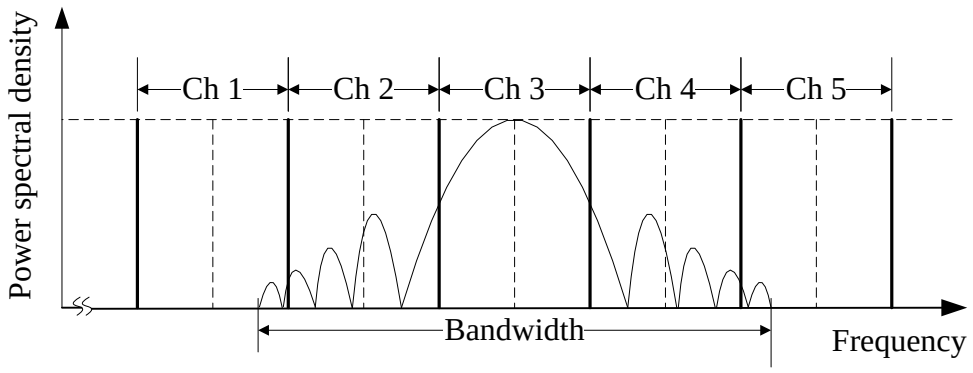

Figure 4-3 Power spectral density of a time-limited signal

To reduce the contention problem and to improve the spectrum utilization, the licensed primary spectrum band is always split into multiple channels. If the bandwidth of the transmitting signal is wider than that of the channel, e.g., in Figure 4-3, signals on one channel will interfere with the signals on the adjacent channels if they are transmitted simultaneously. The interference power on channel *v* due to the transmitter on channel *u*, by applying the two-ray ground propagation model, is derived in [106] as:

$$P_r = d^{-\beta}\left[r,tx\right]P^t I\left(u,v\right)\phi_c \tag{4.13}$$

where *d[r,tx]* is the distance between the transmitter and the receiver; β is the path loss exponent; P^t is the transmission power; ϕ_c is constant and depends only on the heights and gains of the antennas on the transmitter and receiver; *I(u,v)* is the interference factor and equal to 1 when *u=v*. Although *I(u,v)* is used in the derivation process, *I(u,v)* is not necessary when the cancellation is performed.

4.4.2 Method of ICI Cancellation

In general, the received power of an SU consists of three parts: the signal power, the power of the ICI, and the power of the background noise. As a result, sensing primary signals on channel *c*, the receiving power, $p_{s(i,j)}$ at the j^{th} cognitive SU, and *s(i,j)* in cluster *i*, can be expressed by:

$$p_{s(i,j)} = \sum_{m=1}^{M} pl_{s(i,j)}^{m} + N \tag{4.14}$$

where $pl_{s(i,j)}^{m}$ is the power due to the transmitters operating on channel *m* and can be given by:

$$pl_{s(i,j)}^{m} = \phi_c I\left(m,c\right)\sum_{\zeta=1}^{Cm}\left(d^{-\beta}\left[s\left(i,j\right),Tx\left(m,\zeta\right)\right]\cdot p^t\left[Tx\left(m,\zeta\right)\right]\right) \tag{4.15}$$

Each item of the summation in (4.15) corresponds to the ICI power due to the transmitter $Tx\left(m,\zeta\right)$. We let:

$$\vec{\mathbf{D}}\left[s(i,j),Tx(m)\right]=\left\{d^{-\beta}\left[s(i,j),Tx(m,1)\right],\ldots,d^{-\beta}\left[s(i,j),Tx(m,Cm)\right]\right\} \quad (4.16)$$

$$\vec{\mathbf{p}}^{t}(m)=\phi_c I(m,c)\left\{p^{t}\left[Tx(m,1)\right],\ldots,p^{t}\left[Tx(m,Cm)\right]\right\} \quad (4.17)$$

Then, (4.15) can be rewritten in a vector form as:

$$pl^{m}_{s(i,j)}=\vec{\mathbf{D}}\left[s(i,j),Tx(m)\right]\bullet\vec{\mathbf{p}}^{t}(m)^{\#} \quad (4.18)$$

where "#" and "$\bullet$" are the operator of the transpose and dot product, respectively.

Moreover, let:

$$\vec{\mathbf{D}}\left[s(i,j)\right]=\left\{\vec{\mathbf{D}}\left[s(i.j),Tx(1)\right],\ldots,\vec{\mathbf{D}}\left[s(i.j),Tx(M)\right]\right\} \quad (4.19)$$

$$\vec{\mathbf{p}}=\left\{\vec{\mathbf{p}}(1),\ldots,\vec{\mathbf{p}}(M)\right\} \quad (4.20)$$

Since the dimensions of the vector $\vec{\mathbf{D}}\left[s(i,j)\right]$ and the vector $\vec{\mathbf{p}}$ are equal to $n_d=\sum_{m=1}^{M}Cm$, (4.18) can be further rewritten as:

$$p_{s(i,j)}=\vec{\mathbf{D}}\left[s(i,j)\right]\bullet\vec{\mathbf{p}}^{\#}+N \quad (4.21)$$

Note that $\vec{\mathbf{p}}$ has no relation with each cognitive SU. Therefore, the received power of other nodes can also be obtained from (4.21) with the same $\vec{\mathbf{p}}$ and different distance vectors. The received powers of all the cognitive SUs in the cluster *i* can be written in a matrix form:

$$\begin{bmatrix}\vec{\mathbf{D}}\left[s(i,1)\right]\\ \vec{\mathbf{D}}\left[s(i,2)\right]\\ \vdots\\ \vec{\mathbf{D}}\left[s(i,N_i)\right]\end{bmatrix}_{N_i\times n_d}\bullet\vec{\mathbf{p}}^{\#}=\begin{bmatrix}p_{s(i,1)}-N\\ p_{s(i,2)}-N\\ \vdots\\ p_{s(i,N_i)}-N\end{bmatrix} \quad (4.22)$$

or in a more simple form:

$$\vec{\mathbf{D}}\left[s(i)\right]\bullet\vec{\mathbf{p}}^{\#}=\vec{\mathbf{p}}^{*}\left[s(i)\right] \quad (4.23)$$

where $\vec{\mathbf{D}}[s(i)]$ and $\vec{\mathbf{p}}^{*}[s(i)]$ correspond to the coefficient matrix and the vector on the right side of (4.22), respectively.

The items of $\vec{\mathbf{D}}[s(i)]$ are the distances between the cognitive SUs in cluster *i* and the primary transmitters on all primary channels. The items of $\vec{\mathbf{p}}^{*}[s(i)]$ are the differences between the total receiving power of cognitive SUs and the background noise power. Note that the background noise can be estimated through quantized samples, as in [96, 108]. Consequently, $\vec{\mathbf{p}}$ can be solved from (4.23) when the coefficient matrix is given and satisfies some constraints, which will be discussed later.

If we let

$$\vec{\mathbf{T}} = \{Tx(1,1),\ldots,Tx(1,C1),\ldots,Tx(M,1),\ldots,Tx(M,CM)\}; \alpha = \sum_{j=1}^{m-1} Cj \qquad (4.24)$$

and use $p[\eta]$ and $Tx[\eta]$ to index the η^{th} factor of vector $\vec{\mathbf{p}}$ and $\vec{\mathbf{T}}$, respectively; then, the part of the received power at *s(i,j)* due to the transmitter η operating on the primary channel *m* can be extracted from the superposition of receiving power and can be expressed as:

$$p[Tx(m,\eta)] = p[\eta] d^{-\beta}[s(i,j), Tx(\eta)] \qquad (4.25)$$

The part of the received power at *s(i,j)* due to all the primary transmitters on channel *m* can be expressed as:

$$p_m = \sum_{\eta=\alpha+1}^{\alpha+Cm} p[\eta] d^{-\beta}[s(i,j), Tx(\eta)] \qquad (4.26)$$

(4.25) and (4.26) clearly show that the part of the power due to each transmitter on any primary channel can be decomposed from the superposition of the received power. The received power due to all the transmitters operating on each primary channel can thereby be decomposed. If the target channel is *j* and the received power due to all the transmitters on channel *j* is p_j, the corresponding inter-channel interference power can

be expressed by:

$$I_p(j) = \sum_{m=1, m\neq j}^{M} p_m \tag{4.27}$$

Now, the task of ICI cancellation has been transformed into solving the non-homogeneous linear equation set in (4.23), which will be discussed in the next section. After canceling the ICI, the sensing metric will become:

$$T = \sum_{n=0}^{N_S-1} \left|R(n)\right|^2 = \begin{cases} T_0 = \sum_{n=0}^{N_S-1} \left|N(n)\right|^2, H_0 \\ T_0 = \sum_{n=0}^{N_S-1} \left|S(n)+N(n)\right|^2, H_1 \end{cases} \tag{4.28}$$

The corresponding optimal threshold can still be obtained from (4.12) with different means and variances of T_0 and T_1. Consequently, P_{FA} and P_{MD} with the ICI cancellation can also be obtained.

4.4.3 Conditions for ICI Cancellation

Since the positions of all primary transmitters on all channels are assumed to be known, the distance between each transmitter to all SUs can be easily calculated. Therefore, the coefficient matrix in (4.23) is known. According to the property of the non-homogeneous linear equation set, solving for $\vec{\mathbf{p}}$ depends only on the coefficient matrix. By fine-tuning the position of the SUs, the rank of the coefficient matrix can always satisfy:

$$rank\left\{\overline{\mathbf{D}}\left[s(i)\right]\right\} = \min\left(N_i, n_d\right) \tag{4.29}$$

As a result, the solution for the non-homogeneous linear equation set has the following three cases:

1) If $N_i<n_d$, (4.23) has a general solution but no particular solution vector, the ICI cannot be cancelled.

2) If $N_i=n_d$, (4.23) has a unique solution, $\overline{\mathbf{D}}\left[s(i)\right]$ is invertible and the solution can

be obtained from:

$$\vec{\mathbf{p}}^{\#} = \vec{\mathbf{D}}^{-1}\left[s(i)\right] \bullet \vec{\mathbf{p}}^{*}\left[s(i)\right] \tag{4.30}$$

3) If $N_i > n_d$, we can select any k-order complementary minor $\vec{\mathbf{D}}^{*}$ with a rank equal to k from $\vec{\mathbf{D}}\left[s(i)\right]$ to replace $\vec{\mathbf{D}}\left[s(i)\right]$ to get the unique solution vector by (4.30).

As a result, the minimum number of SUs to sense a channel equals the number of PUs operating on all primary channels. In this case, with ICI cancellation, the maximum number of channels that can be sensed simultaneously is the integer part of the quotient of the number of cognitive SUs in the network divided by the number of PUs on all primary channels.

The derivations above also show that ICI cancellation does not require any information about the primary signals and the interference factor. Therefore, it is a non-coherent method.

4.5 Control Channel Allocation

In this section, we will first show the admissible condition for new wireless links, i.e., the links between the receiver and the transmitters in the sensing range of the receiver. Then, we will briefly introduce the multi-radio conflict graph (MCG) proposed in [95] and, finally, give the proposed algorithm for control channel allocation.

4.5.1 Admissible Condition for New Wireless Links

To correctly decode packets at the receiver, $Rx(l_i)$, of the i^{th} link, l_i, the received SINR should be greater than a predefined threshold γ if we assume that the threshold is the same for all the radios in the network. Such a condition can be expressed by:

$$\frac{P_r(l_i)}{N + \sum_{l_j, j \neq i} I_{Rx(l_i)}^{Tx(l_j)}} > \gamma \Leftrightarrow \sum_{l_j, j \neq i} I_{Rx(l_i)}^{Tx(l_j)} < \frac{P_r(l_i)}{\gamma} - N \tag{4.31}$$

Here, l_i and l_j are the i^{th} and the j^{th} link operating on the same channel, respectively. $Tx(l_i)$ and $Rx(l_i)$ are the transmitter and receiver of the link l_i, respectively. $P_r(l_i)$ is the receiving power at $Rx(l_i)$ due to the transmitter $Tx(l_i)$. N is the background noise power. $I_{Rx(l_i)}^{Tx(l_j)}$ is the received interference power at $Rx(l_i)$ due to the transmitter $Tx(l_j)$ of link j operating on the same channel. It can easily be calculated from (4.13) by letting $I(u,v)$ equal 1.

The current maximum admissible interference power (CMAIP) of the receiver on the link l_i in the channel can be obtained from (5.1) as:

$$CMAIP\left[Rx\left(l_i\right)\right] = \frac{P_r\left(l_i\right)}{\gamma} - \sum_{l_j, j \neq i} I_{Rx(l_i)}^{Tx(l_j)} - N \tag{4.32}$$

Then, the interference power P_{itf}, incurred by the new wireless link, which will be scheduled on the same channel with l_i, should be less than the minimum value of the CMAIP of all links on this channel, which can be represented as:

$$P_{itf} < \min_{l_i} \left\{ CMAIP\left[Rx\left(l_i\right)\right] \right\} \tag{4.33}$$

Similarly, the interference power with the new wireless link due to the links on the target channel can also be obtained. It should also satisfy (5.1).

4.5.2 Construction of Multi-radio Conflict Graph (MCG)

Considering the fact that some wireless nodes are equipped with multiple radios (interfaces) to further improve the system capacity, the proposed control channel allocation algorithm should be able to allocate multiple control channels among the heterogeneous networks with partial multi-radio nodes. The MCG proposed in [95] is used to minimize the co-channel interference. It can be described as follows. First, each radio in the mesh network is represented as a vertex in the topology graph G. The edges in G are between radios on different nodes in the mesh network. Then, the vertices in the MCG, M, are represented as the edges in G. The edges between vertices in M are created in this way; i.e., two vertices in M have an edge between each other if the edges in G represented by the two vertices in M interfere with each other. As an example,

Figure 4-4-(b) is the corresponding MCG of the network topology illustrated in Figure 4-4-(a) with the constraint that nodes A, B, C, and D, are equipped with 1, 2, 1, and 1 radio(s), respectively. In Figure 4-4-(b), the vertex (B2:C1) represents the wireless link between the second radio on node B and the first radio on node C.

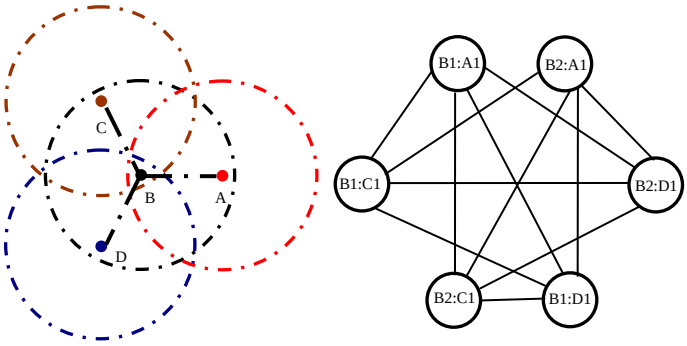

Figure 4-4 Construction of multi-radio conflict graph

4.5.3 Algorithm of Control Channel Allocation

To clearly describe the proposed algorithm of control channel allocation (ACCA), we assume that there are *N* nodes (including cognitive SUs, FCs, and other mesh nodes) in the mesh network. Node *n, n=(1,...,N)*, is equipped with r_n radios, denoted as $rd(n)=\{(n,1),\ldots,(n,r_n)\}$. Then, the wireless links between the radios on node *i* and *j* can be represented as:

$$S_i^j = \left\{(i,\mu):(j,\varepsilon)\middle|\left\langle(i,\mu),(j,\varepsilon)\right\rangle \in rd(i)\times rd(j)\right\} \tag{4.34}$$

where "×" represents the operation of the Cartesian product, $\mu \in (1,\ldots,r_i)$, and $\varepsilon \in (1,\ldots,r_j)$. Obviously, only when nodes *i* and *j* are in the transmission range with each other do the wireless links between the radios on these two nodes exist. Otherwise, such links do not exist and can be denoted by $\boldsymbol{0}$. Since no wireless links exist between the radios on the same node, $S_i^i=\boldsymbol{0}$. Consequently, the wireless links in the cognitive WMN can be represented by:

$$S = [S_i^j]_{N\times N} = \begin{bmatrix} 0 & S_1^2 & \cdots & S_1^N \\ S_2^1 & 0 & \cdots & S_2^N \\ \vdots & \vdots & \ddots & \vdots \\ S_N^1 & S_N^2 & \cdots & 0 \end{bmatrix} \tag{4.35}$$

To implement the control channel allocation, a breadth-first-search (BFS)-based vertex coloring algorithm (VCA) can be applied to the MCG. Since the amount of data transmitted from the cognitive SUs to the FC is much larger than that of the sensing decisions (binary bits) transmitted from the FCs to the gateway, we perform the BFS-based VCA in a bottom-up order. In addition, to ensure that only one channel is allocated to one radio, a significant constraint should be imposed on the BFS-based VCA: once any vertex $(i,\mu):(j,\varepsilon)$ is colored in the MCG, then all the vertices corresponding to the wireless links S_i^j should be completely removed. In this case, there possibly exists a scenario such that the number of orthogonal channels is not enough to be allocated to the links in the interference range or that the number of radios on the node is insufficient. Some of these links have to share channels, although interference will occur when transmitting and/or receiving simultaneously. To minimize the co-channel interference and balance load on each channel, the sharing channel should be selected according to the hop counts of the node from the gateway and the accessible condition for new links. The links with higher hop counts should be assigned higher priority to share channels with fewer links considering traffic pattern in the WMN. Thus, the uncolored vertices encountering this scenario should try to share channels with links with the same priority. In this way, the connectivity of the network is ensured and the topology remains unchanged. The BFS-based VCA in a bottom-up order for control channel allocation can be described by Table 4-1.

Table 4-1 Algorithm of Control Channel Allocation

(BFS-based VCA in a Bottom-Up Order)

Initialization: *V={v|v ∈ MCG}*; *C={all channels}*; *h= maxHopCount*;
while *h>=1* **do**
Queue={v|v∈V and *notVisisted(v)* and *hopCount(v)=h}*
while *size(Queue)>0* **do**

$v_{current}$=*popHead(Queue)*
if *visited*($v_{current}$)=*True* ***then***
continue
end if
visit($v_{current}$)
$V_{neighbor}$={$v|v \in V$ and *edge*(v,$v_{current}$) exists }
V_{temp}={$v|v \in V_{neighbor}$ and v has been visited}
V'_{temp}={$v|v \in V_{neighbor}$ and v has not been visited}
$C_{available}$={$c|c \in C$ and c does not conflict with the channels that had been assigned to $v_i \in V_{temp}$}
while V'_{temp} is not empty **do**
if $C_{available}$ is not empty **then**
Assign a randomly selected channel from $C_{available}$ to v_m, {$v_m \in V'_{temp}$}
Remove all the vertices corresponding to S_i^j from MCG with $(i,\mu):(j,\varepsilon)$ denoting V_m
Update V_{temp}, V'_{temp} and $C_{available}$
else
Assign channel to v_m, {$v_m \in V'_{temp}$ } according to the admissible condition
Remove all the vertices corresponding to S_i^j from MCG with $(i,\mu):(j,\varepsilon)$ denoting V_m
Update V_{temp}, V'_{temp} and $C_{available}$
end if
end while
end while
h=h-1
end while

4.6 Simulation-based Performance Evaluation

In this section, we will first evaluate the efficiency of the proposed algorithm of control channel allocation (ACCA) by using the average end-to-end packet delay as the evaluation metric. Then, we will evaluate the performance of the proposed SS method through two metrics: probabilities of false alarms and missed detection in soft combination (SC) and hard combination (HC) scenarios, similar to [101]. In HC, the transmitted data from SUs to FC are the binary decisions made by the SUs based on the

sensed data. Then, the FCs make the final decision according to the received binary results from the SUs in "AND," "OR," or other rules [69]. However, in SC, the SUs will not make any decisions; instead, they report the sensed data to the corresponding FCs, which make the final decisions. Obviously, the amount of transmitted data from the SUs to the FCs in an SC is much larger than that in an HC; therefore, an SC can benefit more than an HC from the utilization of multiple in-band control channels.

The main parameters in our simulation are as follows. We randomly distributed 12 PUs operating on 4 primary channels (each channel has 3 PUs) in a 20Km-by-20Km square area. There are 4 clusters, each of which contains 12 SUs and an FC in the cognitive WMN. The other nodes are also randomly distributed with two constraints in the 20Km-by-20Km area listed above. First, the SUs in each cluster are able to exchange data with the corresponding FC without any relay. Second, the 4 FCs are able to exchange data with the gateway through 2 hops. To simplify the simulation, we assume that the number of radios equipped on the FCs, the gateway, and the relay nodes in the WMN is the same as the number of available secondary orthogonal channels. The two-ray ground propagation model is used and the path loss exponent β is set at 3. We model the transmission powers of PUs and background noise as normal random variables with different means and variances. The decrease in SINR is implemented by increasing the ICI while the background noise remains unchanged. The increase in ICI is achieved by improving the means of transmission power of PUs operating in the adjacent channels. The optimal threshold corresponding to different SINRs is used in the simulation of the proposed SS method. Consequently, for different SINRs, the threshold is also different.

We compare the proposed ACCA with the Rama method proposed in [95], which can also be used for control channel allocation in terms of average end-to-end packet delay. We perform this simulation in an SC in order to explicitly demonstrate the benefit of using multiple control channels. When performing the simulation, to saturate the control channels, we decrease the SINR to get enough power samples. Then, we fix the SINR and compare the two methods by changing the packet size. We compare these two methods with 2 and 4 available secondary orthogonal channels, respectively. The plot of the average end-to-end packet delay corresponding to different packet sizes is

shown in Figure 4-5. Each point in the figure is an average of 30 runs with randomly generated topologies. The error bars show the 95% confidence intervals for the difference of each run.

Figure 4-5 shows that the proposed ACCA can achieve lower end-to-end packet delay than the Rama method when both 2 and 4 channels are available for control channels. It also indicates that the delay increases with the increase in packet size when the packet size is less than 1100 bytes and then becomes flat with the increase in packet size. In addition, Figure 4-5 indicates that the delay decreases as the number of control channels increases. The comparison shows that the proposed ACCA can achieve lower latency, which is important for SS to trace the variation of occupancy of the primary spectrum by PUs.

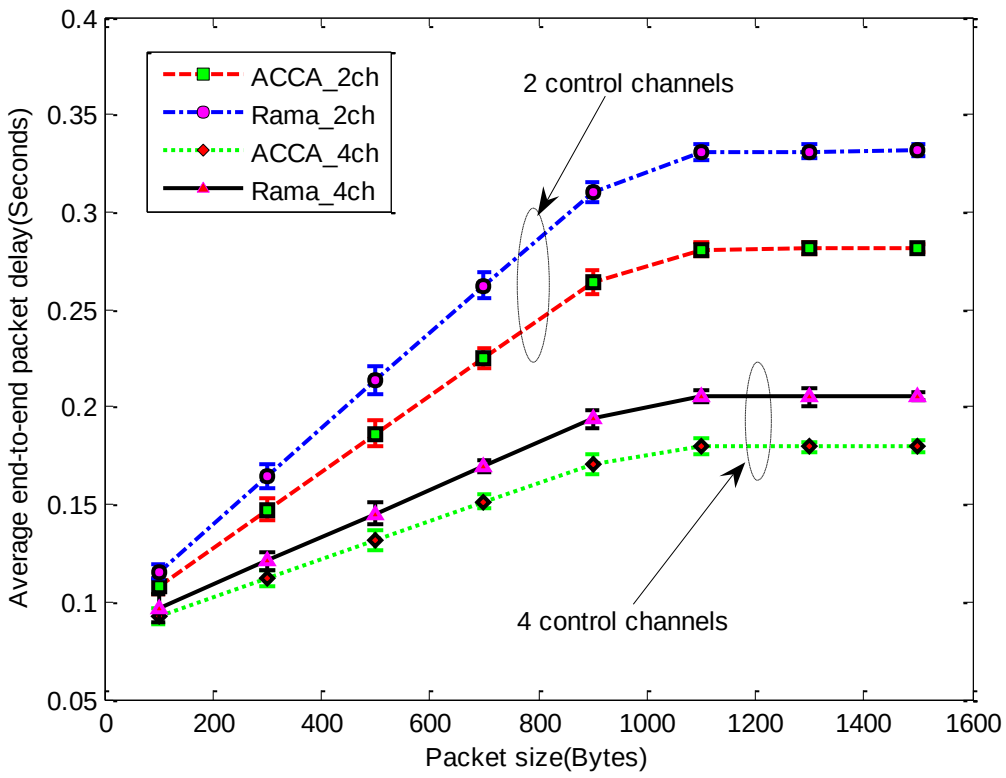

Figure 4-5 The average packet delay for multiple control channels

When evaluating the performance of the proposed cooperative SS method, to ensure the accuracy of the optimal threshold, we perform the simulation in the relatively

low SINR range (from -24dB to -20dB). In the simulation, 4 secondary orthogonal channels are used as control channels for a case study. For each combining method, we compare the P_{FA} and P_{MD} achieved by the ICI cancellation method with those achieved by the conventional method (without canceling the ICI). The curves of the P_{FA} and P_{MD} with different SINRs are shown in Figure 4-6 and Figure 4-7, respectively. In Figure 4-6 and Figure 4-7, CON, ICI, HC, and SC denote the conventional method without ICI cancellation, the ICI cancellation method, the hard combination scenario, and the soft combination scenario, respectively. We run the simulation 30 times with different seeds for the random number generator for each SINR value. Each time, we get the averaged value of P_{FA} and P_{MD} of the 4 clusters. The points in Figure 4-6 and Figure 4-7 are the average value of the 30 runs. The error bars show the 95% confidence intervals for the difference of each run.

Figure 4-6 and Figure 4-7 show that the conventional method works very poorly, but the ICI method can achieve much better performance in the low SINR range in terms of P_{FA} and P_{MD}. In particular, Figure 4-6 indicates that the P_{FA} using the conventional method in both the HC and SC scenarios increases rapidly with the decrease in SINR; however, P_{FA} using the ICI method remains almost flat with the decrease in SINR; in addition, SC always offers lower P_{FA} than HC, as shown in most of the previous literature [1, 101]. Figure 4-7 indicates that ICI cancellation can achieve lower P_{MD} in the low SINR range; with the decrease in SINR, P_{MD} increases sharply when the conventional method is used in both the SC and the HC; however, P_{MD} remains flat in both the SC and HC when ICI cancellation is applied; also, the SC can provide a lower probability of missed detection than the HC, as shown in previous literature [1, 101].

Both Figure 4-6 and Figure 4-7 show that the proposed method can efficiently cope with the ICI when the SINR is less than -2 dB; the SC can work better than the HC regardless of whether ICI is used or not; in addition, the ICI method in the SC scenario can achieve the best performance among the 4 combinations of ICI and the conventional method with the SC and HC.

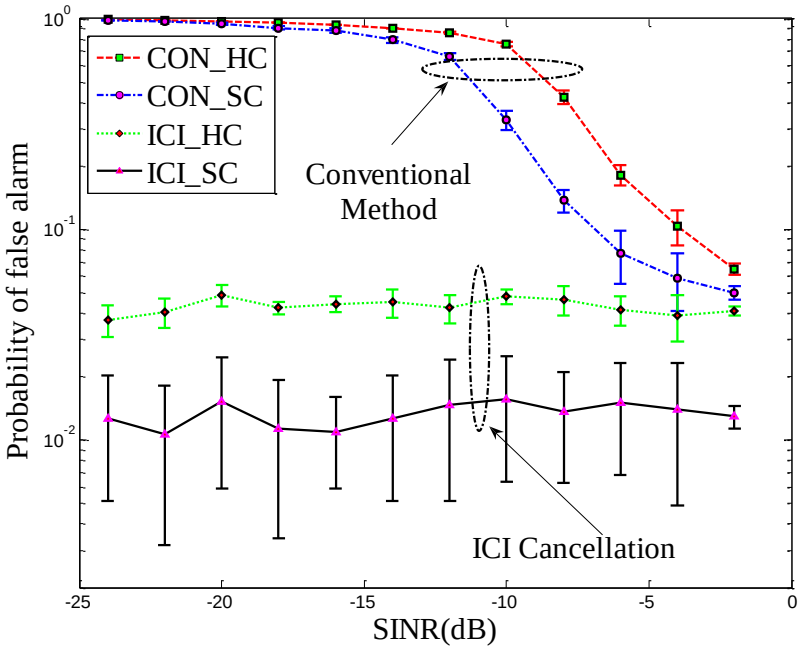

Figure 4-6 Probability of false alarms with optimal threshold.

The SINRs are calculated before ICI cancellation

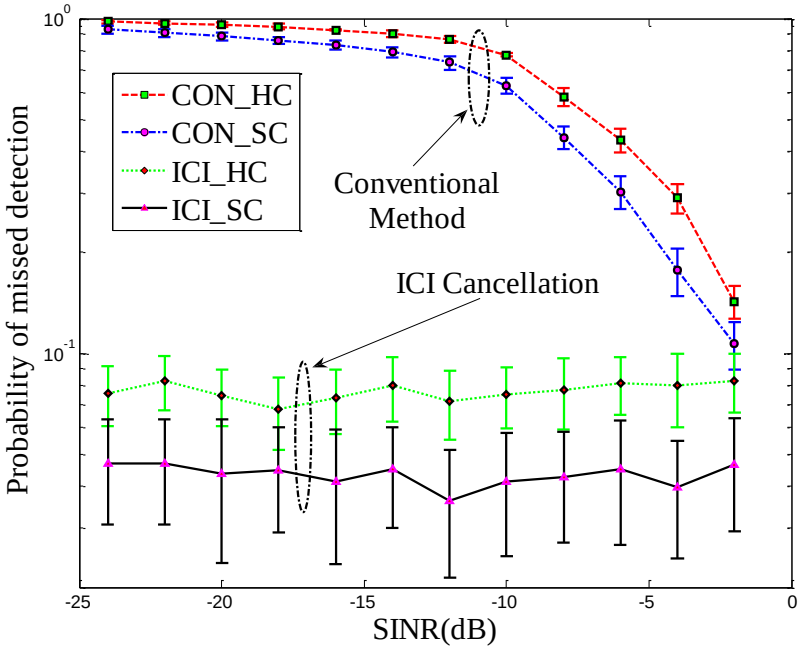

Figure 4-7 Probability of missed detection with optimal threshold.

The SINRs are calculated before ICI cancellation

4.7 Conclusions

This chapter proposed an optimal cooperative SS method with ICI cancellation for a cognitive WMN. Unlike the previous methods to determine the threshold for SS with given probability of false alarms, in the proposed optimal method, the optimal threshold is determined based on the means and variances of the power samples when the primary signals are present and absent, respectively, and is aimed at minimizing the sum of the probabilities of false alarms and missed detection. In addition, to decrease the sensing delay, we proposed an algorithm of control channel allocation to utilize multiple control channels for the transmitting the sensed data from the cognitive SUs to the corresponding FCs. Considering the architecture of the WMN, ACCA is performed by the gateway in a centralized way.

To cope with the ICI, we proposed a non-coherent ICI cancellation method. It is implemented indirectly by solving a non-homogeneous linear equation set with a coefficient matrix depending only on the distances between the primary transmitters and cognitive secondary users. The proposed SS method does not require any prior knowledge of the primary signals. The minimum number of SUs to sense a single channel in accordance with the ICI cancellation is also derived. Then, the number of channels that can be sensed simultaneously by a cognitive radio network can also be calculated. The simulation results show that the proposed SS method is able to decrease the sensing delay compared with the Rama method. They also indicate that the proposed method is able to cope with the ICI and can achieve better performance than the conventional method in terms of probabilities of false alarms and missed detection.

Chapter 5

Two-stage Coordination M2MAC MAC Protocol for Cognitive WMN

Within the secondary network in cognitive WMN, a bottleneck problem arises as the number of concurrent traffic flows (NCTF) increases over a single common control channel, as arises in most conventional networks. To alleviate this problem, this chapter proposes a two-stage coordination multi-radio multi-channel MAC (TSC-M2MAC) protocol that designates all available channels as both control channels and data channels in a time division manner through a two-stage coordination. On the first stage, a load balancing breadth-first-search-based vertex coloring algorithm for multi-radio conflict graph is proposed to intelligently allocate multiple control channels. On the second stage, a REQ/ACK/RES mechanism is proposed to realize dynamical channel allocation for data transmission. On this stage, the Channel-and-Radio Utilization Structure (CRUS) maintained by each node is able to alleviate the hidden nodes problem; also, the proposed adaptive adjustment algorithm for the Channel Negotiation and Allocation (CNA) sub-interval is able to cope with the variation of NCTF. In addition, a power saving mechanism for the TSC-M2MAC is designed to decrease its energy consumption. Simulation results show that the proposed protocol is able to achieve higher throughput and lower end-to-end packet delay than conventional schemes. They also show that the TSC-M2MAC can achieve load balancing, save energy, and remain stable when the network becomes saturated.

5.1 Introduction

As an emerging and promising technology, a wireless mesh network (WMN) can provide high QoS to end users as the last mile technique for data delivery over the Internet. Different from mobile ad hoc networks (MANET), WMN has its own unique

features [8]. At first, it has an infrastructure consisting of stationary or slow mobile wireless routers and gateways through which mesh clients connect to the Internet. Obviously, the gateway has much stronger computing capability than other nodes. Secondly, its traffic pattern is mainly from the clients to the gateways or in the inverse direction. Therefore, the links closer to the gateway are more likely to be burdened with a higher traffic load. Therefore, the design of protocol for WMN should take such unique features into full consideration in order to achieve better performance.

Compared to single channel MAC protocols, multi-channel MAC protocols can achieve much higher time-spatial-reuse efficiency and thus considerably improve system performance. The multi-radio multi-channel MAC (M2MAC) [89, 91, 93, 95] can further improve the flexibility of resource allocation, and it provides at least two more advantages over the single radio multi-channel MAC [89, 90]. First, radios do not always need to switch among different channels, which will simplify the design and significantly reduce the protocol overhead. Second, M2MAC can further improve network capacity, because it features nodes that can communicate simultaneously on different radios. Considering the fact that IEEE 802.11b/g and 802.11a can respectively provide as many as 3 and 13 orthogonal channels [112], it makes sense to study M2MAC for practical applications.

To the best of our knowledge, almost all the previous M2MAC protocols [89, 91, 93, 95] specify an out-of-band or in-band single channel as the common control channel (CCC) for exchanging control messages so that the protocol can coordinate the communication pair nodes and mitigate hidden nodes problem. In this chapter, we consider only the in-band control channels. Obviously, the use of dedicated CCC could cause resource waste when the Number of available Orthogonal Channels (NOC) is small (e.g., 1/3 orthogonal channels have to be used as a control channel in IEEE 802.11 b/g), so it may face the bottleneck problem when the Number of Concurrent Traffic Flows (NCTF) grows immense. In the latter case, the collision of control messages will lead to system performance degradation in terms of throughput and end-to-end packet delay.

In this chapter, we propose a Two-Stage Coordination M2MAC (TSC-M2MAC), which not only solves the abovementioned bottleneck problem for control messages

exchanging but also alleviates hidden node problems and achieves load balancing among different channels. The proposed TSC-M2MAC exploits all available orthogonal channels for both control messages exchanging and data transmission through a time division manner. Compared to conventional M2MAC, the proposed TSC-M2MAC has the following new features:

a) Instead of exploring a single dedicated CCC, all the available channels are designated as control channels and data channels on Channel Negotiation and Allocation (CNA) and Data Transmission (DT) sub-intervals, respectively, in a time division manner. It can also address the scenario of large NCTF.

b) An intelligent control channel allocation algorithm, which considers co-channel interference, is proposed on the first stage. It is able to achieve load balancing among all channels, and it minimizes co-channel interference.

c) On the second stage, a REQ/ACK/RES mechanism is proposed to realize dynamical channel allocation for data transmission. The hidden node problem can also be alleviated with channel and radio utilization structures.

d) An adaptive adjustment algorithm (AAA) for the CNA sub-interval is proposed to cope with the variation of the number of traffic flows at different times.

e) A Power Saving Mechanism (PSM) designed specifically for the TSC-M2MAC is presented to improve the efficiency of its energy consumption.

The remainder of this chapter is organized as follows. Section 5.2 presents the system model. Section 5.3 reports the admissible conditions for new wireless links. Sections 5.4 and 5.5 show the proposed Control Channel Allocation Algorithm (CCAA) and the dynamic data channel allocation, respectively. We present the AAA for the CNA sub-interval and PSM in sections 5.6 and 5.7, respectively. Section 5.8 describes the simulation-based performance evaluation. We conclude this chapter in section 5.9.

5.2 System Model of TSC-M2MAC

TSC-M2MAC is designed for a heterogeneous system environment. There is no requirement for the radio communication or sensing range, the physical layer

technology of each radio, or the number of radios equipped on each node. The two main assumptions in TSC-M2MAC include: 1) all the nodes in the network are synchronized, similar to [7]; and 2), all the radios used in the network are half-duplex, which means the radio cannot transmit data and receive data at the same time. The TSC-M2MAC is a virtual MAC running on the top of all radios equipped on each node. Figure 5-1 demonstrates the schematic of a multi-radio node. This node's objectives are to increase throughput, to decrease end-to-end delay, and to reduce energy consumption.

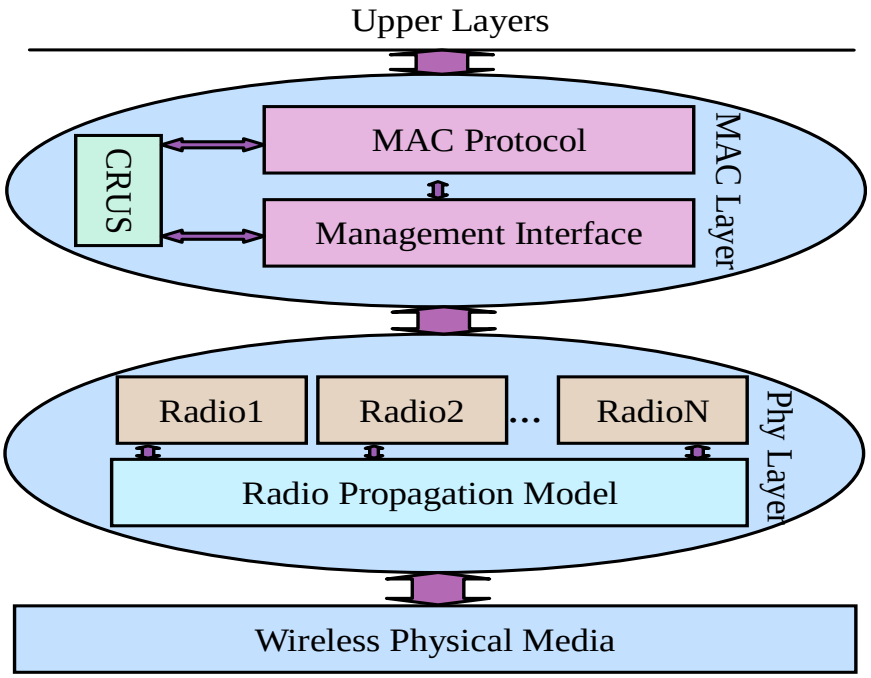

Figure 5-1. Schematic of a Multi-Radio Node

To realize such objectives by efficiently utilizing the available channels, TSC-M2MAC consists of a two-stage coordination process: control channel allocation and data channel allocation, which are performed in a centralized and distributed manner, respectively. On the first stage, in order to minimize co-channel interference and to decrease the collision probability of control messages (similar to [95]), we apply the Multi-radio Conflict Graph (MCG) to model the interference, but we use a different BFS-based vertex coloring algorithm (VCA) in order to consider load balancing among all channels. The VCA can figure out control channel allocation results for radios on different nodes. VCA is performed through the gateway and is triggered by topology variations. Given the complexity of VCA and the slow change of traffic patterns, this

algorithm can be executed for a long period, e.g., at 100 beacon intervals, so as to alleviate its demand on the gateways. As an example, given that all the nodes are equipped with 3 radios and that 3 orthogonal channels are available, Figure 5-2 demonstrates a control channel allocation result obtained from this stage. In this figure, all of the three channels are used as control channels. Each node turns its radios on different control channels.

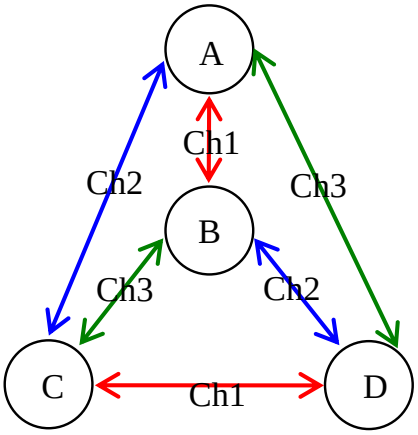

Figure 5-2. Control Channel Allocation Result Obtained from the First Stage

On the second stage, a REQ/ACK/RES mechanism is used to dynamically allocate channels for data transmission. Control messages (i.e., beacon, data pilot, REQ, ACK, RES) are transmitted over allocated control channels on the first stage. Similar to the RTS/CTS mechanism, the REQ/ACK/RES also has an exponential backoff mechanism to avoid collision.

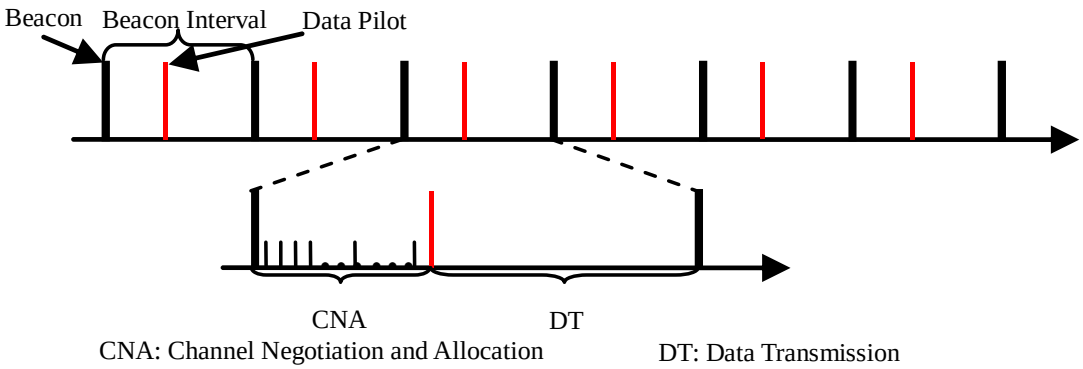

Figure 5-3. Time Division Method in TSC-M2MAC

On the second stage in TSC-M2MAC, the timeline is divided into equal beacon intervals. The periodical data pilots further divide each beacon interval into the CNA sub-interval and the DT sub-interval, as shown in Figure 5-3. The CNA sub-interval is used for channel allocation for data packets. In CNA, control messages like REQ, ACK, and RES are exchanged over the allocated control channels. The REQ/ACK/RES mechanism can allocate every communication radio-pair with an appropriate channel for data packets. We exploit the AAA for the CNA sub-interval to cope with the variation of NCTF. In the DT sub-interval, data packets are transmitted over the negotiated data channels.

The sequence diagram for control messages exchanging and data packet transmission is as Figure 5-4.

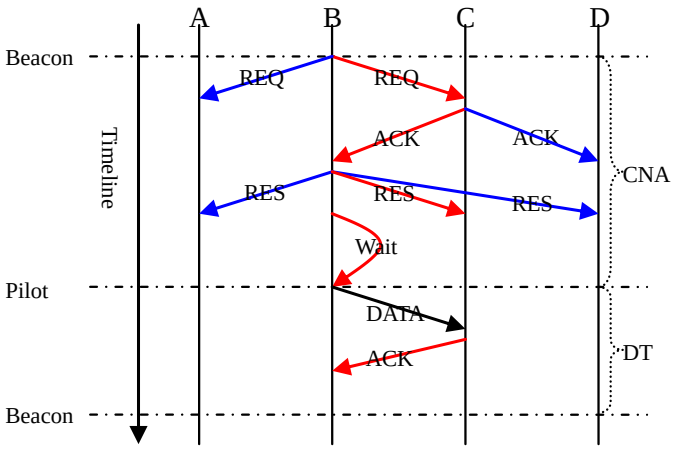

Figure 5-4. Sequence Diagram for Control Message Exchanging and Data Transmission

5.3 Admissible Conditions for New Wireless Links

Generally speaking, NCTF in the network is much bigger than NOC. So, it is inevitable that more than one wireless link, i.e., the links between the receiver and the transmitters in the sensing range of the receiver, share one channel. To schedule a new wireless link to share a channel, the schedule algorithm should be satisfied with two conditions. First, the interference caused by the new link should not lead to decoding errors in the existing receiving nodes operating on the channel. Second, the existing interference in the channel should not be strong enough to impact the correct decoding

on the receiving node of the new wireless link. The method to determine these two conditions is as follows.

To correctly decode packets at the receiver, $Rx(l_i)$, of the i^{th} link, l_i, the received SINR should be greater than a predefined threshold γ if we assume that the threshold is the same for all the radios in the network. Such a condition can be expressed by:

$$\frac{P_r(l_i)}{N+\sum_{l_j, j\neq i} I_{Rx(l_i)}^{Tx(l_j)}} > \gamma \Leftrightarrow \sum_{l_j, j\neq i} I_{Rx(l_i)}^{Tx(l_j)} < \frac{P_r(l_i)}{\gamma} - N \tag{5.1}$$

Here, l_i and l_j are the i^{th} and the j^{th} link operating on the same channel, respectively. $Tx(l_i)$ and $Rx(l_i)$ are the transmitter and receiver of the link l_i, respectively. $P_r(l_i)$ is the receiving power at $Rx(l_i)$ due to the transmitter $Tx(l_i)$. N is the background noise power. $I_{Rx(l_i)}^{Tx(l_j)}$ is the received interference power at $Rx(l_i)$ due to the transmitter $Tx(l_j)$ of link j operating on the same channel. If the two-ray ground propagation model is used, $I_{Rx(l_i)}^{Tx(l_j)}$ can be easily calculated according to [113].

The current maximum admissible interference power (CMAIP) of the receiver on the link l_i in the channel can be obtained from (5.1) as:

$$CMAIP\left[Rx(l_i)\right] = \frac{P_r(l_i)}{\gamma} - \sum_{l_j, j\neq i} I_{Rx(l_i)}^{Tx(l_j)} - N \tag{5.2}$$

Then, the interference power P_{itf}, incurred by the new wireless link, which will be scheduled on the same channel with l_i, should be less than the minimum value of the CMAIP of all links on this channel. This interference can be represented as:

$$P_{itf} < \min_{l_i}\left\{CMAIP\left[Rx(l_i)\right]\right\} \tag{5.3}$$

Similarly, the interference power with the new wireless link due to the links on the target channel can also be obtained. The interference power should also satisfy (5.1).

When any new wireless link is scheduled to use or release the channel, P_{itf} should be updated.

5.4 Control Channel Allocation Algorithm

The conflict graph is applied to minimize the co-channel interference in the cellular network in [114]. Then, the vertex coloring algorithm (VCA) is exploited to determine whether a set of transmissions can occur simultaneously or not. The conflict graph in WMN can be constructed as follows. Consider a graph, *G*, with vertices corresponding to mesh nodes and with edges corresponding to the single hop wireless links. The resulting conflict graph, *F*, which comes from *G*, has vertices corresponding to the edges in *G*, and has an edge between vertices in *F* if and only if the wireless links denoted by the vertices in *F* interfere with each other in the network topology. For example, in Figure 5-5-(a), there are three single-hop wireless links: BA, BC, and BD. The corresponding conflict graph should be as shown in Figure 5-5-(b). Obviously, if three different orthogonal channels are allocated to the vertices in Figure 5-5-(b), and node B has at least 3 radios tuned on different channels, there would be no interference among the 3 links. However, in practical networks, it is impossible to equip any node with an unlimited number of radios in most cases. For instance, if there are only two radios equipped on node B, that node cannot operate on three orthogonal channels simultaneously. So, its conflict graph cannot be directly applied to our system model without a constraint on the number of radios.

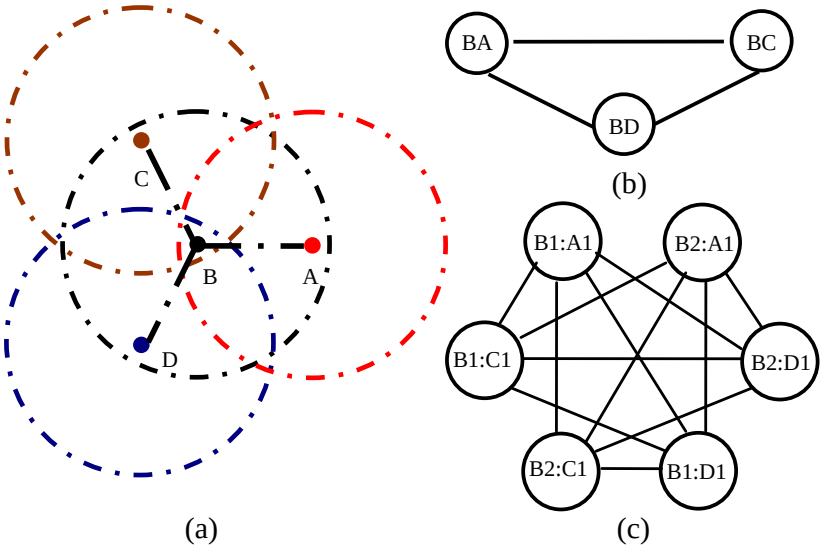

Figure 5-5. (a) Network topology; (b) Conflict graph; (c) MCG

To tackle the above problem, a Multi-radio Conflict Graph (MCG) is proposed to model the interference in [95], which this chapter calls the Rama scheme. Edges between radios on different nodes are represented as vertices in MCG rather than representing them between nodes in the conflict graph. Thus, the construction of MCG can be described as follows. First, each radio in the mesh network is represented as a vertex in the topology graph $G^{'}$. The edges in $G^{'}$ are between radios on different nodes. Then, the vertices in the MCG, notated as M, are represented as the edges in $G^{'}$. The edges between the vertices in M are created in this way, i.e., two vertices in M have an edge between each other if the edges in $G^{'}$ (as represented by the two vertices in M) interfere with each other. Figure 5-5-(c) is the corresponding MCG of the network topology illustrated in Figure 5-5-(a). The MCG comes with the constraint that nodes A, B, C, and D must be equipped with 1, 2, 1, and 1 radio(s), respectively. In Figure 5-5-(c), the vertex (B2:C1) represents the wireless link between the second radio on node B and the first radio on node C.

To ensure connectivity, the Rama scheme requires that at least one radio of each node tunes to the single common channel, which is also used as the single CCC, and one of data channels. Additionally, regarding coloring any vertex in MCG, the Rama scheme has a constraint that all uncolored vertices in MCG that contain any radio from the just-colored vertex must be removed. In this case, this method will lead to a considerable imbalance in load among channels and serious co-channel interference on the common channel, which in turn significantly degrades the network performance. For example, if node A in Figure 5-5-(a) is closest to the gateway, after allocating channel 1 and 2 to link AB and BC, respectively, all the vertices in Figure 5-5-(c) should be removed. In this case, link BD should be allocated a randomly selected channel without considering the interference and load according to the Rama scheme.

Unlike our method in the Rama scheme, we discard the requirement in TSC-M2MAC as well as the constraint in the Rama scheme. Instead, we avoid the scenario of removing the vertices representing the wireless links to which orthogonal channels are unallocated, from the view of the mesh node rather than the radio. For example, after allocating channels to link AB and BC, vertices like (B1:D1) and (B2:D1), which present the unassigned link BD, should not be removed.

Without loss of generality, assume that there are N nodes in a WMN, and that node K has N_K radios, denoted by $R_K = \left(K_1, K_2, \ldots, K_{N_K}\right), K \in \left(1, \ldots N\right)$. Then, the wireless links between the radios on node P and Q can be denoted by

$$S_{PQ} = \left\{ Ps : Qt \middle| \left\langle Ps, Qt \right\rangle \in R_P \times R_Q \right\}, P, Q \in \left(1, 2, \ldots N\right) \tag{5.4}$$

Where "×" represents the operation of the Cartesian product. Obviously, if node P and node Q are in transmitting range of each other, such a link exists; otherwise, it does not exist and can be denoted by $\boldsymbol{0}$. Clearly, $S_{PP}=\boldsymbol{0}$, $P \in (1, 2, \ldots, N)$. As a result, the wireless links in the mesh network can be represented by a matrix:

$$S = [S_{PQ}]_{N \times N} = \begin{bmatrix} 0 & S_{12} & \cdots & S_{1N} \\ S_{21} & 0 & \cdots & S_{2N} \\ \vdots & \vdots & \ddots & \vdots \\ S_{N1} & S_{N2} & \cdots & 0 \end{bmatrix} \tag{5.5}$$

In order to solve the problem in the Rama scheme and to ensure only one channel is allocated to each radio, a significant constraint should be imposed in CCAA when using BFS-based VCA to color the MCG: once any vertex (Ps,Qt) is colored, then all the vertices corresponding to the wireless links in S_{PQ} should be completely removed. In this way, there could exist a scenario whereby there are not enough orthogonal channels to be allocated to the links in the interference range, or there may be an insufficient number of radios on the node. In this case, some of these links must share channels, although interference will occur when transmitting and/or receiving simultaneously. Such a scenario is inevitable when the scale of a network is large and the density of nodes is intensive. To minimize co-channel interference in such a scenario and to balance the load on each channel, the sharing channel should be selected according to the hop counts of the node from the gateway and the accessible conditions for new wireless links. The links with less hop counts should be assigned higher priority to share channels that have a smaller number of links, considering the traffic pattern in WMN. So, the uncolored vertices encountering this scenario should try to share channels that have links of the same priority. In this way, the connectivity of the network is ensured and the topology remains unchanged. The CCAA is demonstrated in Table 5-1.

Table 5-1. Control Channel Allocation Algorithm (CCAA)

Initialization: $V=\{v|v \in MCG\}$; $C=\{all\ \ channels\}$; $h=1$;
while $h<=maximumHopCount$ **do**
  $Queue=\{v|v \in V$ and $notVisisted(v)$ and $hopCount(v)=h\}$
  while $size(Queue)>0$ **do**
    $v_{current}=popHead(Queue)$
    if $visited(v_{current})=True$ ***then***
      continue
    end if
    $visit(v_{current})$
    $V_{neighbor}=\{v|v \in V$ and $edge(v,v_{current})$ exists $\}$
    $V_{temp}=\{v|v \in V_{neighbor}$ and v has been visited$\}$
    $V'_{temp}=\{v|v \in V_{neighbor}$ and v has not been visited$\}$
    $C_{available}=\{c|c \in C$ and c does not conflict with the channels that had been assigned to $v_i \in V_{temp}\}$
    while V'_{temp} is not empty **do**
      if $C_{available}$ is not empty **then**
        Assign a randomly selected channel from $C_{available}$ to v_m, $\{v_m \in V'_{temp}\}$
        Remove all the vertices corresponding to S_{PQ} from MCG with $(Ps:Qt)$ denote V_m
        Update V_{temp}, V'_{temp} and $C_{available}$
      else
        Assign channel to v_m, $\{v_m \in V'_{temp}\}$ according to the admissible condition
        Remove all the vertices corresponding to S_{PQ} from MCG with $(Ps:Qt)$ denote V_m
        Update V_{temp}, V'_{temp} and $C_{available}$
      end if
    end while
  end while
  $h=h+1$
end while

In contrast to the single CCC in the Rama scheme, CCAA uses all available channels as control channels. This type of allocation can indicate which radio on each node should tune to which channel to exchange control messages. It also requires few system resources as long as the executing frequency is not large, which is crucial for the gateway. If the gateway is overloaded, then it will not have enough resources to deal

with functions like forwarding packets between the mesh network and the outside Internet.

In addition to these advantages, CCAA perfectly solves the broadcast problem in multiple control channels because of two factors. First, it ensures the connectivity of the nodes in WMN. Second, the CRUS, defined in section 5.1, is shared by all radios on each node and can therefore ensure that all radios are accessible as long as one of them on the node captures the broadcast packet. In these ways, CCAA can reduce the overhead caused by transmitting duplicated broadcast packets in the previous broadcast mechanism.

5.5 Dynamic Data Channel Allocation

5.5.1 Criterion Determining the Channel and Radio Utilization structure (CRUS)

In TSC-M2MAC, the available channels are categorized into two groups: idle channels and busy channels. The priority for every idle channel is the same, and they are selected randomly. The priority of idle channels is higher than that of busy channels. For busy channels, the priority for each channel is determined by CMAIP, as defined in (5.2). The more interference a channel has, the lower its priority is. If CMAIP is the same, then the channel with the lowest traffic load has the highest priority. CRUS is a data structure consisting mainly of three items: node ID, a list of sorted available channels in terms of priority, and a map indicating the radios' channel utilization on the node. Every node maintains its own CRUS.

5.5.2 Dynamic Channel Allocation for Data Transmission

In TSC-M2MAC, a REQ/ACK/RES mechanism is used to allocate the channels for data transmission. All control messages are exchanged over the CCAA's resulting channels. The second coordination stage contains five steps:

Step 1: Once a beacon comes, if a source node (node B) has data pending for a

destination (node C), B should check its $CRUS_B$ to find whether a radio and an available channel can be used for data transmission. If so, B waits for T_{DIFS} and a random exponential backoff value, and then transmits a packet REQ($CRUS_B$) to C and broadcasts it to B's neighbors. If node B does not have data pending, then B must wait until the next beacon comes.

Step 2: Once node C receives the packet REQ($CRUS_B$), C has to check whether it has idle radios. If it does not, then C sends an acknowledgment message ACK(INVALID) to B and broadcast it to C's neighbors to inform them that all radios on C are busy. If it does have idle radio, then C needs to select a channel for data transmission according to $CRUS_B$ and $CRUS_C$. If the intersection between $CRUS_B$ and $CRUS_C$ is empty, node C sends an ACK(NULL) message to tell B that no channel is available for data transmission, and also broadcasts it to C's neighbors. It is clear that whether a receiver can decode the data correctly or not depends only on the SNIR at the receiver. So, it has no relation to $CRUS_B$ on the condition that a common channel can be found in the intersection between $CRUS_B$ and $CRUS_C$. Therefore, if the intersection is not empty, then the channel to be selected should be satisfied with one condition: it must have the highest priority in the intersection between $CRUS_B$ and $CRUS_C$, according to the sorted priority of $CRUS_C$ rather than $CRUS_B$. If the channel selected by C is CH_k, then the C will send the ACK(CH_K) to B and broadcast it to the neighbors of C.

Step 3: Once B receives the ACK message, it will check whether the information carried by ACK is NULL, INVALID, or CH_K. If it is NULL or INVALID, B cancels the negotiation process and goes to step 1. If it is CH_K, then B will check if this channel can still be used. If that is the case, B updates its $CRUS_B$ and then broadcasts a reservation message RES(CH_k) across the network. When C receives this reservation message, it updates its $CRUS_C$.

Step 4: After the exchanging process for control messages is finished, both B and C have to wait for the coming of the data pilot.

Step 5: All the nodes start to transmit data to their destinations when the data pilot arrives, and they continue to transmit data until the next beacon comes.

One must note that all the control messages, REQ, ACK, and RES, are transmitted over the allocated control channels from the first coordination stage. On this stage, CCAA is able to indicate the mapping relationship for which radio should be tuned to which control channel. Obviously, the hidden node problem can be alleviated in TSC-M2MAC. For example, there are three nodes, A, B and C. The pairing of A and B and the pairing of B and C are within the transmission range of each other, respectively. But, the pairing of A and C are beyond the transmission range of each other. If a channel is assigned to the link between A and B, it would not be selected from $CRUS_B$ when C negotiates the transmission channel with B.

5.6 AAA for CNA Sub-interval

In TSC-M2MAC, the fixed size of the CNA sub-interval greatly impacts the network's performance. Performance mainly depends on the NCTF scheduled on each orthogonal channel. If the NCTF is small, it will require a short time for negotiation and will need a small size of CNA sub-interval. Otherwise, the collision probability of control messages will become high, and the negotiation will take more time, which requires a large size of CNA sub-interval. So, its size should be adaptively adjusted according to the practical NCTF. On the other hand, the CNA size should not be infinitely increased, since enough time should be left for data transmission. So, a threshold should be set to limit the increase of the CNA size. If the CNA size has been equal to the threshold, those communication pairs that have not yet finished negotiation will be denied. Such a threshold heavily depends on the network's topology and its traffic patterns, so the threshold should be determined according to the practical case.

In addition, the efficiency of AAA heavily depends on whether the scheduling of traffic flows on the available channels is balanced or not, because the same time division method is used for all the channels. For example, if one channel was overloaded whereas others were under-loaded, there would be no ideal dynamic adjustment scheme available. Consequently, in TSC-M2MAC, load balancing should be taken into consideration on both coordination stages.

To cope with the instability of the network, the size of the CNA sub-interval can only be increased or decreased a one-step size. In the meantime, when the size is

decreased, a margin of one step size should be reserved so that it can be used to avoid CNA oscillation and also to ensure that the size of the CNA sub-interval is able to converge into a stable state. The AAA of the CNA sub-interval is in Table 5-3, and the related notations in the algorithm are in Table 5-2.

Table 5-2. Notations in AAA for CNA Sub-interval

Notations	**Meaning**
CNA	The size of CNA sub-interval
CNA_{min}	The minimum size of CNA sub-interval
CNA_{max}	The maximum size of CNA sub-interval
Step	The length of time that the CNA sub-interval takes to increase or decrease one time
$AccIdleT_i$	The accumulated idle time of channel *i*
$Threshold_{adj}$	The threshold to adjust the size of CNA sub-interval

Table 5-3. AAA for CNA Sub-interval

Initialization: All the radios begin with $CNA = CNA_{min}$

When time approaches the end of *CNA*

if $minimum(AccIdleT_i) <= Threshold_{adj}$ **then**

if $CNA_{max} <= CNA + Step$ **then**

$CNA = CNA_{max}$

else increase *CNA* by step

end if

else if $minimum(AccIdleT_i) > CNA + Step$ **then**

if $CNA - Step < CNA_{min}$ **then**

$CNA = CNA_{min}$

else decrease *CNA* by *Step*

end if

else

remain *CNA* unchangeable

end if

Repeat the above process until all the events are scheduled

In TSC-M2MAC, the gateway executes such an adjustment algorithm. The algorithm may occupy much system resource in order to time synchronize and coordinate all nodes. So, similar to CCAA, it should also be executed for a relatively long period rather than every time interval if the traffic pattern varies slowly.

5.7 Power Saving Mechanism in TSC-M2MAC

Energy consumption is a key challenge that requires an urgent solution due to current concerns about cost, the environment, the limitation of non-renewable resources, etc. Various types of measures can be taken to tackle this problem. However, this chapter will focus only on how to intelligently let radios on each node transit among the state space to save power without adversely affecting the performance of the network.

5.7.1 Problem Formulation

A radio usually has the following four states: busy (transmitting or receiving), idle (ready to transmit or receive data), doze (cannot transmit or receive and thus consuming little energy) and off state (consuming no energy). Table 5-4 outlines the energy consumption of two typical commercial radios [115-117]. It shows that energy can be saved by switching a radio from idle state to doze state if it has no packets to exchange. When they are needed, the radios in doze state should be awaked. The switching process among state spaces can be described by a discrete event dynamic system. In the process, the transition is driven by different events that are arriving at the system. Each event is triggered by the timeout mechanism set on each radio. For each arrived event, corresponding decisions should be made according to the given rules. Consequently, energy consumption in TSC-M2MAC can be formulated as an optimization problem: how to make a decision for each radio when a new event comes such that the total energy consumption is minimized subject to the constraint that the requirement for system performance is satisfied. The main assumption in the proposed PSM is that the time spent on transition from one state to another is far less than the time interval used in the proposed TSC-M2MAC protocol. Otherwise, such a mechanism will become meaningless.

Table 5-4. Power Consumption (unit: watt)

Type	***Tx***	***Rx***	***idle***	***doze***
Laucent WaveLAN	1.65	1.4	1.15	0.045
Cisco AIR-PCM 350	1.88	1.3	1.08	0.045

The off state is not considered in the proposed PSM, since it is different to awake. As a result, the state space contains three states: S={busy, idle, doze}. The event set can be represented as E={Et, t⩾0}. The decision space can be denoted by D={D1, D2, …, Dn}. Below, the state evolution process is illustrated by Figure 5-6.

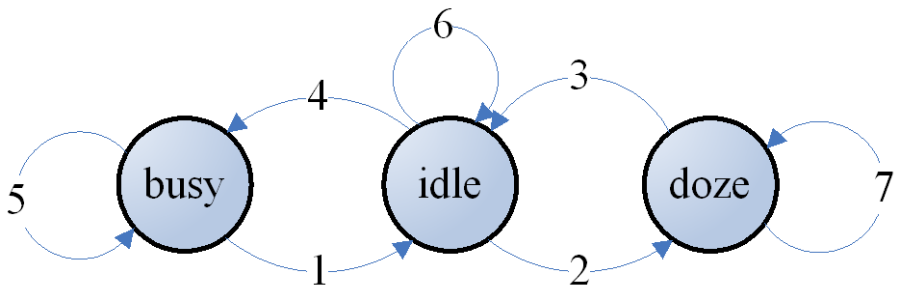

Figure 5-6. The state evolution process of each radio

5.7.2 Decisions for Power Saving

As far as the radios in our scheme are concerned, there are only 7 decisions (denoted by the numbers 1 to 7 shown in Figure 5-6) no matter which event comes. Among them, only decision 2, 3, and 7 are related to power saving. The mapping relationship between events and the 3 decisions can be described as follows:

Decision 2: this decision will be made if two conditions are satisfied. First, the period between the epoch when one radio finishes transmitting or receiving messages and the following time indicator (beacon or pilot) is longer than the time spent on the sleeping process (transition from idle to doze) and the waking process (inverse transition). Second, the saved energy by means of making the decision is larger than the additional energy spent on the sleeping and waking processes.

Decision 3: if the following time indicator is a beacon, then such a decision should

be made at the moment of a period spent on the waking process before the next beacon comes. If the following time indicator is a pilot and the radio also has data to exchange, then this decision will be made at the moment of a period spent on the waking process before the next pilot comes.

Decision 7: this decision will be made if the radio finishes the coordination during the CNA sub-interval and has no data to exchange with other radios.

Decision 3 indicates that the radio can transit from doze state to idle state through the timing mechanism, which does not require any additional control information. The timing mechanism can also be used in decision 7.

As a result, as long as events corresponding to the three decisions listed above come, the resulting action from the corresponding decision will be taken. Consequently, these economical decisions can decrease the total energy consumption.

5.8 Simulation-based Performance Evaluation

5.8.1 Performance of the Control Channel Allocation Algorithm (CCAA)

From section 4, it can be seen that the CCAA mainly depends on the network topology, NOC, the traffic pattern, etc. It is difficult to completely evaluate the algorithm from all aspects. So, we use the case study method to simplify the simulation. We assume that there is one gateway, 3 available orthogonal channels, 10 and 100 nodes with one and two hops respectively from the gateway. We use the throughput fairness index defined in [118] to measure the load balancing, i.e., throughput balancing among available channels. Obviously, the higher the fairness index is, the better the performance is, in terms of load balancing. We compare the proposed CCAA with the Rama scheme using different randomly generated topologies.

Table 5-5. Fairness Index with Randomly Generated Topologies

Topology	**1st**	**2nd**	**3rd**	**4th**	**5th**
CCAA	0.72	0.68	0.86	0.83	0.79
Rama scheme	0.47	0.44	0.52	0.54	0.63

Table 5-5 shows that the proposed CCAA outperforms the Rama scheme with respect to fairness of throughput among available channels. The reason why the fairness for CCAA is less than 1 is that the links closer to the gateway have higher priority on allocating channels than those far from the gateway. Load balancing plays an important role in the proposed TSC-M2MAC, since the channels with the heaviest load determine the size of the CNA sub-interval, and this determination significantly impacts the network's overall performance.

5.8.2 Performance of TSC-M2MAC

5.8.2.1 Efficiency of TSC-M2MAC

The performance of TSC-M2MAC is characterized by efficiency and stability. We use average aggregated throughput and end-to-end packet delay to evaluate its efficiency, and we use packet loss rates to evaluate its stability, similar to [119-121]. Although few similar protocols with TSC-M2MAC exist in the previous literatures, measures have been taken to decrease the contentions in the single CCC [122-125]. To evaluate the efficiency of the proposed TSC-M2MAC, we compare it with three schemes: 1) the "pure" IEEE 802.11 MAC protocol with a single CCC and a single data channel; 2) the Rama scheme, proposed in [95], with a single CCC and multiple data channels; 3) the enhanced Rama (en_Rama) scheme with an additional mechanism of the adaptive contention window proposed in [122]. We apply the same number of orthogonal channels in all of our comparisons of the TSC-M2MAC, Rama, and en_Rama. Additionally, to evaluate the stability of the TSC-M2MAC, we observe the packet loss rate when the aggregated transmission rate is increased from a small value to a value that is large enough to saturate the network. We perform the simulations using the ns2 simulator with CMU wireless extensions [126]. The number of radios equipped

on each node is a uniformly distributed integral number with two bounds: the lower bound is 1 and the upper bound corresponds to the number of orthogonal channels. The handover time for a radio from one channel to another is assumed to be 224 μs, and the time interval is assumed to be 100ms (refer to [8, 89]). In this part, we set the size of the CNA sub-interval as a fixed value (20% of the time interval) and we devote the rest of the time interval for DT. We will simulate the AAA of the CNA sub-interval in part 8.3. The following common parameters are used in the simulation. The radio power and threshold levels are set such that the transmission range and the carrier sensing range are 250m and 550m, respectively. The bandwidth of each channel (including the CCC and data channels) is 1Mbps. We use a wired-cum-wireless topology on a 1500m-by-1500m area with one gateway, one wired node, and 23 randomly positioned wireless nodes in the wireless domain of the gateway. The bandwidth, delay, and propagation model of the duplex-wired link between the wired node and the gateway are 100Mbps, 1ms and drop tail, respectively. The two-ray ground reflection model is used to model the wireless propagation. There are 13 CBR flows with source-destination pairs. Three of the CBR flows are destined to the wired node via the gateway, and the others are random selected pairs. Each simulation is performed long enough to saturate the network. Each data point in the plot has the averaged value of 30 runs with different topologies. The error bars show 95% confidence intervals for the difference of each run.

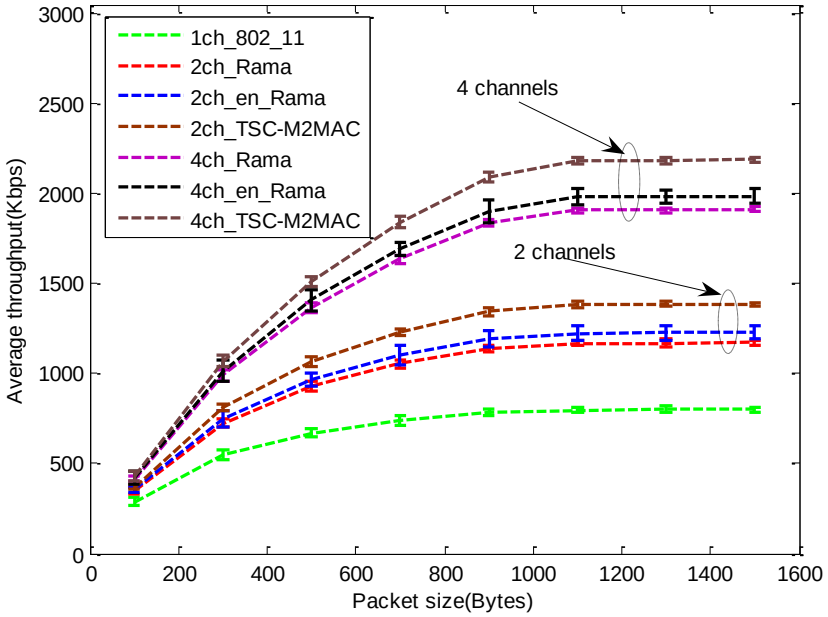

Figure 5-7. Average aggregated throughput with different packet sizes

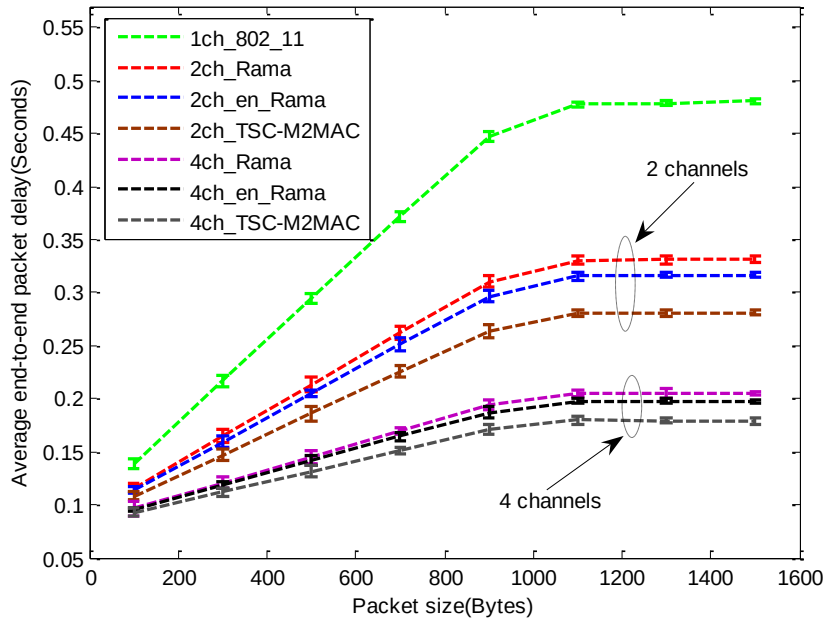

Figure 5-8. End-to-end packet delay with different packet sizes

We plotted the average aggregated throughput and the average end-to-end packet

delay in Figure 5-7 and Figure 5-8, respectively, for the TSC-M2MAC, pure 802.11, the Rama schemes, and the enhanced Rama scheme with an adaptive contention window. The abbreviations in Figure 5-7 and Figure 5-8 are as follows: 1ch_802_11 denotes the 802.11 scheme; 2ch_TSC-M2MAC, 4ch_TSC-M2MAC denote the TSC-M2MAC with 2, 4 orthogonal channels, respectively; 2ch_Rama, 4ch_Rama denote the Rama scheme with 2, 4 orthogonal channels, respectively; and 2ch_en_Rama, 4ch_en_Rama denote the enhanced Rama scheme with 2, 4 orthogonal channels, respectively. Figure 5-7 depicts that: 1) the average aggregated throughputs increase as the number of orthogonal channels increases in TSC-M2MAC, Rama, and enhanced Rama schemes for any specific packet size; however, the throughputs achieved by TSC-M2MAC using 2 and 4 channels are always higher than the throughputs achieved by Rama and enhanced Rama schemes using the same number of channels, although enhanced Rama can achieve higher throughput than Rama, which shows the efficiency of the utilization of multiple control channels; 2) the increasing speed of the throughputs becomes moderate with the increase in packet size when the packet size is less than 1100bytes; and the throughputs become nearly stable when the packet size is larger than 1100bytes; 3) TSC-M2MAC, Rama, and enhanced Rama schemes can achieve much higher throughputs than 802.11, and this shows the advantage of using multiple orthogonal channels; 4) the improvement on throughput over 802.11 MAC is still less than *k* times when *k* orthogonal channels are used in TSC-M2MAC, which may be caused by the fact that the REQ/ACK/RES is more complex and requires more coordination time than the RTS/CTS used in 802.11. In short, utilizing multiple orthogonal channels for data transmission within a single control channel can improve higher throughput over 802.11. Also, the TSC-M2MAC with multiple control channels outperforms the Rama and the enhanced schemes with a single common control channel in terms of throughput when the same number of in-band orthogonal channels is used.

Figure 5-8 shows the comparison of the average end-to-end packet delays in the TSC-M2MAC, Rama, enhanced Rama, and 802.11 schemes as the packet size increases. The results indicate that: 1) the delay decreases as the number of orthogonal channels increases when it has the same packet size; 2) the delays increase with the increase in packet size when the packet size is smaller than 1100 bytes, and it becomes nearly stable when it is larger than 1100 bytes in all three schemes; 3) the increasing speed of

delays becomes moderate with the increasing of packet sizes for any specific number of channels; 4) the delays in both TSC-M2MAC and Rama schemes are lower than those in 802.11; 5) the delay in TSC-M2MAC is always lower than the delay in Rama and in the enhanced Rama schemes with the same orthogonal channels, although enhanced Rama can achieve lower delay than the Rama scheme. In short, the utilization of multiple control channels can achieve lower end-to-end packet delay than that of a single, dedicated common control channel.

Figure 5-7 and Figure 5-8 show that TSC-M2MAC can achieve the highest throughput and the lowest end-to-end packet delay among the four schemes. On the opposite end of the spectrum, the 802.11 scheme has the worst performance in terms of throughput and delay. It can be seen that the proposed TSC-M2MAC can further improve the throughput and reduce end-to-end packet delay better than the Rama and enhanced Rama schemes using the same number of orthogonal channels. This ability shows the advantage of using multiple control channels over a single common control channel, and the TSC-M2MAC does not face the bottleneck that arises in the single dedicated CCC. Notice the fact that the existing 802.11a, 802.11b/g can provide 13 and 3 available orthogonal channels, respectively, and the widely used 802.11 MAC wastes a lot of spectrum resource, resulting in performance degradation; it is therefore the worst one among the 4 schemes compared here.

5.8.2.2 Stability of TSC-M2MAC

In our stability evaluation, we use the same parameters as we used in section IV-A. Similar to [119-121], packet loss rate is selected as the evaluation metric. We observe the packet loss rate when the transmission rate increases with a specific packet size (210 bytes). We use the packet loss rate of the pure IEEE 802.11 as the baseline. The packet loss rate appears in Figure 5-9.

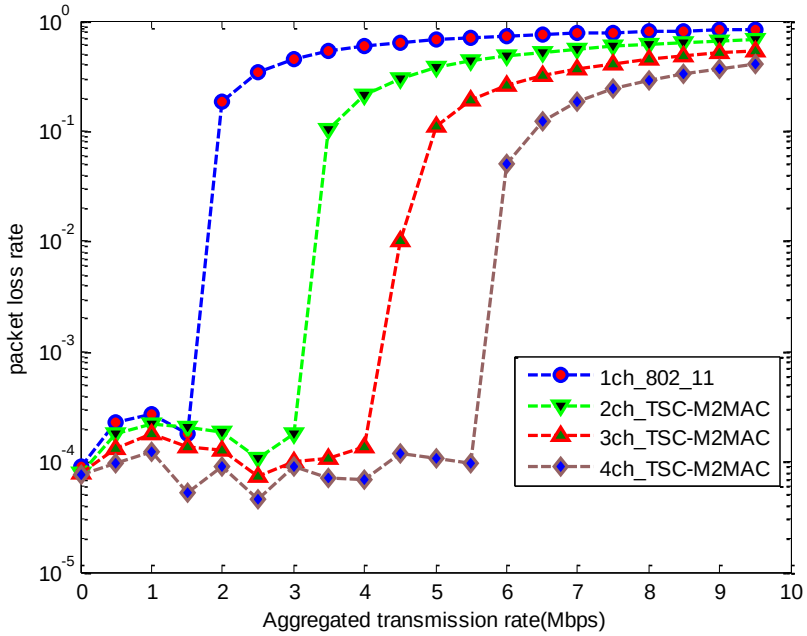

Figure 5-9. Packet loss rate with a given packet size (210 bytes)

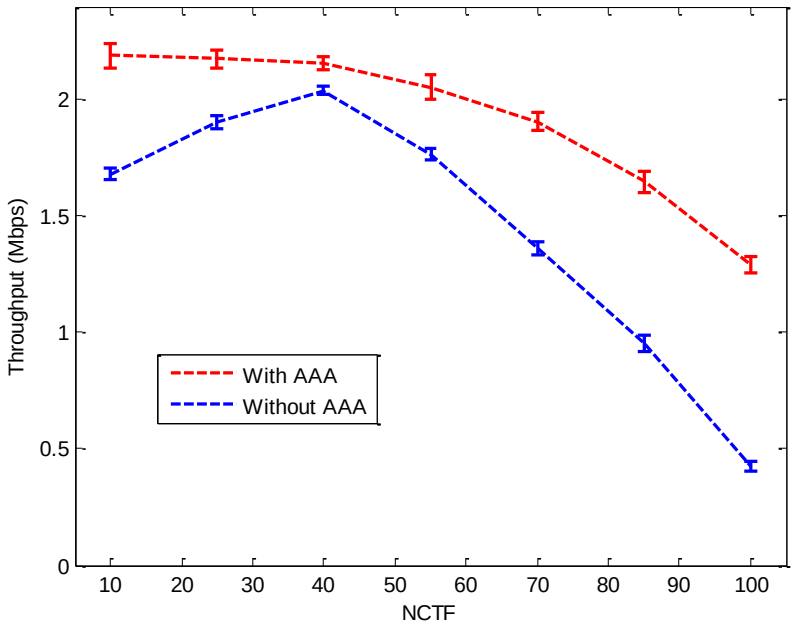

Figure 5-10. Impact of AAA on the throughput

Figure 5-9 shows that the packet loss rate in both pure 802.11 and TD-MAMAC fluctuate before the network is saturated. Recall that the bandwidth of each channel is

assumed to be the same, but the corresponding aggregated transmission rates for saturation with a different number of channels appear differently in Figure 5-9. This appearance also indicates that both pure 802.11 and the proposed TSC-M2MAC will become stable when the network saturates. In addition, Figure 5-9 shows that the packet loss rate decreases with the increase in the number of orthogonal channels. Since the loss rate is defined as the ratio between the number of packets unsuccessfully accepted by the destinations and the total transmitted packets, all 4 curves approach 100% when the transmission rate increases.

5.8.3 Evaluation of AAA for CNA sub-interval

As mentioned before, the contention time for channel negotiation has a dominating impact on the performance of TSC-M2MAC. Thus, at first, we simulate the consumed contention time as NCTF increases, as shown in Table 5-6. Table 5-6 indicates that the average contention time increases sharply as NCTF increases, because the exponential backoff mechanism begins when collision happens.

Table 5-6. Averaged contention time vs. Number of concurrent traffic flows

NCTF	10	25	40	55	70	85	100
Contention time (ms)	3.78	7.31	12.61	23.07	38.44	57.81	80.62

We also apply a case study method to evaluate the efficiency of the proposed AAA of the CNA sub-interval, since the measurement varies with many factors, such as NOC, NCTF, etc. We take 4 available channels as a special case and measure the aggregated throughput as the NCTF increases. In the simulation, we set the threshold for the CNA sub-interval at 50ms, which is half of the time interval. We compare the achieved throughput by exploiting AAA of the CNA sub-interval, with that employing a fixed CNA sub-interval to 20ms. Figure 5-10 shows that the throughput achieved using AAA is always higher than that using fixed CNA size. It also shows that the throughput with AAA drops slowly and sharply when NCTF is less and more than 40, respectively. This is because the time available for data transmission becomes shorter and shorter as NCTF increases. However, with the fixed CNA sub-interval, the throughput increases when NCTF is less than 40 and drops rapidly when NCTF is more than 40. This is

because the CNA sub-interval is so large that it becomes wasteful when there are few concurrent flows, and then it becomes too small for negotiation, resulting in service denial for the flows not finishing negotiation when NCTF becomes large. It also shows that when there are 100 concurrent flows, the achieved throughput for the fixed CNA sub-interval is much less than that for the AAA case. The reason is that too many flows with large contention time are denied for the fixed sub-interval case, while for AAA, time for negotiation can occupy as much as half of the time interval, which is much larger than the fixed CNA sub-interval. Thus, the adaptive adjustment of CNA outperforms the fixed case in terms of aggregated throughput.

5.8.4 Performance of the Power Saving Mechanism

In order to evaluate the performance of the proposed PSM with a simple simulation, we must establish a few main assumptions. First, the buffer on each node is infinite and there is always data to transmit. Second, the sequence of the packet for transmission follows the rule of FCFS (First Come, First Serve). Third, the transmitted data for each request follows an exponential distribution with a mean equal to 100M bits. Fourth, the powers of the radio on each state are referred to the interface card of *Laucent WaveLAN*, and the data transmission rate on each channel is 1Mbps. Each point in the plot is the average of the achieved results of our simulation, which made 30 runs at different seeds. In our simulation, we take the scenario with two orthogonal channels as an example to demonstrate the performance of the proposed PSM. It is easy to generalize such a mechanism to other scenarios with variant numbers of orthogonal channels. The consumed energy with and without PSM is compared in our simulation.

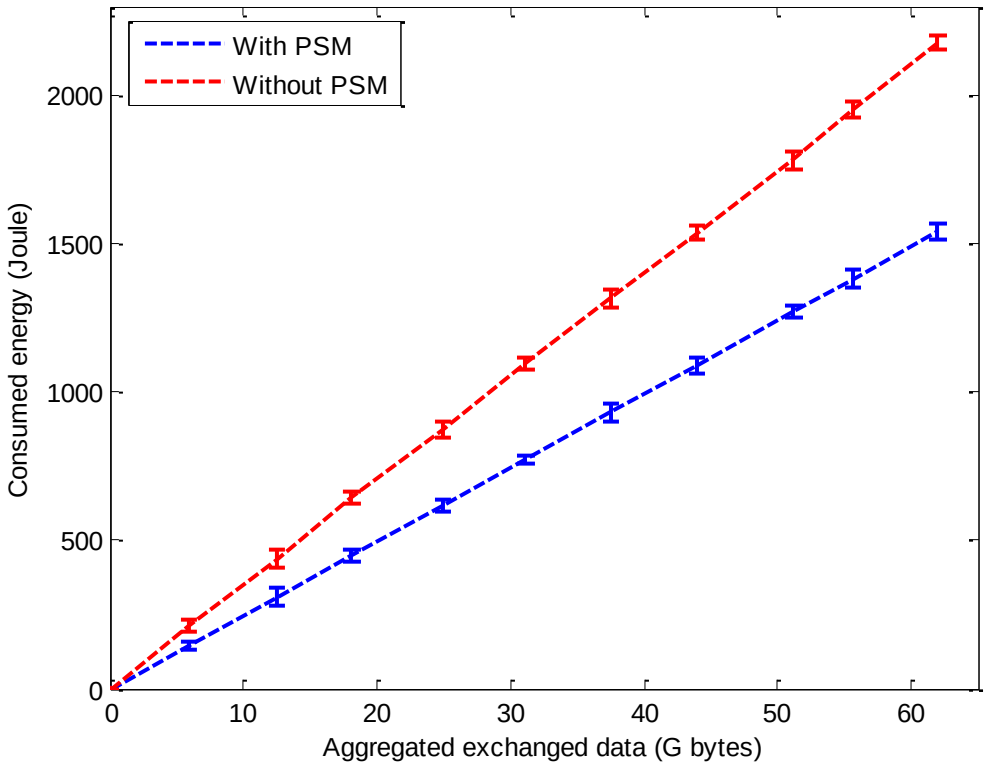

Figure 5-11. Performance of the power saving mechanism (PSM)

The comparison of energy consumption with and without PSM is shown in Figure 5-11. We have calculated that the energy saved in the case with PSM is approximately 29% compared to the energy in the case without PSM. It can therefore be expected that the system with PSM can save more energy during the period of less requests from clients, e.g., the period near dawn for the multimedia Video on Demand (VoD) system.

5.9 Conclusions

Instead of using a single dedicated Common Control Channel (CCC), the proposed TSC-M2MAC designates all available channels as control channels on the Channel Negotiation and Allocation (CNA) sub-interval and the data channels on the Data Transmission (DT) sub-interval in a time division manner through a two-stage coordination. On the first coordination stage, a Multi-radio Conflict Graph (MCG) is used to model the co-channel interference, and the Breadth-First-Search (BFS)-based

Vertex Coloring Algorithm (VCA) is used to realize an intelligent control channel allocation. As a result, the co-channel interference decreases. On the second stage, a REQ/ACK /RES mechanism is proposed to implement the dynamical channel allocation for data transmission. The hidden node problem is successfully alleviated by using a Channel and Radio Utilization Structure (CRUS). Then, the problems that arise from the variation of Number of Concurrent Traffic Flows (NCTF) are mitigated using the Adaptive Adjustment Algorithm (AAA) for the CNA sub-interval. Simulation results show that TSC-M2MAC can achieve load balancing among multiple channels; as the NCTF increases, it can achieve higher throughput and lower end-to-end packet delay than conventional methods. Also, TSC-M2MAC converge into stability when the network saturates; finally, the effectiveness of the Power Saving Mechanism (PSM) proposed specially for TSC-M2MAC has also been verified, because it helps to save 29% of the total power consumption.

Chapter 6

Conclusions and Future Works

Due to the scientific and technological progress over the last decades, various new wireless applications have been developed, such as WLAN, wireless sensor networks, ad hoc networks, etc. Therefore, more and more wireless spectrum resources are demanded. This makes some of the spectrum band such as the ISM band very crowded. In the meanwhile, it has been shown by the US FCC that the allocated spectrum bands are significantly underutilized in vast geographic locations and different times. For example, in New York city, one of the most crowded places in the world, the maximum total spectrum occupancy is only 13.1% from 30 MHz to 3 GHz [127, 128]. Obviously, there exist an unbalanced problem between the very crowded ISM band and most of the underutilized allocated spectrum bands. However, the current spectrum regulatory rule exclusively allocates wireless spectrum to different specific applications, and no violation from unlicensed users is allowed. In order to solve this unbalanced spectrum problem, dynamic spectrum access techniques are necessary.

Dynamic spectrum access allows the unlicensed secondary users to access the vacant white spaces in the primary spectrum band as long as they can limit the interference with the primary users at an acceptable level. The typical technique of dynamic spectrum access is cognitive radio, which can adapt their parameters to its working environment and can switch its transceiver between the unlicensed spectrum band and the primary spectrum band. In order to utilize the primary spectrum band, the secondary cognitive radio users should find the white spaces in the primary spectrum band. There are two ways to achieve this goal. The first way is to query the remote database which can provide the information of the white spaces. The second way is to detect the primary signals and infer whether they are present or absent by the cognitive radio itself. Although both ways are accepted by the FCC as feasible solutions for TV white spaces, more and more researchers focus on the spectrum sensing since it can be used to detect other signals in addition to the TV signals.

Many local sensing techniques such as energy detection, covariance detection, eigenvalue detection, matched filter detection, cyclostationary detection, and wavelet detection have been proposed in the previous literature. However, because of the multi-path fading, shadowing, and receiver uncertainty, local spectrum sensing cannot work well; thus, the cooperative spectrum sensing is proposed. In cooperative spectrum sensing, multiple cognitive radio users are coordinated to perform spectrum sensing. The sensed data are transmitted to the fusion centre, which makes the final decision whether the primary signals are present or not.

Although many architectures for cooperative spectrum sensing can be employed, the mesh architecture is one of the most attractive architectures due to its unique features such as self-organizing, self-healing, and self-configuring. In addition, the connections between the mesh clients and the affiliated mesh routers are similar to the architecture of cooperative spectrum sensing, which make it very suitable for the cooperative spectrum sensing. Therefore, cooperative spectrum sensing for cognitive wireless mesh network is investigated in this dissertation.

However, there are several challenges to be addressed in the cooperative spectrum sensing for cognitive WMN.

1. The performance of the local spectrum sensing is always compromised by the inter-channel interference. How to deal with it?
2. The threshold setting in energy detection has an important impact on both probability of false alarm and probability of missed detection, how to obtain the optimal threshold?
3. The sensed data of each local cognitive radio should be transmitted to the fusion centre in the soft combining method through the reporting channel, which will become the bottleneck when the number of cognitive radios is large, how to solve it?
4. In the secondary cognitive WMN, the widely used common control channel will become the bottleneck when the number of the concurrent traffic flows need to be coordinated becomes large. How to design the MAC protocol for the

multiple radios multiple channels scenarios to improve the network performance?

Focusing on the above mentioned problems, this dissertation proposed the following schemes to address them.

In chapter 3, a non-coherent power decomposition based energy detection scheme is proposed for cooperative spectrum sensing. It is able to decompose the signal power, the interference power, and the background noise power individually. As a result, the useful signal power for energy detection can be extracted but the interference power and background power can be excluded from the composed received power. Thus, the impact of the interference and background noise uncertainty can be alleviated and the detection performance can be improved. The power decomposition method is implemented indirectly by solving a non-homogeneous linear equation set with a coefficient matrix that involves only the distances between the primary transmitters and the cognitive secondary users. The optimal number of cognitive radio users for sensing a single channel and the number of channels that can be sensed simultaneously are also derived accordingly. The simulation results show that the proposed method is able to cope with the expected interference variation and achieve higher probability of detection and lower probability of false alarm than the conventional method in both hard combining and soft combining scenarios.

In chapter 4, the optimal threshold is derived to minimize the sum of the probability of false alarm and probability of missed detection. It depends only on the means and variances of the power samples when the primary signals are absent and when they are present. Then, it is successfully applied in the power decomposition method described in chapter 3. In addition, in order to address the bottleneck problem of the reporting channel in soft combining scenario, multiple in-band orthogonal channels are designated as reporting channels. In this scheme, a multi-radio conflict graph is utilized to model the co-channel interference, and the vertex colouring algorithm is applied to the multi-radio conflict graph to figure out the reporting channel allocation results. Simulations verify the feasibility of the optimal threshold setting and show that it can work well in the low SINR range and can achieve low sensing delay.

In chapter 5, in order to address the bottleneck problem of common control channel, a two-stage coordination (TSC) M2MAC is proposed. It designates all the available orthogonal channels as both control channels and data channels in a time division manner through a two-stage coordination. On the first stage, similar to the reporting channel allocation in chapter 4, the multiple control channels allocation is performed. On the second stage, a REQ/ACK/RES mechanism is proposed to dynamically channel allocation for data transmission. The control messages are exchanged in the pre-allocated control channels on the first stage. In this stage both the primary channel and the secondary channels can be allocated. The proposed TSC-M2MAC is able to alleviate the hidden terminal problem when using multiple control channels and cope with the variation of the number of concurrent traffic flows. In addition, a power saving mechanism is designed for TSC-M2MAC to decrease its power consumption. Simulation results show that the TSC-M2MAC protocol is able to achieve higher throughput and lower end-to-end packet delay than conventional schemes. They also show that the TSC-M2MAC can achieve load balancing, save energy, and remain stable when the network becomes saturated.

For the future works, the proposed power decomposition method will be tried to be used for a real time in-band energy detection-based spectrum sensing. In the existing schemes, the spectrum sensing is performed periodically for a duration period, called quiet period. That is to say, in the quiet period, the secondary network should stop transmission and keep silent since the conventional energy detection method cannot differentiate the primary signals from the secondary signals. As a result, the performance of the secondary network will be inevitablely degraded. For example, the quiet period will interrupt the ongoing sessions, which will some real time application such as a voice IP phone available when the quiet period is long. Moreover, it will decrease the secondary network throughput and increase the transmission delay. However, as it is described in this dissertation, the power decomposition method has the potential to address this problem. It will be utilized to implement a real time energy detection based real time spectrum sensing to avoid the quiet period. Accordingly, the new MAC protocol should be considered.

Bibliography

[1] I. F. Akyildiz, B. F. Lo, and R. Balakrishnan, "Cooperative spectrum sensing in cognitive radio networks: A survey," *Physical Communication*, vol. 4, No. 1, 2011, pp. 40-62.

[2] T. Yucek and H. Arslan, "A Survey of Spectrum Sensing Algorithms for Cognitive Radio Applications," *IEEE Communications Surveys and Tutorials*, vol. 11, No. 1, 2009, pp. 116-130.

[3] C. Li and J. Xie, "Spectrum borrowing balancing-based spectrum management in cognitive radio," *IEEE Transactions on Consumer Electronics*, vol. 56, No. 2, 2010, pp. 441-446.

[4] M. E. Sahin, I. Guvenc, J. Moo-Ryong, and H. Arslan, "Handling CCI and ICI in OFDMA femtocell networks through frequency scheduling," *IEEE Transactions on Consumer Electronics*, vol. 55, No. 4, 2009, pp. 1936-1944.

[5] C. You, H. Kwon, and J. Heo, "Cooperative TV spectrum sensing in cognitive radio for Wi-Fi networks," *IEEE Transactions on Consumer Electronics*, vol. 57, No. 1, 2011, pp. 62-67.

[6] J. Mitola III and G. Q. Maguire Jr, "Cognitive radio: making software radios more personal," *IEEE Personal Communications*, vol. 6, No. 4, 1999, pp. 13-18.

[7] J. Mitola, "Cognitive radio: an integrated agent architecture for software defined radio," *Doctor of Technology, Royal Inst. Technol.(KTH), Stockholm, Sweden*, 2000, pp. 271-350.

[8] I. F. Akyildiz and X. Wang, *Wireless mesh networks*: John Wiley & Sons Inc, 2009.

[9] I. F. Akyildiz, X. Wang, and W. Wang, "Wireless mesh networks: a survey," *Computer Networks*, vol. 47, No. 4, 2005, pp. 445-487.

[10] Z. Ping, W. Xudong, and R. Rao, "Asymptotic Capacity of Infrastructure Wireless Mesh Networks," *IEEE Transactions on Mobile Computing*, vol. 7, No. 8, 2008, pp. 1011-1024.

[11] V. Navda, A. Kashyap, and S. R. Das, "Design and evaluation of iMesh: an infrastructure-mode wireless mesh network," in the *Proc. of Sixth IEEE International Symposium on a World of Wireless Mobile and Multimedia Networks (WoWMoM)*, giardini naxos, italy, 2005, pp. 164-170.

[12] L. Krishnamurthy, S. Conner, M. Yarvis, J. Chhabra, C. Ellison, C. Brabenac, and E. Tsui, "Meeting the demands of the digital home with high-speed multi-hop wireless networks," *Intel Technology Journal*, vol. 6, No. 4, 2002, pp. 57–68.

[13] I. F. Akyildiz and I. H. Kasimoglu, "Wireless sensor and actor networks: research challenges," *Ad Hoc Networks*, vol. 2, No. 4, 2004, pp. 351-367.

[14] FCC, "Spectrum policy task force Report," ET Docket No. 02-135, 2002.

[15] I. F. Akyildiz, W. Y. Lee, M. C. Vuran, and S. Mohanty, "NeXt generation/dynamic spectrum access/cognitive radio wireless networks: a survey," *Computer Networks*, vol. 50, No. 13, 2006, pp. 2127-2159.

[16] FCC. *ET Docket No 03-222 Notice of proposed rule making and order*. Available: http://hraunfoss.fcc.gov/edocs_public/attachmatch/FCC-03-322A1.pdf

[17] B. Letaief and W. Zhang, "Cooperative communications for cognitive radio networks," *Proceedings of the IEEE*, vol. 97, No. 5, 2009, pp. 878-893.

[18] Y. R. Kondareddy, N. Andrews, and P. Agrawal, "On the capacity of secondary users in a cognitive radio network," in the *Proc. of IEEE Sarnoff Symposium*, Princeton, NJ, USA, 2009, pp. 1-5.

[19] S. Haykin, "Cognitive radio: brain-empowered wireless communications," *IEEE Journal on Selected Areas in Communications*, vol. 23, No. 2, 2005, pp. 201-220.

[20] R. V. Prasad, P. Pawelczak, J. A. Hoffmeyer, and H. S. Berger, "Cognitive functionality in next generation wireless networks: standardization efforts," *IEEE Communications Magazine*, vol. 46, No. 4, 2008, pp. 72-78.

[21] B. Zhao and S. Shimamoto, "Non-Coherent Power Decomposition-based Energy Detection for Cooperative Spectrum Sensing in Cognitive Radio Networks," *IEICE Transactions on Communications*, vol. E95-B, No. 01, 2012, To appear.

[22] B. Zhao and S. Shimamoto, "Optimal cooperative spectrum sensing with non-coherent inter-channel interference cancellation for cognitive wireless mesh networks," *IEEE Transactions on Consumer Electronics*, vol. 57, No. 3, 2011, pp. 1049-1056.

[23] B. Zhao and S. Shimamoto, "Energy-Aware Cooperative Spectrum Sensing with Inter-Channel Interference Cancellation for Cognitive Radio Networks," in the *Proc. of the 20th International Conference on Computer Communications and Networks (ICCCN)*, Maui, HI, USA, 2011, pp. 1-6.

[24] B. Zhao and S. Shimamoto, "Two-Stage Coordination Multi-Radio Multi-channel MAC Protocol for Wireless Mesh Networks," *International Journal of Computer Networks and Communications*, vol. 3, No. 4, 2011, pp. 99-116.

[25] B. Zhao and S. Shimamoto, "Time division based multi-radio multi-channel MAC protocol for wireless mesh networks," in the *Proc. of the 11th International Conference onTelecommunications (ConTEL)*, Graz, Austria, 2011, pp. 293-300.

[26] Y. Zeng, Y. C. Liang, A. T. Hoang, and R. Zhang, "A review on spectrum sensing for cognitive radio: challenges and solutions," *Eurasip Journal on Advances in Signal Processing*, vol. 2010, 2010, pp. 1-15.

[27] D. Cabric, I. D. O'Donnell, M. S. W. Chen, and R. W. Brodersen, "Spectrum sharing radios," *IEEE Circuits and Systems Magazine*, vol. 6, No. 2, 2006, pp. 30-45.

[28] B. Wild and K. Ramchandran, "Detecting primary receivers for cognitive radio applications," in the *Proc. of the First IEEE International Symposium on New Frontiers in Dynamic Spectrum Access Networks*, Baltimore, Maryland, USA, 2005, pp. 124-130.

[29] I. F. Akyildiz, L. Won-Yeol, M. C. Vuran, and S. Mohanty, "A survey on spectrum management in cognitive radio networks," *IEEE Communications Magazine*, vol. 46, No. 4, 2008, pp. 40-48.

[30] A. Sahai, N. Hoven, and R. Tandra, "Some fundamental limits on cognitive radio," in the *Proc. of Forty-second Allerton Conference on Communication, Control, and Computing*, Monticello, Illinois, USA, 2004, pp. 1662–1671.

[31] Y. Zeng and Y.-C. Liang, "Spectrum-Sensing Algorithms for Cognitive Radio Based on Statistical Covariances," *IEEE Transactions on Vehicular Technology*, vol. 58, No. 4, 2009, pp. 1804-1815.

[32] Y. Zeng and Y.-C. Liang, "Covariance Based Signal Detections for Cognitive Radio," in the *Proc. of the 2nd IEEE International Symposium on New Frontiers in Dynamic Spectrum Access*

Networks (DySPAN), Dublin, Ireland, 2007, pp. 202-207.

[33] Y. Zeng and Y. C. Liang. *Eigenvalue based sensing algorithms*. Available: www.ieee802.org/22/Meeting.../22-06-0118-00-0000_I2R-sensing.doc

[34] Y. Zeng and Y.-C. Liang, "Maximum-Minimum Eigenvalue Detection for Cognitive Radio," in the *Proc. of IEEE 18th International Symposium on Personal, Indoor and Mobile Radio Communications (PIMRC)*, Athens, Greece, 2007, pp. 1-5.

[35] Y. Zeng and Y. C. Liang, "Eigenvalue-based spectrum sensing algorithms for cognitive radio," *IEEE Transactions on Communications*, vol. 57, No. 6, 2009, pp. 1784-1793.

[36] P. Bianchi, J. Najim, G. Alfano, and M. Debbah, "Asymptotics of eigenbased collaborative sensing," in the *Proc. of IEEE Information Theory Workshop (ITW)*, taormina, sicily, Italy, 2009, pp. 515-519.

[37] P. Bianchi, J. Najim, M. Maida, and M. Debbah, "Performance analysis of some eigen-based hypothesis tests for collaborative sensing," in the *Proc. of IEEE/SP 15th Workshop on Statistical Signal Processing (SSP)*, Cardiff, Wales, UK, 2009, pp. 5-8.

[38] F. Penna, R. Garello, and M. A. Spirito, "Cooperative spectrum sensing based on the limiting eigenvalue ratio distribution in Wishart matrices," *IEEE Communications Letters*, vol. 13, No. 7, 2009, pp. 507-509.

[39] Y. Zeng, C.-L. Koh, and Y.-C. Liang, "Maximum Eigenvalue Detection: Theory and Application," in the *Proc. of IEEE International Conference on Communications (ICC)*, Beijing, China, 2008, pp. 4160-4164.

[40] A. I. Perez-Neira, M. A. Lagunas, M. A. Rojas, and P. Stoica, "Correlation Matching Approach for Spectrum Sensing in Open Spectrum Communications," *IEEE Transactions on Signal Processing*, vol. 57, No. 12, 2009, pp. 4823-4836.

[41] A. Sahai and D. Cabric, "Spectrum sensing: fundamental limits and practical challenges," in the *Proc. of IEEE International Symposium on New Frontiers in Dynamic Spectrum Access Networks (DySPAN)*, Baltimore, Md, USA, 2005.

[42] S. M. Kay, *Fundamentals Of Statistical Processing, Volume 2: Detection Theory*: Pearson Education, 2009.

[43] H.-S. Chen, W. Gao, and D. G. Daut, "Signature Based Spectrum Sensing Algorithms for IEEE 802.22 WRAN," in the *Proc. of IEEE International Conference on Communications (ICC)*, Glasgow, Scotland, 2007, pp. 6487-6492.

[44] D. Cabric, S. M. Mishra, and R. W. Brodersen, "Implementation issues in spectrum sensing for cognitive radios," in the *Proc. of the Thirty-Eighth Asilomar Conference on Signals, Systems and Computers*, Pacific Grove, CA, USA, 2004, pp. 772-776.

[45] J. Lunden, V. Koivunen, A. Huttunen, and H. V. Poor, "Collaborative Cyclostationary Spectrum Sensing for Cognitive Radio Systems," *IEEE Transactions on Signal Processing*, vol. 57, No. 11, 2009, pp. 4182-4195.

[46] M. Derakhshani, M. Nasiri-Kenari, and L.-N. Tho, "Cooperative Cyclostationary Spectrum Sensing in Cognitive Radios at Low SNR Regimes," in the *Proc. of IEEE International Conference on Communications*, Cape Town, South Africa, 2010, pp. 1-5.

[47] N. Han, S. Shon, J. H. Chung, and J. M. Kim, "Spectral correlation based signal detection method for spectrum sensing in IEEE 802.22 WRAN systems," in the *Proc. of the 8th*

International Conference Advanced Communication Technology (ICACT), Phoenix Park, South Korea, 2006, pp. 1765-1770.

[48] W. Gardner, W. Brown, and C. Chih-Kang, "Spectral Correlation of Modulated Signals: Part II--Digital Modulation," *IEEE Transactions on Communications*, vol. 35, No. 6, 1987, pp. 595-601.

[49] W. Gardner, "Spectral Correlation of Modulated Signals: Part I--Analog Modulation," *IEEE Transactions on Communications*, vol. 35, No. 6, 1987, pp. 584-594.

[50] W. A. Gardner, "Exploitation of spectral redundancy in cyclostationary signals," *IEEE Signal Processing Magazine*, vol. 8, No. 2, 1991, pp. 14-36.

[51] J. Lunden, V. Koivunen, A. Huttunen, and H. V. Poor, "Spectrum Sensing in Cognitive Radios Based on Multiple Cyclic Frequencies," in the *Proc. of the 2nd International Conference on Cognitive Radio Oriented Wireless Networks and Communications (CrownCom)*, Orlando, FL, USA, 2007, pp. 37-43.

[52] M. Oner and F. Jondral, "On the extraction of the channel allocation information in spectrum pooling systems," *IEEE Journal on Selected Areas in Communications*, vol. 25, No. 3, 2007, pp. 558-565.

[53] Z. Tian and G. B. Giannakis, "A Wavelet Approach to Wideband Spectrum Sensing for Cognitive Radios," in the *Proc. of the 1st International Conference on Cognitive Radio Oriented Wireless Networks and Communications (CrownCom)*, Mykonos Island, Greece, 2006, pp. 1-5.

[54] G. W. Wornell, "Emerging applications of multirate signal processing and wavelets in digital communications," *Proceedings of the IEEE*, vol. 84, No. 4, 1996, pp. 586-603.

[55] S. Chantaraskul and K. Moessner, "Experimental Study of Multi-Resolution Spectrum Opportunity Detection Using Wavelet Analysis," in the *Proc. of 2010 IEEE Symposium on New Frontiers in Dynamic Spectrum*, Singapore, 2010, pp. 1-6.

[56] S. Chantaraskul and K. Moessner, "Implementation of wavelet analysis for spectrum opportunity detection," in the *Proc. of IEEE 20th International Symposium on Personal, Indoor and Mobile Radio Communications (PIMRC)*, Tokyo, Japan, 2009, pp. 2310-2314.

[57] K.-H. Chen and T.-D. Chiueh, "A Cognitive Radio System Using Discrete Wavelet Multitone Modulation," *IEEE Transactions on Circuits and Systems I: Regular Papers*, vol. 55, No. 10, 2008, pp. 3246-3258.

[58] Y. Hur, J. Park, W. Woo, J. S. Lee, K. Lim, C. H. Lee, H. S. Kim, and J. Laskar, "A Cognitive Radio (CR) System Employing A Dual-Stage Spectrum Sensing Technique : A Multi-Resolution Spectrum Sensing (MRSS) and A Temporal Signature Detection (TSD) Technique," in the *Proc. of IEEE Global Telecommunications Conference (GLOBECOM)*, San Francisco, CA, USA, 2006, pp. 1-5.

[59] G. Ganesan and Y. Li, "Agility improvement through cooperative diversity in cognitive radio," in the *Proc. of IEEE Global Telecommunications Conference (GLOBECOM)*, St. Louis, MO, USA, 2005, pp. 2505-2509.

[60] S. M. Mishra, A. Sahai, and R. W. Brodersen, "Cooperative Sensing among Cognitive Radios," in the *Proc. of IEEE International Conference on Communications (ICC)*, Istanbul, Turkey, 2006, pp. 1658-1663.

[61] T. Weiss, "A diversity approach for the detection of idle spectral resources in spectrum pooling

systems," in the *Proc. of the 48th International Scientific Colloquium*, Ilmenau, Germany, 2003, pp. 37-38.

[62] A. Ghasemi and E. S. Sousa, "Opportunistic spectrum access in fading channels through collaborative sensing," *Journal of Communications,* vol. 2, No. 2, 2007, pp. 71-82.

[63] A. Ghasemi and E. S. Sousa, "Spectrum sensing in cognitive radio networks: the cooperation-processing tradeoff," *Wireless Communications and Mobile Computing,* vol. 7, No. 9, 2007, pp. 1049-1060.

[64] A. Ghasemi and E. S. Sousa, "Collaborative spectrum sensing for opportunistic access in fading environments," in the *Proc. of the First IEEE International Symposium on New Frontiers in Dynamic Spectrum Access Networks (DySPAN)*, Baltimore, MD, USA, 2005, pp. 131-136.

[65] M. Gandetto and C. Regazzoni, "Spectrum sensing: A distributed approach for cognitive terminals," *IEEE Journal on Selected Areas in Communications,* vol. 25, No. 3, 2007, pp. 546-557.

[66] E. Visotsky, S. Kuffner, and R. Peterson, "On collaborative detection of TV transmissions in support of dynamic spectrum sharing," in the *Proc. of the First IEEE International Symposium on New Frontiers in Dynamic Spectrum Access Networks (DySPAN)*, Baltimore, MD, USA, 2005, pp. 338-345.

[67] G. Ganesan and Y. Li, "Cooperative Spectrum Sensing in Cognitive Radio, Part II: Multiuser Networks," *IEEE Transactions on Wireless Communications,* vol. 6, No. 6, 2007, pp. 2214-2222.

[68] G. Ganesan and Y. Li, "Cooperative Spectrum Sensing in Cognitive Radio, Part I: Two User Networks," *IEEE Transactions on Wireless Communications,* vol. 6, No. 6, 2007, pp. 2204-2213.

[69] W. Zhang, R. K. Mallik, and K. Ben Letaief, "Cooperative Spectrum Sensing Optimization in Cognitive Radio Networks," in the *Proc. of IEEE International Conference on Communications*, Beijing, China, 2008, pp. 3411-3415.

[70] V. Kostylev, "Energy detection of a signal with random amplitude," in the *Proc. of IEEE International Conference on Communications*, New York, NY, USA, 2002, pp. 1606-1610.

[71] H. Urkowitz, "Energy detection of unknown deterministic signals," *Proceedings of the IEEE,* vol. 55, No. 4, 1967, pp. 523-531.

[72] F. F. Digham, M. S. Alouini, and M. K. Simon, "On the energy detection of unknown signals over fading channels," in the *Proc. of IEEE International Conference on Communications*, Anchorage, Alaska, USA, 2003, pp. 3575-3579.

[73] S. Yngve, H. Tullberg, and J. Kronander, "Sensor Selection for Cooperative Spectrum Sensing," in the *Proc. of the 3rd IEEE Symposium on New Frontiers in Dynamic Spectrum Access Networks (DySPAN)*, Chicago, IL, USA, 2008, pp. 1-11.

[74] W. Jin and Z. Xi, "Energy-Efficient Distributed Spectrum Sensing for Wireless Cognitive Radio Networks," in the *Proc. of INFOCOM IEEE Conference on Computer Communications Workshops*, San Diego, CA, USA, 2010, pp. 1-6.

[75] A. C. Malady and C. da Silva, "Clustering methods for distributed spectrum sensing in cognitive radio systems," in the *Proc. of IEEE Military Communications Conference (MILCOM)*, San Diego, CA, USA, 2008, pp. 1-5.

[76] S. Chunhua, Z. Wei, and K. Ben, "Cluster-Based Cooperative Spectrum Sensing in Cognitive Radio Systems," in the *Proc. of IEEE International Conference on Communications (ICC)*,

Glasgow, Scotland, UK, 2007, pp. 2511-2515.

[77] G. Chen, P. Tao, X. Shaoyi, W. Haiming, and W. Wenbo, "Cooperative Spectrum Sensing with Cluster-Based Architecture in Cognitive Radio Networks," in the *Proc. of IEEE 69th Vehicular Technology Conference (VTC Spring)*, Barcelona, Spain, 2009, pp. 1-5.

[78] W. Saad, H. Zhu, M. Debbah, A. Hjorungnes, and T. Basar, "Coalitional Games for Distributed Collaborative Spectrum Sensing in Cognitive Radio Networks," in the *Proc. of IEEE INFOCOM*, Rio de Janeiro, Brazil, 2009, pp. 2114-2122.

[79] J. Ma and Y. Li, "Soft Combination and Detection for Cooperative Spectrum Sensing in Cognitive Radio Networks," in the *Proc. of IEEE Global Telecommunications Conference (GLOBECOM)*, Washington, DC, USA, 2007, pp. 3139-3143.

[80] F. Cali, M. Conti, and E. Gregori, "Dynamic tuning of the IEEE 802.11 protocol to achieve a theoretical throughput limit," *IEEE/ACM Transactions on Networking*, vol. 8, No. 6, 2000, pp. 785-799.

[81] M. Takai, J. Martin, R. Bagrodia, and A. Ren, "Directional virtual carrier sensing for directional antennas in mobile ad hoc networks," in the *Proc. of* the 3rd ACM international symposium on Mobile ad hoc networking and computing (MOBIHOC), Lausanne, Switzerland, 2002, pp. 183-193.

[82] R. R. Choudhury, X. Yang, R. Ramanathan, and N. H. Vaidya, "Using directional antennas for medium access control in ad hoc networks," in the *Proc. of* the 8th annual international conference on Mobile computing and networking, Atlanta, Georgia, USA, 2002, pp. 59-70.

[83] L. Krishnamurthy, "Making radios more like human ears: alternative MAC techniques and innovative platforms to enable large-scale meshes," in *Microsoft Mesh Networking Summit*, ed, 2004.

[84] X. Wang, W. Wang, and M. P. Nova, "Distributed TDMA for wireless mesh network," United States Patent, 2005.

[85] C. Eklund, R. B. Marks, K. L. Stanwood, and S. Wang, "IEEE standard 802.16: a technical overview of the WirelessMAN TM air interface for broadband wireless access," *IEEE Communications Magazine*, vol. 40, No. 6, 2002, pp. 98-107.

[86] *High Rate Ultra Wideband PHY and MAC Standard*. Available: www.ecma-international.org/publications/files/ECMA-ST/ECMA-368.pdf

[87] X. Yang and G. d. Veciana, "Inducing spatial clustering in MAC contention for spread spectrum ad hoc networks," in the *Proc. of* the 6th ACM international symposium on Mobile ad hoc networking and computing, Urbana-Champaign, IL, USA, 2005, pp. 121-132.

[88] A. A. Bertossi and M. A. Bonuccelli, "Code assignment for hidden terminal interference avoidance in multihop packet radio networks," in the *Proc. of the Eleventh Annual Joint Conference of the IEEE Computer and Communications Societies (INFOCOM)* Florence , Italy, 1992, pp. 701-709.

[89] J. So and N. H. Vaidya, "Multi-channel mac for ad hoc networks: handling multi-channel hidden terminals using a single transceiver," in the *Proc. of the 5th ACM international symposium on Mobile ad hoc networking and computing*, New York, NY, USA, 2004, pp. 222-233.

[90] P. Bahl, R. Chandra, and J. Dunagan, "SSCH: slotted seeded channel hopping for capacity improvement in IEEE 802.11 ad-hoc wireless networks," in the *Proc. of the 10th annual*

international conference on Mobile computing and networking, Philadelphia, PA, USA, 2004, pp. 216-230.

[91] A. Adya, P. Bahl, J. Padhye, A. Wolman, and L. Zhou, "A multi-radio unification protocol for IEEE 802.11 wireless networks," in the *Proc. of the First International Conference on Broadband Networks (BroadNets)*, San Jose, CA, USA, 2004, pp. 344-354.

[92] B. Raman and K. Chebrolu, "Design and evaluation of a new MAC protocol for long-distance 802.11 mesh networks," in the *Proc. of* the 11th annual international conference on Mobile computing and networking, Cologne, Germany, 2005, pp. 156-169.

[93] B. Raman, "Channel allocation in 802.11-based mesh networks," in the *Proc. of 25th IEEE International Conference on Computer Communications (INFOCOM)*, Barcelona, Spain, 2006, pp. 1-10.

[94] K. Xing, X. Cheng, L. Ma, and Q. Liang, "Superimposed code based channel assignment in multi-radio multi-channel wireless mesh networks," in the *Proc. of* the 13th annual ACM international conference on Mobile computing and networking, Montreal, Quebec, Canada, 2007, pp. 15-26.

[95] K. N. Ramachandran, E. M. Belding, K. C. Almeroth, and M. M. Buddhikot, "Interference-aware channel assignment in multi-radio wireless mesh networks," in the *Proc. of 25th IEEE International Conference on Computer Communications (INFOCOM)*, Barcelona, Spain, 2006, pp. 1-12.

[96] K. R. Chowdhury and I. F. Akyildiz, "Cognitive wireless mesh networks with dynamic spectrum access," *IEEE Journal on Selected Areas in Communications*, vol. 26, No. 1, Jan 2008, pp. 168-181.

[97] C. Song, Y. D. Alemseged, T. Ha Nguyen, G. Villardi, C. Sun, S. Filin, and H. Harada, "Adaptive Two Thresholds Based Energy Detection For Cooperative Spectrum Sensing," in the *Proc. of 7th IEEE Consumer Communications and Networking Conference (CCNC)*, Las Vegas, NV, USA, 2010, pp. 1-6.

[98] C. SONG, M. A. RAHMAN, R. FUNADA, and H. HARADA, "Robust Spectrum Sensing of DVB-T Signals," *IEICE technical report*, vol. 110, No. 252, 2010, pp. 161-168.

[99] I. F. Akyildiz, W. Y. Lee, and K. R. Chowdhury, "CRAHNs: Cognitive radio ad hoc networks," *Ad Hoc Networks*, vol. 7, No. 5, Jul 2009, pp. 811-836.

[100] W. A. Gardner, "Signal interception: a unifying theoretical framework for feature detection," *IEEE Transactions on Communications*, vol. 36, No. 8, 1988, pp. 897-906.

[101] C. SONG, Y. D. Alemseged, T. Ha Nguyen, G. Villardi, C. Sun, S. Filin, and H. Harada, "Adaptive Two Thresholds Based Energy Detection For Cooperative Spectrum Sensing," in the *Proc. of the 7th IEEE Consumer Communications and Networking Conference (CCNC)*, Las Vegas, Nevada, USA, 2010, pp. 1-6.

[102] "IEEE 802. 22TM/ P802.22/D2.0 Draft Standard for Wireless Regional Area Network Part 22: Cognitive Wireless RAN Medium Access Control (MAC) and Physical Layer (PHY) Specifications: Policies and procedures for operation in the TV Bands," ed, 2011, pp. 1-657.

[103] A. Ghasemi and E. S. Sousa, "Spectrum sensing in cognitive radio networks: requirements, challenges and design trade-offs," *IEEE Communications Magazine*, vol. 46, No. 4, 2008, pp. 32-39.

[104] S. J. Shellhammer, A. K. Sadek, and W. Zhang, "Technical challenges for cognitive radio in the TV white space spectrum," in the *Proc. of Information Theory and Applications Workshop*, La Jolla, CA, USA, pp. 323-333.

[105] C. Stevenson, G. Chouinard, L. Zhongding, H. Wendong, S. Shellhammer, and W. Caldwell, "IEEE 802.22: The first cognitive radio wireless regional area network standard," *IEEE Communications Magazine*, vol. 47, No. 1, 2009, pp. 130-138.

[106] A. Mishra, V. Shrivastava, S. Banerjee, and W. Arbaugh, "Partially overlapped channels not considered harmful," *SIGMETRICS Perform. Eval. Rev.*, vol. 34, No. 1, 2006, pp. 63-74.

[107] T. S. Rappaport, *Wireless communications: Principles and Practice, 2nd Edition*: Prentice-Hall, 2001.

[108] J. Lehtomaki, M. Juntti, H. Saarnisaari, and S. Koivu, "Threshold setting strategies for a quantized total power radiometer," *IEEE Signal Processing Letters*, vol. 12, No. 11, 2005, pp. 796-799.

[109] S. Shellhammer, V. Tawil, G. Chouinard, M. Muterspaugh, and M. Ghosh, "Spectrum sensing simulation model," *IEEE 802.22-06/0028r10*, 2006, pp. 1-18.

[110] C. Adrados, I. Girard, J.-P. Gendner, and G. Janeau, "Global Positioning System (GPS) location accuracy improvement due to Selective Availability removal," *Comptes Rendus Biologies*, vol. 325, No. 2, 2002, pp. 165-170.

[111] Y. Tachwali, F. Basma, and H. H. Refai, "Cognitive radio architecture for rapidly deployable heterogeneous wireless networks," *IEEE Transactions on Consumer Electronics*, vol. 56, No. 3, 2010, pp. 1426-1432.

[112] B. Wang, G. Zeng, M. Mutka, and L. Xiao, "Routing for minimum length schedule in multi-channel TDMA based wireless mesh networks," in the *Proc. of IEEE International Symposium on a World of Wireless Mobile and Multimedia Networks (WoWMoM)*, Montreal, QC, Canada, 2010, pp. 1-6.

[113] K. Fal and K. Varadhan. *The ns Manual*. Available: http://www.isi.edu/nsnam/ns/doc/ns_doc.pdf

[114] I. Katzela and M. Naghshineh, "Channel assignment schemes for cellular mobile telecommunication systems: A comprehensive survey," *IEEE Personal Communications*, vol. 3, No. 3, 1996, pp. 10-31.

[115] T. Pering, Y. Agarwal, R. Gupta, and R. Want, "CoolSpots: reducing the power consumption of wireless mobile devices with multiple radio interfaces," in the *Proc. of the 4th international conference on Mobile systems, applications and services*, New York, NY, USA, 2006, pp. 220-232.

[116] M. Stemm and R. H. Katz, "Measuring and reducing energy consumption of network interfaces in hand-held devices," *IEICE Transactions on Communications*, vol. 80, No. 8, 1997, pp. 1125-1131.

[117] W. van der Moolen, "IEEE 802.11 WaveLAN PC Card User's Guide," *Lucent Technologies*, 1998, pp. A-1.

[118] R. Jain, A. Durresi, and G. Babic. *Throughput fairness index: an explanation*. Available: http://www1.cse.wustl.edu/~jain/atmf/a99-0045.htm

[119] C. L. Robinson and P. R. Kumar, "Optimizing controller location in networked control systems with packet drops," *IEEE Journal on Selected Areas in Communications*, vol. 26, No. 4, 2008,

pp. 661-671.

[120] H. Shawn and Y. Wei-Yong, "Stability of Networked Control Systems Under a Multiple-Packet Transmission Policy," *IEEE Transactions on Automatic Control*, vol. 53, No. 7, 2008, pp. 1706-1711.

[121] J. Xiong and J. Lam, "Stabilization of linear systems over networks with bounded packet loss," *Automatica*, vol. 43, No. 1, 2007, pp. 80-87.

[122] J. Daewon, H. Jaeseon, L. Hyuk, P. Kyung-Joon, and J. C. Hou, "Adaptive contention control for improving end-to-end throughput performance of multihop wireless networks," *IEEE Transactions on Wireless Communications*, vol. 9, No. 2, 2010, pp. 696-705.

[123] D. Der-Jiunn, K. Chih-Heng, C. Hsiao-Hwa, and H. Yueh-Min, "Contention window optimization for ieee 802.11 DCF access control," *IEEE Transactions on Wireless Communications*, vol. 7, No. 12, 2008, pp. 5129-5135.

[124] B. Hirantha Sithira Abeysekera, T. Matsuda, and T. Takine, "Dynamic Contention Window Control Mechanism to Achieve Fairness between Uplink and Downlink Flows in IEEE 802.11 Wireless LANs," *IEEE Transactions on Wireless Communications*, vol. 7, No. 9, 2008, pp. 3517-3525.

[125] S. Pudasaini, K. Moonsoo, S. Seokjoo, and J. A. Copeland, "COMIC: Intelligent Contention Window Control for Distributed Medium Access," *IEEE Communications Letters*, vol. 14, No. 7, 2010, pp. 656-658.

[126] *NS simulator, version 2.29*. Available: http://isi.edu/nsnam/ns/

[127] M. McHenry, E. Livsics, T. Nguyen, and N. Majumdar, "XG dynamic spectrum access field test results," *IEEE Communications Magazine*, vol. 45, No. 6, 2007, pp. 51-57.

[128] M. A. McHenry, D. McCloskey, and G. Lane-Roberts. *Spectrum Occupancy Measurements*. Available: http://www.sharedspectrum.com/wp-content/uploads/4_NSF_NYC_Report.pdf

Research Achievements

Category (Subheadings)	
Articles in refereed journals	○ Bingxuan Zhao and Shigeru Shimamoto, "Non-Coherent Power Decomposition-based Energy Detection for Cooperative Spectrum Sensing in Cognitive Radio Networks," *IEICE Transactions on Communications*, vol. E95-B, No. 01, 2012, 10 pages. (To appear). ○ Bingxuan Zhao and Shigeru Shimamoto, "Optimal Cooperative Spectrum Sensing with Non-coherent Inter-Channel Interference Cancellation for Cognitive Wireless Mesh Networks," *IEEE Transactions on Consumer Electronics*, vol. 57, No. 3, 2011, pp.1049-1056. ○ Bingxuan Zhao and Shigeru Shimamoto, "Two-Stage Coordination Multi-Radio Multi-channel MAC Protocol for Wireless Mesh Networks," *International Journal of Computer Networks and Communications*, vol. 3, No. 4, 2011, pp. 99-116.
Presentations at International conferences	○ Bingxuan Zhao and Shigeru Shimamoto, "Energy-aware Cooperative Spectrum Sensing with Inter-Channel Interference Cancellation for Cognitive Radio Networks," *In the Proc. of ICCCN Workshop on Cognitive and Resource-aware Wireless Communications*, Maui, Hawaii, USA, 2011, pp. 1-6. ○ Bingxuan Zhao and Shigeru Shimamoto, "Time Division based Multi-Radio Multi-Channel MAC Protocol for Wireless Mesh Networks," *In the Proc. of The 11th International Conference on Telecommunications*, Graz, Austria, 2011, pp. 293-300

Other papers	Bingxuan Zhao, Song Wang, Xutao Lv, and Gang Wu, "Study on Data Frame Synchronization Fast Algorithm of Radio Data System," *Journal of Computer Applications (In Chinese)*, vol. 28, No. 1, 2008, pp. 9-10,13 Xiaoli Wang, Zhaosheng Yang, Xutao Lv, and Bingxuan Zhao, "Shortest Path Algorithm Based on Limiting Parallelogram and Its Application in Traffic Networks," *Journal of Jilin University (Engineering and Technology Edition) (In Chinese)*, vol. 36, No. 1, 2006, pp. 123-127
Others (Innovation patents)	Jian Yang, Hongsheng Xi, Baoqun Yin, Bingxuan Zhao, and Jing Li, the Implementing Approach of On-line Service Migration in the Streaming Media Server Cluster, Chinese innovation patents, CN 101252546 Jian Yang, Hongsheng Xi, Baoqun Yin, Xiaoqiang Yang, Fei Wang, and Bingxuan Zhao, The Approach of Separating Up-link and Down-link Data on Transport-layer in Load Balancing System, Chinese innovation patents, CN 101252591 B Jian Yang, Bingxuan Zhao, Baoqun Yin, Ming Zhu, and Hongsheng Xi. The Load Balancing System and the Approach of Load Balancing for Multi-Services, Chinese innovation patents, CN 101207550 B Jian Yang, Bingxuan Zhao, Baoqun Yin, Ming Zhu, and Hongsheng Xi. The Adapter for Multi-Protocols and the Approach of Load Balancing for Multi-Service, Chinese innovation patents, CN 101207568 Song Wang, Quan Zheng, Jun Li, Ming Zhu, Bingxuan Zhao. The Approach of Data Transmission, Chinese innovation patents, CN 101155296 B

Others (Presentations)	Bingxuan Zhao, and Shigeru Shimamoto, “Energy-aware Cooperative Spectrum Sensing with Inter-channel Interference Cancellation,” Tsinghua - Waseda Exchange Workshop, Tsinghua University, Beijing, China, Mar. 2011. Bingxuan Zhao, and Shigeru Shimamoto, “Energy-aware Cooperative Spectrum Sensing with Inter-channel Interference Cancellation,” Exchange Workshop at Beijing University, Beijing, China, Mar. 2011. Bingxuan Zhao, and Shigeru Shimamoto, “Energy-aware Cooperative Spectrum Sensing with Inter-channel Interference Cancellation,” Exchange seminar between Hanyang University and Waseda University, Waseda University, Tokyo, Japan, Nov. 2010.